Distribution Agreement

In presenting this thesis or dissertation as a partial fulfillment of the requirements for an advanced degree from Emory University, I hereby grant to Emory University and its agents the non-exclusive license to archive, make accessible, and display my thesis or dissertation in whole or in part in all forms of media, now or hereafter known, including display on the world wide web. I understand that I may select some access restrictions as part of the online submission of this thesis or dissertation. I retain all ownership rights to the copyright of the thesis or dissertation. I also retain the right to use in future works (such as articles or books) all or part of this thesis or dissertation.

Signature:

Alexander John Mesko	Date

Studies of the Ices and Chiral Molecules of the Interstellar Medium

By

Alexander John Mesko
Master of Science
Chemistry

Susanna Widicus Weaver, Ph.D
Advisor

Michael Heaven, Ph.D
Committee Member

Francesco Evangelista, Ph.D
Committee Member

Accepted:

Lisa A. Tedesco, Ph.D
Dean of the James T. Laney School of Graduate Studies

Date

Studies of the Ices and Chiral Molecules of the Interstellar Medium

By

Alexander John Mesko
B.S., University of Tulsa, 2013

Advisor: Susanna Widicus Weaver, Ph.D

An abstract of
A thesis submitted to the Faculty of the
James T. Laney School of Graduate Studies of Emory University
in partial fulfillment of the requirements for the degree of
Master of Science
in Chemistry
2016

Abstract

Studies of the Ices and Chiral Molecules of the Interstellar Medium

By Alexander John Mesko

Our understanding of the chemical diversity of the interstellar medium is ever increasing. With better observational technology and experimentation, the detection of ices, ions, radicals, and chiral molecules have all been confirmed. Millimeter/submillimeter spectroscopy is one tool which has driven advances in observational astronomy and laboratory spectroscopy. The work presented here focuses on two experiments: the study of interstellar ices and the study of propylene oxide, the first chiral molecule detected in the interstellar medium. Millimeter/submillimeter spectroscopy is the primary technique employed in both experiments. The premise of the interstellar ice analogue experiment is to understand the chemical mechanisms which can lead to the formation and desorption of key molecules in the interstellar medium. Millimeter/submillimeter spectroscopy allows us to study the gas-phase over the surface of the ice at high sensitivity and excellent resolution. To this point we have studied thermal and photodesorption of water from pure water ices, and the evolution of CO as a result of photo-processing of pure methanol ices. The motivation of the propylene oxide experiment is to provide new laboratory spectra so that it can be a target for further astronomical searches. The spectrum from 70 GHz to 1 THz is presented, the molecular constants are determined, and the internal rotation of the methyl group is analyzed and discussed.

Studies of the Ices and Chiral Molecules of the Interstellar Medium

By

Alexander John Mesko
B.S., University of Tulsa, 2013

Advisor: Susanna Widicus Weaver, Ph.D

A thesis submitted to the Faculty of the
James T. Laney School of Graduate Studies of Emory University
in partial fulfillment of the requirements for the degree of
Master of Science
in Chemistry
2016

Acknowledgement

Firstly, I would like to thank Emory University and Dr. Susanna Widicus Weaver for funding me throughout my time here. To further thank Dr. Widicus Weaver I would like to say that she has always been a very encouraging and understanding boss and mentor. I would not have made it this far without her. I would also like to thank Dr. Michael Heaven and Dr. Francesco Evangleista, the members of my committee, for being good mentors and providing excellent feedback and advice. Lastly, all of the members of the Widicus Weaver research group have been a pleasure to work with, with special consideration for Luyao Zou who contributed greatly to the work on propylene oxide and Houston Smith who has worked with me on the ice experiment since he started as a freshman.

Table of Contents

List of Figures

List of Tables

Chapter 1 A Brief Overview of The Interstellar Environment

The scope of chemistry encompasses 118 different unique elements capable of bonding together to form innumerable distinct chemical species; and yet just over 190 different molecules, ions, and radicals have been detected in the incomprehensible immensity of the interstellar medium (ISM) [1]. It is by knowing which molecules exist in an astronomical environment, their densities, and their energy distributions that we gain an idea of what kind of chemistry occurs there. A crucial tool in the detection of molecules in the interstellar medium is mm/submm astronomy. In this wavelength regime, every molecule has a distinct set of rotational lines which can allow for unambiguous determination of what molecules are present and their temperatures and densities. As observational studies have progressed, chemical models have adapted accordingly. With the backing of laboratory spectroscopy, further astronomical searches can be conducted and the models can be examined.

In the vast expanse of interstellar space, gas-phase collisions between neutral species are extremely unlikely with time scales on the order of 10^5 – 10^6 years [2]. As a result, in early models of astrochemistry, ion-molecule gas-phase reactions had been considered to be the primary method of formation of most complex organic molecules (COMs), defined to be carbon containing molecules of six or more atoms [2]. The electrostatic attraction of an ion to a permanent molecular dipole considerably enhances the reaction rate over neutral-neutral molecular reactions. Ion-molecule pathways are still a major part of interstellar chemical models, but these reactions are not sufficient to explain the observed concentrations of many interstellar species such as the high concentrations of methyl formate in cold cores [3–5] and glycolaldehyde [6] in hot cores. As a result, icy-grain chemistry has become a critical model by which much

interstellar COM chemistry is thought to occur. Silicate and carbonaceous grains in cold regions of the interstellar medium adsorb almost any species that comes into contact with them, due to the high sticking probabilities resulting from the very low thermal energies. Thus these grains act as a meeting ground for simple molecular and atomic species. The low thermal energies in these regions have a second effect: species, with the exception of hydrogen, that have stuck to the grain are unable to move across the surface of it. As a result, the icy grain remains relatively inert, with the exception of hydrogenation reactions, until a source of energy is found. The molecular clouds in which icy grains exist in can begin to gravitationally collapse, and over thousands of years, as the cloud falls inward, the core of the cloud begins to heat up, becoming a prestellar core. If the cloud is massive enough a star can be born. The star bathes everything in the surrounding areas with radiation. Ultraviolet radiation, produced either directly by the star or from cosmic-ray induced VUV emission within clouds, coupled with the increasing temperature of the environment, mobilizes and photylizes the species composing the icy grains. These icy grains become a breeding ground for complex organic molecules.

Over extensive time, the processing of ices and gasses produce a high diversity of molecules which have been detected in the ISM [1]. Nitrogen containing species [7, 8], organic molecules up to 12 atoms in size [9], the C_{60} [10–14] and C_{70} [10] fullerenes, and recently the first chiral molecule, propylene oxide [15], have been discovered in interstellar space. The detection of chiral molecules is a prime area of interest in the astrochemistry and astrobiology communities because of the implications it has to the origin of homochirality on Earth. If a particular enantiomer of a given chiral molecule can be preferentially selected in interstellar clouds, the decedents of those clouds can then inherent and further amplify an enantiomeric excess, eventually producing homochirality, a necessity for the evolution of life.

The overarching motivation for the work of this thesis is to further understand the

chemical makeup and resulting chemistry of astrophysical environments, with a focus on interstellar ices and propylene oxide. Here I present two distinct experiments: One, a prototype ice experiment designed to study the gas-phase chemistry above the ice during photo and thermal processing; and the other a gas-phase spectroscopy study of propylene oxide. Understanding the pathways which can take place as a result of UV irradiation and heating of icy grains is the goal of the ice experiment. The motivation for our work on propylene oxide is to provide new mm/submm laboratory spectra to bolster observational efforts in the identification of propylene oxide in the interstellar medium. I present the details of both of these experiments in the following chapters.

Chapter 2 Rotational Spectroscopy of Gases Above Interstellar Ice Analogues

2.1 Introduction

Cold interstellar cores are composed primarily of hydrogen, with approximately 1% of the mass of the cloud existing in carbonaceous and silicate dust grains. Over a long enough time scale in the cold temperatures of interstellar clouds, adsorption of atomic species and simple molecules onto interstellar dust grains leads to hydrogenation reactions to form the molecules that will become the bulk of an interstellar ice [16], i.e.:

$$O + H \rightarrow OH + H \rightarrow H_2O \tag{2.1}$$

$$N + H \rightarrow NH + H \rightarrow NH_2 + H \rightarrow NH_3 \tag{2.2}$$

$$CO + H \rightarrow HCO + H \rightarrow CH_2CO + H \rightarrow CH_3O + H \rightarrow CH_3OH \tag{2.3}$$

Most of the information on the composition and structural features of interstellar ices have been collected by analyzing vibrational features characterized by infrared absorption observations. Water is the primary component of interstellar ices with varying concentrations of methanol, ammonia, and carbon monoxide ranging from 5-50% of the amount of water present [2].

The majority of radiative processing of interstellar ices as they rest in cold cores occurs as the result of Lyman-α and cosmic-ray induced vacuum ultra-violet (VUV) emission. Photons of this character can result in photolysis and photodesorption of the molecules which compose interstellar ices. Methanol photodissociation is given

as an example [17–20]:

$$\mathrm{CH_3OH} + h\nu \rightarrow \mathrm{CH_3} + \mathrm{OH} \tag{2.4a}$$

$$\rightarrow \mathrm{CH_3O} + \mathrm{H} \tag{2.4b}$$

$$\rightarrow \mathrm{CH_2OH} + \mathrm{H} \tag{2.4c}$$

$$\rightarrow \mathrm{CH_2} + \mathrm{H_2O} \tag{2.4d}$$

$$\rightarrow \mathrm{HCOH} + \mathrm{H_2} \tag{2.4e}$$

$$\rightarrow \mathrm{H_2CO} + \mathrm{H_2} \tag{2.4f}$$

$$\rightarrow \mathrm{CO} + 2\mathrm{H_2} \tag{2.4g}$$

Products of these types of photodissociation reactions can then react on the grain surface to form more complex species, or desorb into the gas-phase. Recent experiments done on methanol ices show that methanol does not photodesorb from icy grains intact in detectable quantities, but rather will fragment to many different species, the most abundant of which being CO [20]. Results from these experiments have large consequences on the astronomical models. Relatively large abundances of methanol have been detected in cold regions of space, abundances which do not agree with the result from these new laboratory studies. The production of gas-phase methanol from an icy grain, whether it be from primary photodesorption or a recombination of other desorbed species, is an excellent prospect of study for our experiment.

A complex organic molecule (COM) that is thought to be formed by a radical combination mechanism on the surface of an ice is glycine. The detection of glycine in the interstellar medium is controversial; however, it has been definitively detected in numerous carbonaceous chondrite meteorites [21–25] and comets [26], thus it is likely formed by some mechanism related to condensed-phase chemistry. Computational studies done in the past have shown a number of mechanisms from which glycine could form by icy grain chemistry, none of which have been experimentally confirmed

[27]. The experiment presented in this report will offer a method for studying the icy grain formation mechanism of glycine and a number of other important interstellar and cometary chemical processes.

To enable studies of prebiotic COMs, simple molecules have been focused on in the development of this experimental method: water, methanol, formaldehyde, and carbon monoxide. Most laboratory studies done on interstellar ices implement IR spectroscopy and mass spectrometry to analyze the chemistry occurring directly in or on the icy bulk [28, 29]. The new method presented here focuses on the significant amount of chemistry that can occur in the gas-phase over the surface of the ice as the bulk is thermally processed or photo-processed. This offers the added benefit of being able to detect desorbed products of surface reactions. The combination of these two techniques – ice chemical studies and rotational spectroscopy – brings a new approach to this field of study. Temperature information on the products of icy grain reactions can be analyzed to give insight into the reactions which produce them, and the data collected can be directly compared to radioastronomical observations of interstellar clouds and comets.

Herein I report on a novel experimental design and initial results from this experiment. Water and methanol have been used for the interstellar ice analogues in these initial studies. Formaldehyde has been detected as a room-temperature gas-phase photoproduct of methanol photolysis. Water has been observed in the gas-phase over an ice as a thermal desorption product as well as a photodesorption product. Likewise, carbon monoxide has been detected as a photolysis product from UV irradiation of a methanol ice.

2.2 Experimental

2.2.1 General Methods

The experiments set forth in this paper are carried out in a new experimental setup that is conceptually based on the CRYOPAD experiments conducted at the University of Leiden [28], combined with a millimeter and submillimeter spectrometer based on the designs previously implemented in our lab [30]. A schematic of this experiment is shown in Figure 2.1. A closed circuit compressed helium cryostat (APD Cryogenics Expander DE-202B assembly with a APD Cryogenics HC-2 compressor) is used to chill an inert gold plated stage which acts as a substrate for ice formation. Vapor is introduced to the substrate in a controlled manner through a sample line situated 3 cm above the chilled stage. Small doses are introduced into the vacuum chamber which is pumped with a Œrlikon Leybold TW 690 MS turbomolecular pump to a baseline pressure of 1×10^{-7} Torr, via a Matheson Model 4170 Series 316, needle valve to allow for controlled ice formation. By use of the needle valve a chamber pressure of 1×10^{-6} Torr was maintained during dosing. Less than a minute after closing the needle valve, the pressure in the chamber decreased back down to baseline as all of the sample vapor deposited onto the stage and cold head of the cryostat.

Ultra-pure water samples were produced from a Nanopure water filtration system. All experiments conducted on organic ices were performed with CH_3OH of purity 99.8% from Sigma-Aldrich. Both the water and methanol samples have been put through a freeze-pump-thaw process to remove excess gases.

All experiments are monitored by use of pure rotational direct absorption spectroscopy in the 150-750 GHz range. Microwave radiation is produced by an Agilent Technologies E8257D analog signal generator at frequencies of 22 to 46 GHz and passed through a Virginia Diodes S270 multiplier chain to generate harmonics and reach the desired mm/submm frequencies. The output radiation beam passes over

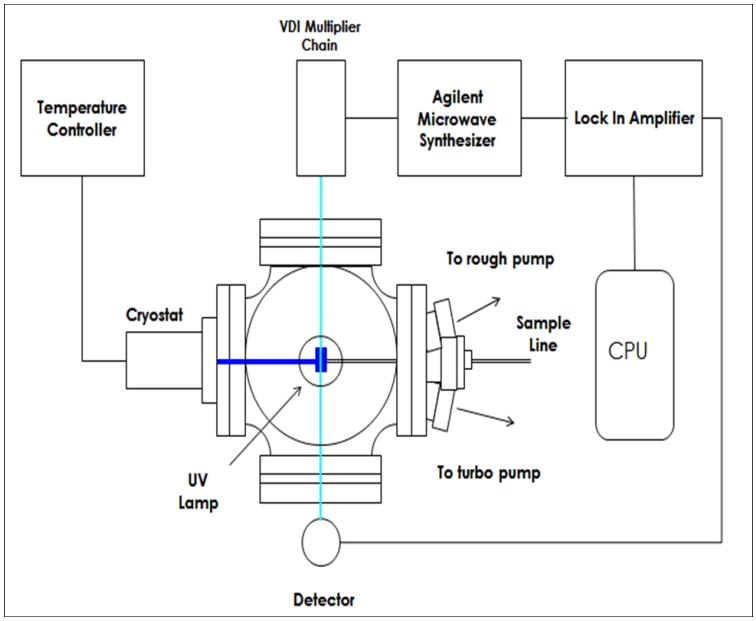

Figure 2.1: Experimental Schematic

the ice surface and is detected by one of two detectors. A Virginia Diodes zero bias detector (ZBD) is used for detection in experiments below 210 GHz, whereas a QMC QFI/XBI InSb hot electron bolometer is used as a detector in experiments with higher frequencies. The signal from the detector is passed into a lock-in amplifier that is referenced to the input radiation with a modulation frequency of 15 kHz. Second harmonic detection is utilized and the resulting 2f lineshapes can be modeled with a second derivative Gaussian function as seen in the results presented below. The spectral resolution is 100 kHz for all experiments.

For ice studies, two primary types of experiments have been conducted: Temperature Programmed Desorption (TPD) experiments and photo-processing experiments, both of which will be described in the sections below. These experiments are not mutually-exclusive, meaning that they can, if the situation requires, be conducted in tandem. A significant part of the experimental method is also shared by both techniques; those parts of the experiment were outlined above.

2.2.2 Temperature Programmed Desorption of Ices

They key to TPD experiments is strict control of the temperature of the ice by an autotuning temperature controller. The temperature is controlled by the joule heating of small resistors (Advanced Research Systems: HTR-TF-36-2) epoxied (Omega: OB-200-2) to the bottom of the sample stage (Advanced Research Systems: SHNO-1B flat plate sample holder). Voltages applied to the heaters are controlled by a Lakeshore Model 330 Autotuning Temperature Controller interfaced with a thermocouple (Omega engineering: WTE-6-24 Washer T/C Assembly striped ends) also mounted on the sample stage. Measurements in TPD experiments are taken after the system is equilibrated at the desired temperature. A slow heating rate of 2 K/min is used in experiments so as to not affect the structure of the ice with sudden powerful heating.

2.2.3 Photo-Processing of Ices

The photochemistry experiments performed utilize the 121 nm line of an Opthos Lyman-α microwave discharge lamp. The lamp is positioned 10 cm above the sample stage at an inclination of 15° from the normal. The UV flux density of the lamp at the 121nm line is approximately 2x10^{12} photons $s^{-1}cm^{-2}$ [31].

Photo-processing experiments have been done on gas-phase methanol as well as pure methanol and water ices. Gas-phase experiments were conducted in static cell conditions (i.e., without active vacuum pumping) with the mercury lamp lit at a forward power of 60 W and a reflected power of 2 W for 10 minutes. The mercury lamp emits at 184 nm and was used in this experiment because the Lyman-α was broken at the time of these experiments. Spectra were collected after the lamp was turned off. The ice experiments were conducted in both static and dynamic cells (i.e., without and with the pump, respectively) with the Lyman-α lamp continuously on at a similar power.

2.3 Results

2.3.1 Temperature Programmed Desorption

Initial experiments focused on proof-of-concept TPD experiments that could be compared to previously-reported literature results. A pure water ice was deposited on the sample stage at a temperature of 15 K. At these temperatures, vapor deposition leads to amorphous ices because the molecules freeze out without being able to reorganize themselves into a crystalline lattice. In this experiment, the thickness of the ice was not a controlled parameter. The TPD experiments, as shown in Figure 2.2, enabled the detection of the desorption of water beginning at 152 K, in good agreement with the literature [32].

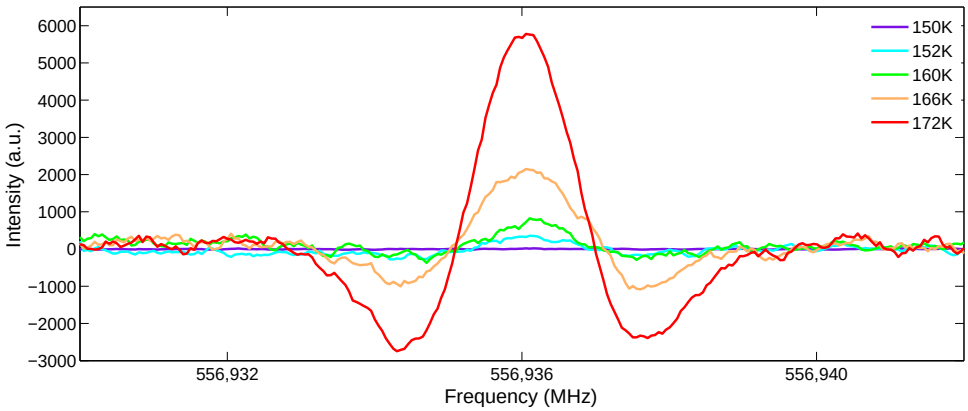

Figure 2.2: TPD experiment of pure water ice

The fits can be seen in the Appendix Figures A.1–A.7.

2.3.2 Room Temperature gas-phase photolysis of Methanol

In preparation for photolysis studies of pure methanol ices, room temperature photolysis experiments were conducted with gaseous methanol. Formaldehyde was detected as the primary product of the methanol photolysis at room temperature, as is shown in Figures 2.3 and 2.4.

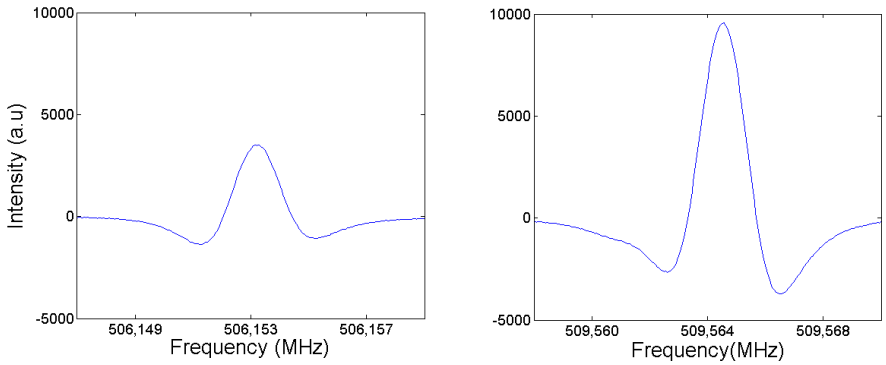

Figure 2.3: Room Temperature Methanol Detection

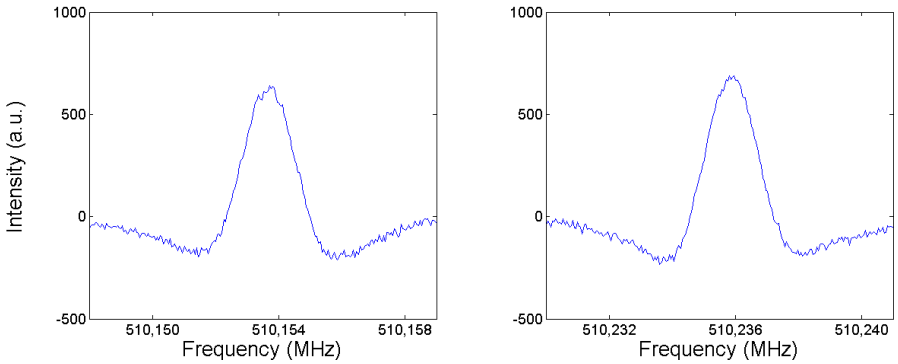

Figure 2.4: Room Temperature Formaldehyde Detection

2.3.3 Photodesorption of Water from an Ice Surface

Moving beyond the gas-phase studies, initial ice processing studies focused on pure water ice. A pure water ice was grown on the sample stage at 30 K by dosing gaseous water into a static chamber to a pressure of 10^{-5} Torr for one minute. Following the collection of a background spectrum, the Lyman-α lamp was lit at a forward power of 50 W and a reverse power of 3 W. The first scan took 17 minutes to collect due to a 6 s integration time, 2 s wait time, and a time constant of 1 s. The first scan revealed detection of the 557 GHz water signal. The lamp was then turned off and over a period of 45 minutes the signal returned to baseline. This is seen in Figure 2.5. The chamber pressure followed the same trend: as the lamp was on, the pressure increased to 10^{-5} Torr and dropped back to baseline after the lamp was powered down.

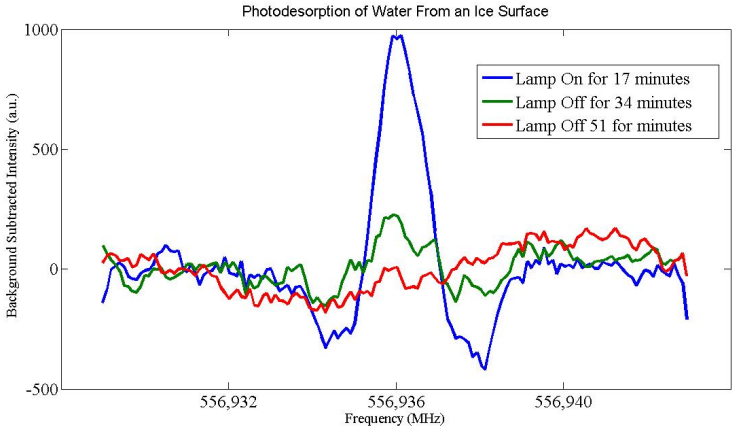

Figure 2.5: Water Photodesorption Signal

2.3.4 The Search for Methanol Photodesorption from an Ice Surface

The next logical step in the experiment was to observe photodesorption of a COM from an ice surface. Methanol was chosen as the obvious candidate since it is a large component of interstellar ices and it is readily available. After many months of testing, no lines were observed.

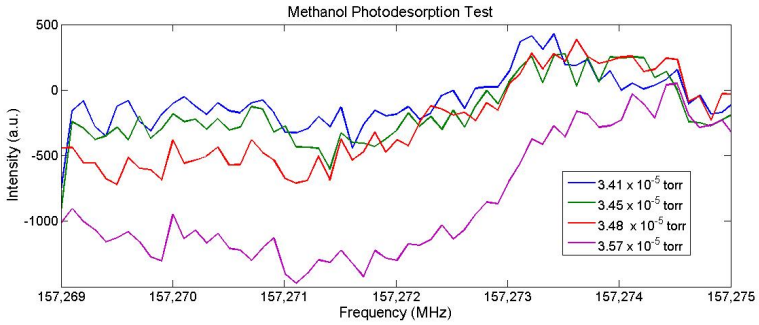

Figure 2.6: The irradiation of the sample in a dynamically pumping experiment caused an increase in the pressure but no molecular lines of methanol was observed: 157270.832 MHz, or 157272.338 MHz

Meanwhile, a paper published by Bertin et. al. demonstrated that methanol does not photodesorb from ice surfaces intact in detectable quantities. Rather, it photofragments into a number of small molecules, the most abundant being CO. [20] This was a surprising result given the high number densities of methanol observed in the gas-phase throughout the ISM. More work will need to be done to discover new

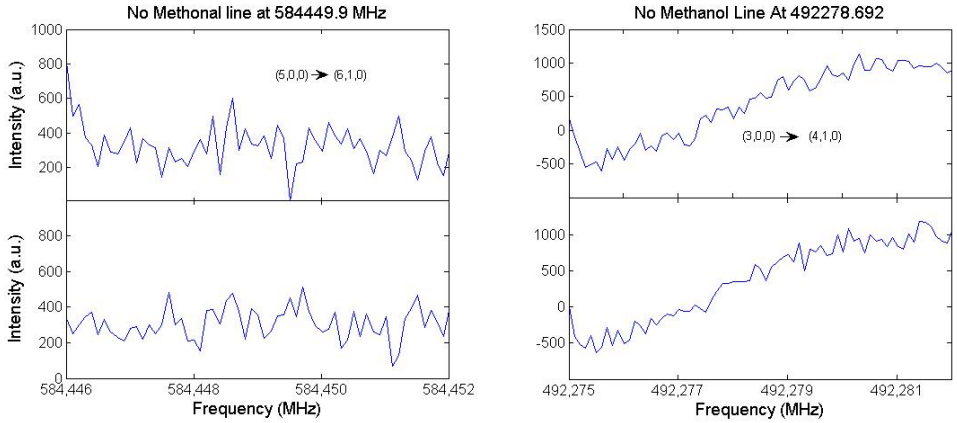

Figure 2.7: The irradiation of the sample in a static pumped cell experiment caused an increase in the pressure but no molecular lines of methanol was observed here either.

chemical mechanisms or find a better balance of the ones currently known to account for these observational results. However, this does explain the lack of methanol photodesorption we observed in our experiments.

2.3.5 Detection of Carbon Monoxide as the Result of Irradiation of Methanol Ice

Shifting focus based on the new information regarding methanol photolysis, a pure methanol ice was grown on the sample stage at 30 K with a chamber pressure of 3×10^{-7} Torr. Irradiation of the ice over multiple hours in a static cell did not produce detectable gas-phase CO. The first detection of CO was made after the cryostat was turned off. The temperature of the stage was unknown at the time of CO detection. Nonetheless, this result indicated that warming of the ice was necessary for CO desorption.

To quantify this, a TPD experiment was run on an irradiated pure methanol ice grown at 30 K. The ice was held at 30 K while it was irradiated for 1 hour with the Lyman-α lamp, after which the lamp was turned off and a traditional TPD experiment was performed. No CO signal was observed until the ice reached a temperature of 230 K. This is a much higher temperature than expected. Methanol was detectable

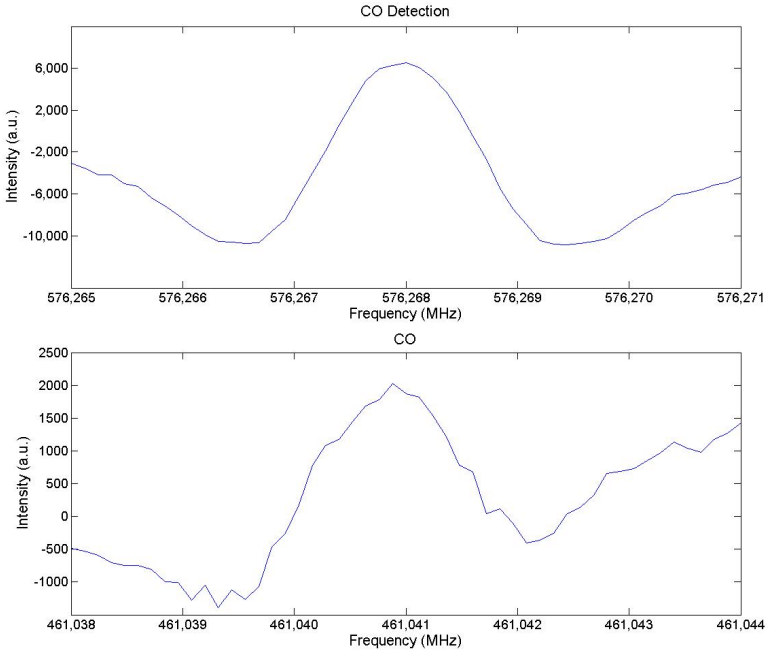

Figure 2.8: CO Molecular signal upon heating of the chamber after ice irradiation

first around 160 K and was still detectable at the point that CO was observed at 230 K.

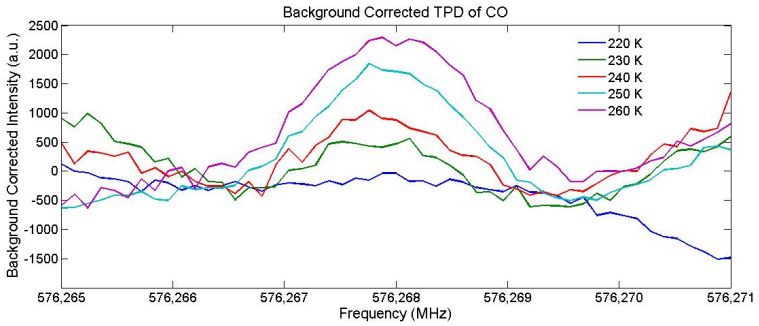

Figure 2.9: Temperature Programmed Desorption experiment of CO from a Methanol Ice

To study this system further, an experiment was conducted in which the TPD was run simultaneously with the UV irradiation. The ice was grown at replicate conditions to the previous experiment and the Lyman-α lamp was again used for irradiation. In contrast to the previous experiment in which CO was not detected until 230 K, the first CO signal was seen at 130 K with the simultaneous heating and irradiation of the ice (as seen in Figure 2.10). More interesting yet was that no CH_3OH signal was

observed until 160 K (Figure 2.11). The evolution of CO gas at a lower temperature than methanol is a particularly intriguing result and has large implications for the interstellar icy grain models, if it can be confirmed by further experimentation.

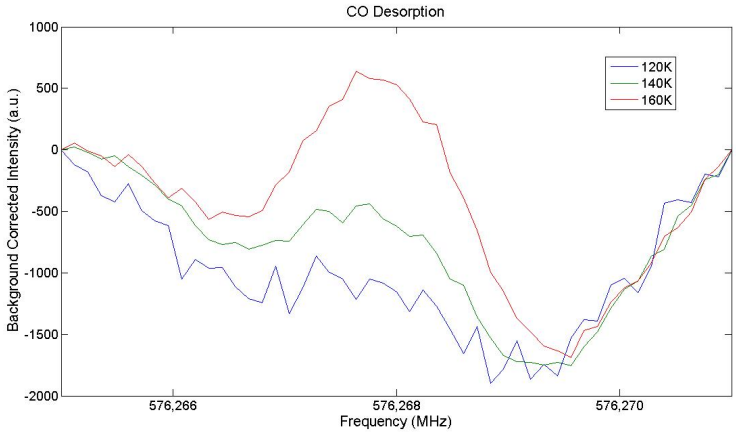

Figure 2.10: Evolution of gaseous carbon monoxide from an ice surface under simultaneous heating and irradiation

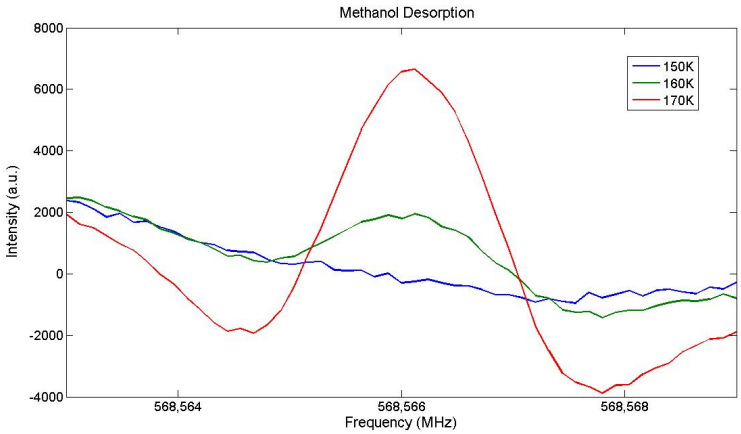

Figure 2.11: Evolution of gaseous methanol from an ice surface under simultaneous heating and irradiation

2.4 Proposed Future Work

A number of additions can be made to the experiment to help further understand the precise conditions to which the ices are being exposed.

To understand the chemistry of the ice and the gas above it, a good physical

understanding of the ice is desirable. The precise thickness of the ice can be measured by observing diffraction fringes produced as a visible laser passes through the ice or by use of IR spectroscopy. It is desirable to have ice thickness as a controlled property because it can have effects on the chemistry occuring in the icy bulk [33]. Two visible lasers of the same wavelength passing through the ice at different angles, or two lasers of different wavelengths passing through ice at the same angle can be used. In either of these techniques, the number of monolayers the beams pass through can be determined by observing the diffraction fringes produced. Alternately, IR spectroscopy is a well-established technique for measuring not only the physical properties of the ice, but also the chemical properties of the icy bulk [28, 29]. This makes addition of an IR spectrometer into the experimental setup the best option because it can be used to simultaneously measure the icy bulk chemical and physical properties in conjunction with what is happening in the gas above the surface of the ice. The conversion of a traditional FTIR instrument into an open-beam Reflection Absorption Infrared (RAIRS) spectrometer that can be utilized on our experiment is possible. In brief, a RAIRS setup passes an IR beam into the vacuum chamber at an angle so that the beam passes down through the ice, reflects off the gold-plated sample stage, passes up through the ice, and then out of the chamber where the absorbance can be detected. This setup could be implemented with the current vacuum chamber by using flanges that have multiple ports for windows that could be the entry point for the IR beam, but it is an in-depth setup that will take time to implement. In lieu of the addition of an FTIR and due to the constraints of the chamber, using the two-wavelength laser method would be a practical way of determining the physical characteristics of the ice.

Real time analysis of the UV flux produced by our Lyman-α discharge lamp via the photoelectric effect would also be an excellent addition to the experiment. The photoelectric effect is a phenomenon that is used in multiple types of common spec-

troscopic detectors including photomultiplier tubes. Incoming radiation, if energetic enough, is capable of ejecting electrons from an anode. The number of photoelectrons ejected is directly related to the number of incident photons. By using a thin gold wire as an anode, it would be possible to observe the photoelectric effect by measuring the resulting current as electrons are ejected from the gold wire and collected on a surrounding collector plate. The current would be directly proportional to the flux of the UV lamp. This would help quantify the efficiency of photodesorption and photolysis in these experiments.

One final addition to the experiment would be the purchase of additional multipliers to extend the working frequency range of the spectrometer to 1.4 THz. This would allow for the observation of the OH radical. The OH radical may play a large part in the chemistry of interstellar ices. Water is the primary component of interstellar ices and OH is produced as water ice is exposed to UV radiation. Observing and quantifying the amount of OH being produced and reacting with other species from mixed water/organic ices would be an interesting area of study for future experiments and would greatly contribute to the interstellar models.

2.5 Conclusion

The results collected from the experiment thus far have been promising, but there is much room for improvement. The temperature programmed desorption data from pure H_2O ice has been found to be in good agreement with the literature. The detection of photodesorbed water from a water ice surface provided proof of concept for this new technique. A significant amount of time and resources were put into the detection of methanol photodesorption, something that the literature has now shown to be an exceptionally difficult detection to make, but it has lead us to our study of CO desorption. The temperatures at which CO have been detected in TPD/irradiation experiments need further study, but have the potential to be significant in under-

standing the composition on interstellar ices in the ISM.

Chapter 3 The Millimeter/Submillimeter Spectrum of Propylene Oxide

3.1 Introduction

One of the most curious and elegant phenomena of molecular biology is nature's selection of specific enantiomers of chiral molecules, molecules that are non-superimposable mirror images of one another. For life on Earth to exist as it does today, it was a necessity for the biochemical makeup of organisms to develop homochirality, or chiral homogeniety [34]. One example is amino acids, the building blocks of proteins. The amino acids we know to exist in living organisms are of the L-type enantiomer, though the R-type enantiomer is of equal physical properties [35]. Several mechanisms have been proposed to elucidate the propagation and amplification of homochirality, usually by assuming a low initial enantiomeric excess (e.e.) [36, 37]. The particularly quizzical problem is how an e.e. comes to exist out of nature when chiral enantiomers share all the same chemical properties. Biochemists believe this process to have occurred from a racemic mixture of chiral molecules in a system of such complexity as an early Earth [36]; however, studies of chiral molecules in meteorites have shown an e.e. to exist in the Murchison meteorite [38]. A number of laboratory studies have shown that it is possible to amplify an e.e. in solution by exposure to circularly polarized light [39, 40]. While it is possible that chemistry occurring on these meteorites could have potentially created an e.e. , it is also possible that the excess was created in the birth place of both meteorites and Earth: interstellar molecular clouds. If an e.e. could be formed in a molecular cloud, it could be inherited and amplified by its descendants, meteorites, comets, and planets alike. Studying chiral molecules in molecular clouds can give great insight into the origin of

homochirality.

In 2016, propylene oxide (CH_3CHCH_2O) became the first chiral molecule detected in the interstellar medium by McGuire and Carroll et al. [15]. Three lines matching with previous laboratory spectroscopy [41] were detected at 12.1 GHz, 12.8 GHz, and 14.0 GHz towards Sagittarius B2(N) [15]. Propylene oxide consists of an oxygen-containing three membered ring with a methyl group extending from one of the carbons, thus making it chiral and subject to an internal rotation under a three-fold barrier arising from the C_3 symmetry of the methyl group [41]. The tunneling through this barrier produces splitting of each rotational state into an A state and doubly-degenerate E states. The magnitude of this splitting is dependent on the energy of the rotational state, the torsional state of the molecule, and the barrier height [42]. The first microwave work on propylene oxide was conducted by Swalen and Herschbach [41]. They measured the spectrum up to 38 GHz. The barrier height was determined to be 895 cm^{-1} for the ground torsional state. Isotopic substitution studies were done with ^{13}C [43] and deuterium [44] to further understand the structure of the molecule in the ground torsional state; these analyses did not consider the internal rotation. Infrared absorption [45–48] and Raman studies [49] have been done to further study the structure and internal barrier. A large area of focus in the previous studies of propylene oxide revolve around enantiomeric distinction by circular dichroism. Electronic circular dichroism has been investigated via experiment [50–53] and theory [54], and vibrational circular dichroism has also been investigated by experiment [55–57] and theory [58].

Extrapolated spectral predictions extending into the mm/submm frequency range are available for propylene oxide based on microwave spectra measured up to 110 GHz [59]. However, in the context of observational astronomy, confirmed line centers with an accuracy better than 1 MHz are crucial. Thus the major goal of the work presented here is to assist in the search for propylene oxide in the interstellar medium in order

to untangle the mystery of the origin of homochirality. Another major goal is to improve upon the molecular constants and better understand the high barrier to internal rotation that the methyl rotor experiences.

Here I present the room temperature mm/submm spectrum of propylene oxide taken from 70 GHz to 1 THz. The SPFIT program of the CALPGM package [60] was used for the analysis of the A state transitions using an asymmetric top Hamiltonian with centrifugal distortion. The internal rotation of the methyl group was then treated using the XIAM program [61]. The combination of these two analyses has resulted in a fit with improved precision of the molecular constants over those in previous studies. Here we report the results of the laboratory work and associated spectral analysis, and provide a spectral line catalog for propylene oxide that extends to 1 THz. This extended catalog will enable more observational studies of propylene oxide in a variety of astronomical sources.

3.2 Experimental

All spectroscopy presented in this section was conducted in a 2.1 m single-pass direct-absorption flow cell at room temperature. Additional details of this spectrometer can be found in a previous study [62]. The propylene oxide was purchased from Acros Organics at a purity of 99%, and used without further purification. The ends of the flow cell were sealed by teflon lenses ($f = 100$ mm). The cell was evacuated by an Edwards 30 Two Stage rotary vane pump. Ultra high purity Ar from Nexair was bubbled through a liquid sample of propylene oxide, and the resultant vapor was directed into the cell. The pressure in the cell was maintained at 50 mTorr throughout the experiments by controlling the flow with the entry valve.

Propylene oxide spectra were collected from 70 GHz to 1 THz. The input microwave signal was generated by an Agilent Technologies E8257D analog signal generator with an internal frequency modulation at 75 kHz. The microwave signal was

multiplied up to the desired frequency range by a Virginia Diodes S270 multiplier chain. A number of detectors were also used in these experiments depending on the specific frequency window. Virginia Diodes Zero Bias detectors (WR10, WR8, WR5.1, WR3.4) were used for the 70 GHz – 110 GHz, 110 GHz – 140 GHz, 140 GHz – 225 GHz, and 225 GHz – 325 GHz frequency windows, respectively. For all frequencies above 325 GHz, a QMC QFI/XBI InSb hot electron bolometer was used for detection. Regardless of the specific detector, the output signal was passed to a Stanford Research Systems model SR830 lock-in amplifier for 2f detection. The intensity output at each frequency point was collected via a digitizer card using a custom computer scanning routine.

Unique scan settings were used for each band. Due to the nature of the lock-in detection scheme, scans must be conducted point-by-point, thus the step size limits the acquisition time. A trade-off comes in the form of spectral resolution versus scanning time. A step size of 50 kHz was used in Band 3 (70 GHz – 110 GHz), 40 kHz in Band 4 (110 GHz – 140 GHz), 60 kHz in Band 5 (140 GHz – 225 GHz), 100 kHz in Band 6 (225 GHz – 325 GHz), 120 kHz in Band 7 (325 GHz – 445 GHz), and 135 kHz for Band 8a (445 GHz – 700 GHz) and Band 9 (700 GHz – 1 THz). For the shorter frequency windows, multiple averages were possible, but for larger windows it was impractical to take more than one average. The spectrum in Band 3 was averaged 4 times, Band 4 had only a single scan, Band 5 and Band 6 were averaged 2 times, and a single scan was taken for Band 7, Band 8a, and Band 9.

3.3 Results and Discussion

Spectra collected from 70 GHz to 1 THz can be seen in Figures 3.1 – 3.7. The line density is large; for example, there is one line per 8 MHz observed in the Band 6 spectrum. Based on the average line densities for different bands, a conservative estimate of about 15,000 lines were observed between 70 GHz and 1 THz. In the

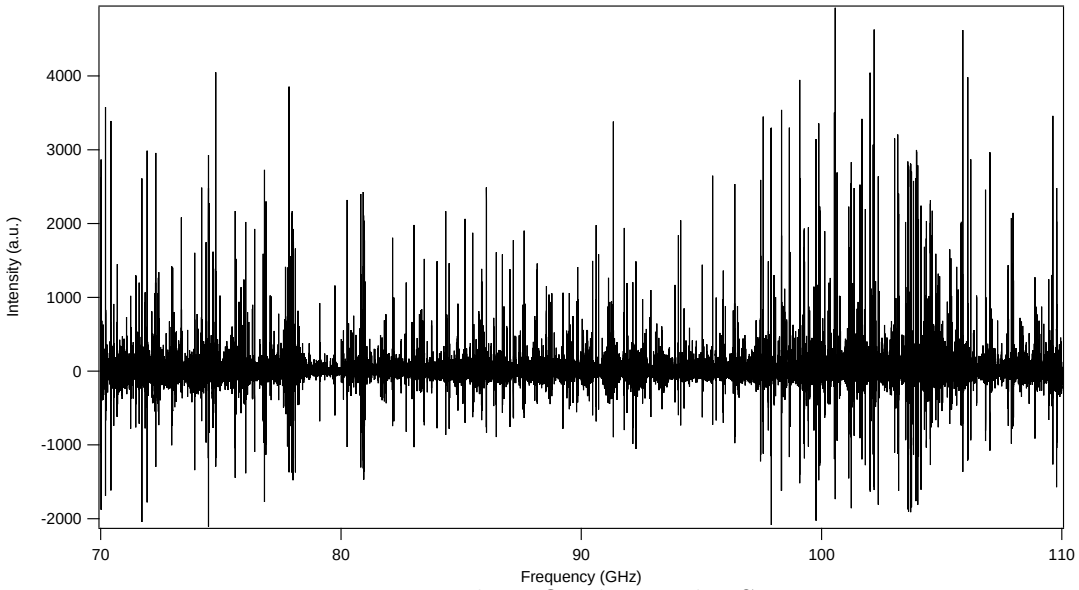

Figure 3.1: Propylene Oxide Band 3 Spectrum

spectra, the strongest lines arise from R branches. A number of Q branches can also be seen buried in the forest of lines.

The average linewidth of the Band 6 (230 GHz – 320 GHz) lines is about 700 kHz. The Doppler linewidth increases moving up in frequency, ranging from 300 kHz in Band 3 (70 GHz – 110 GHz) up to 2.3 MHz near 1 THz. The signal-to-noise-ratio (SNR) also changed significantly band to band. A SNR of 500 was calculated for the strongest line around 100 GHz after 4 averages, whereas a SNR of about 5,000 was calculated for the strongest line around 900 GHz at a single average. This difference is primarily attributed to the use of the hot electron bolometer detector for higher frequency scans. The SNR was greatest at about 10,000 for the line at 336.027 GHz after a single average.

The assignment of the spectra was done using predictions generated by the SPFIT/SPCAT program suite [60] using an asymmetric top Hamiltonian with a Watson A reduction. Visualization of the prediction overlaid on the experimental spectrum was done with the Sub-Millimeter Analysis Program (SMAP) (available at [63]). An A state fit generated from the work of Enye [59] in the microwave region provided an

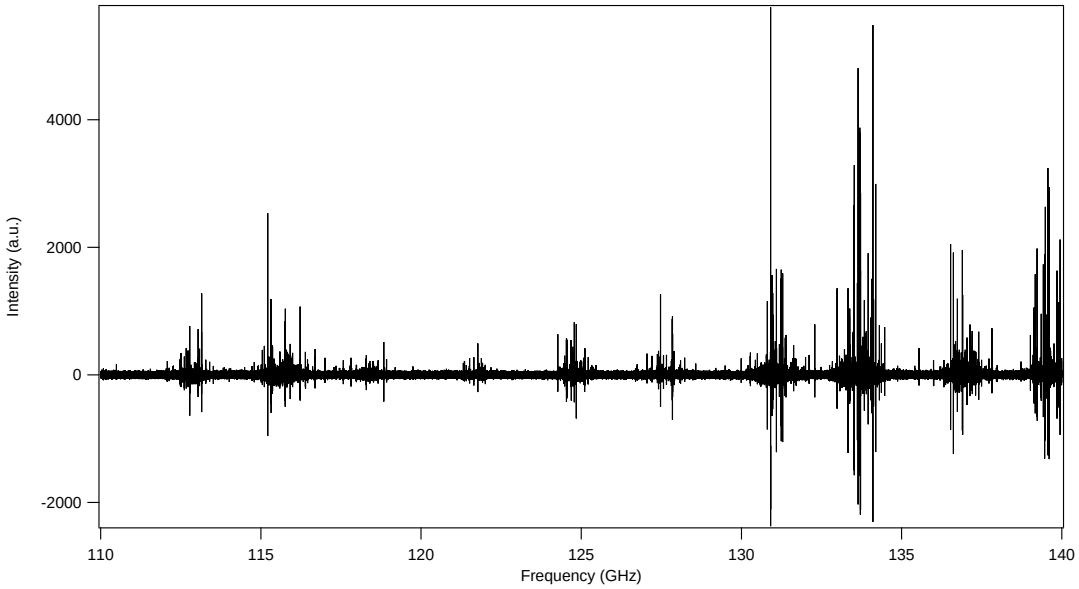

Figure 3.2: Propylene Oxide Band 4 Spectrum

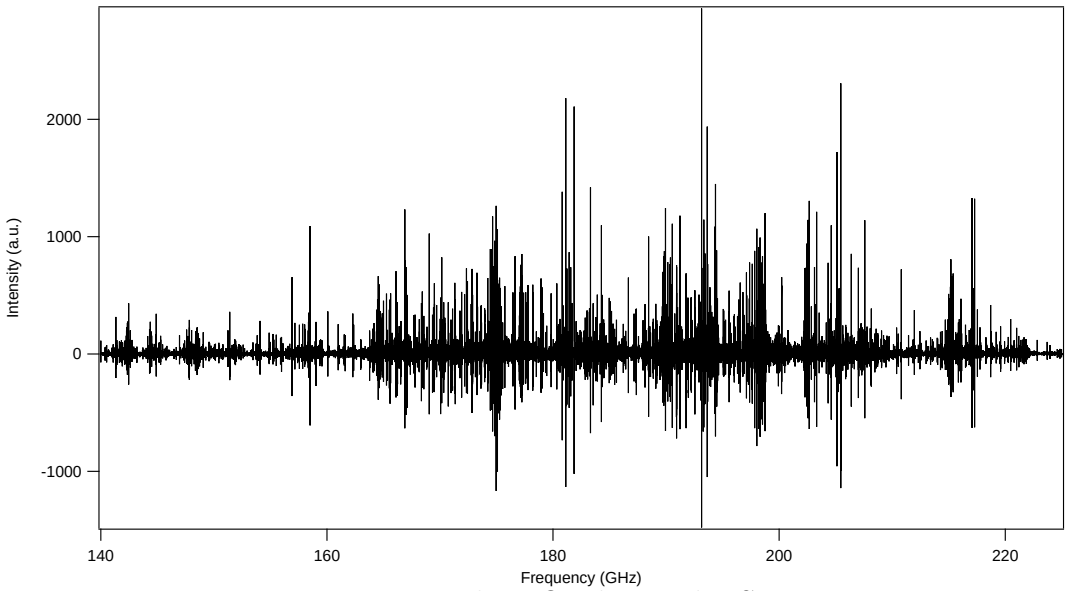

Figure 3.3: Propylene Oxide Band 5 Spectrum

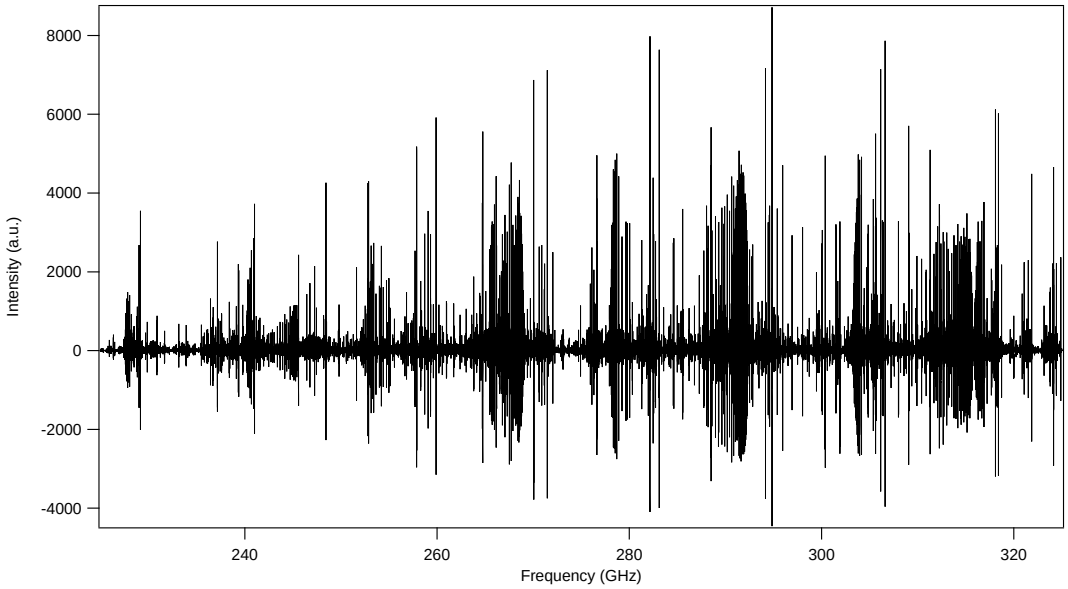

Figure 3.4: Propylene Oxide Band 6 Spectrum

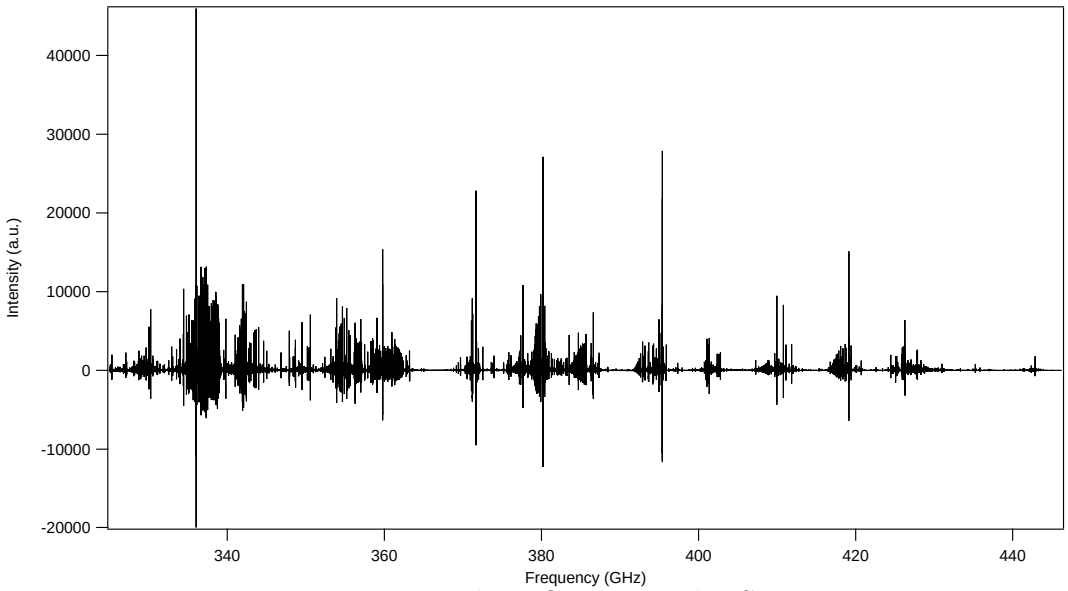

Figure 3.5: Propylene Oxide Band 7 Spectrum

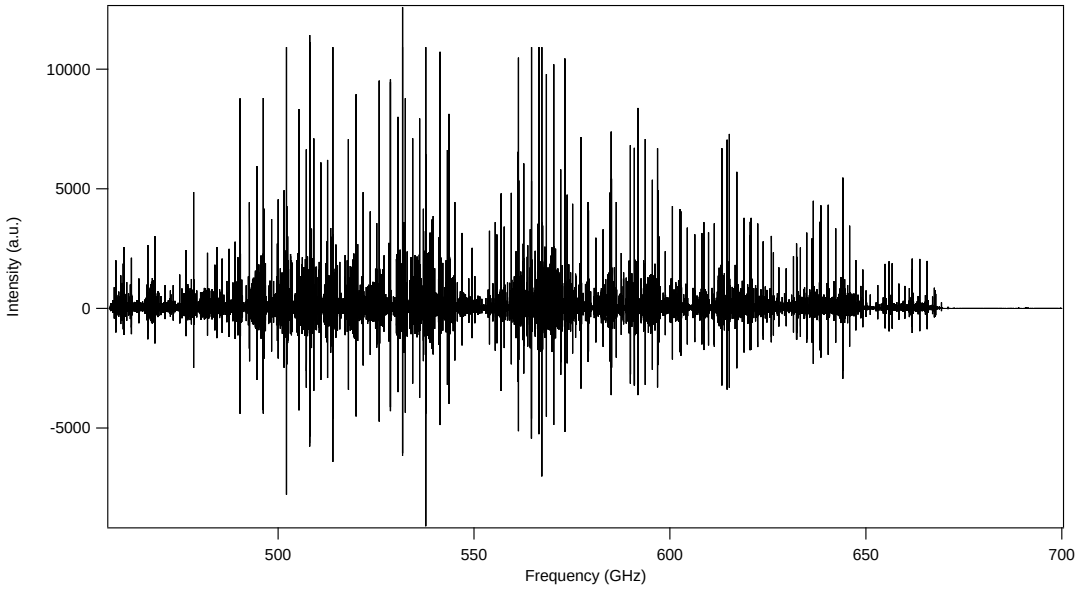

Figure 3.6: Propylene Oxide Band 8 Spectrum

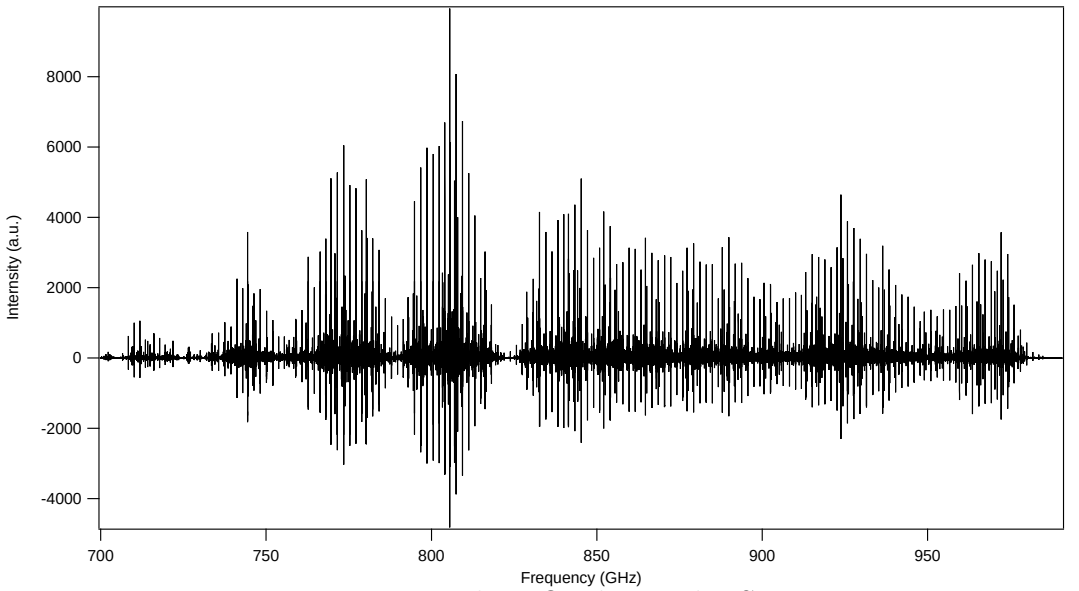

Figure 3.7: Propylene Oxide Band 9 Spectrum

insightful starting point for our assignment. The full A state assignment was achieved by iterative regeneration of SPFIT/SPCAT predictions using new assignments from incremental frequency bands. The final fit included 1152 A state lines in the ground torsional state yielding an RMS of 94 kHz; however, at higher $\tau = (K_a - K_c)$ values the fit began to diverge because of the greater effect of the internal motion splitting. The A state fit generated in SPFIT was invaluable in assigning the E states for the subsequent internal motion analysis in XIAM.

The A/E splitting was observed up to 300 GHz, at which point the A/E lines became blended together due to Doppler broadening. The magnitude of the splitting is on the order of hundreds of kHz to just over 1 MHz, depending on the specific transitions observed. One of the most revealing features of the splitting is shown in Figure 3.8. The resolved A/E splitting exhibited trends over a series of transitions of a given K_a as a function of J. These trends were useful in the assignment of A/E splittings in dense regions of the spectra. Additionally, similar trends were seen in the spectra analyzed by Swalen and Herschbach in which they demonstrated that propylene oxide ought be treated as a high barrier case [64]. Though some splittings of significantly greater magnitude were observed, which is indicative of higher torsional states, only the ground torsional state is analyzed here due to the line confusion of these higher energy vibrational states.

To fit the E states and quantify the barrier to internal rotation, the program XIAM [61] was used for the remainder of the analysis. XIAM uses a modified internal axes method [65] in which the Hamiltonian matrix is set up in the principal axis system, while the internal rotation operator is set up in an internal axis system. The resulting eigenvalues from the internal rotation operator are then transformed into the principal axis system and combined with the rest of the Hamiltonian matrix for the final result. The final fit includes the 17 parameters listed in Table 1. Given that the assignments went up to $J = 70$, sextic distortion constants were included. The internal rotational

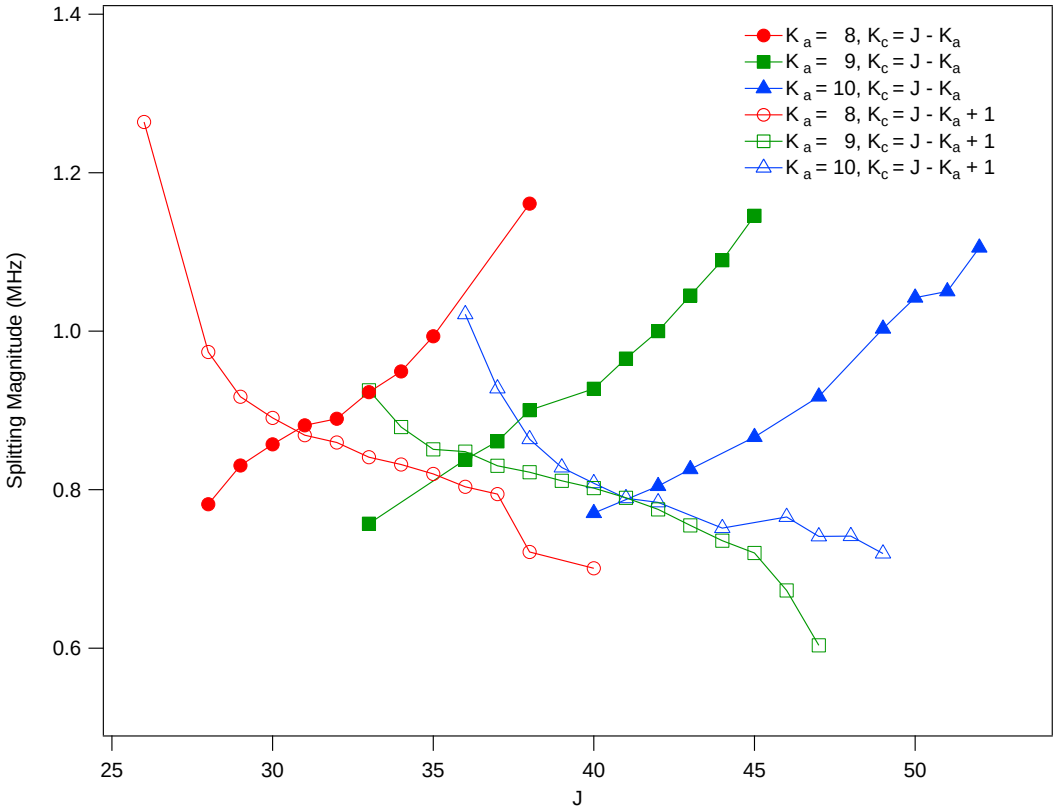

Figure 3.8: Splitting Magnitude vs J for $K_a = 8, 9, 10$. Two clear trends can be observed for each of two separate branches within each K_a level.

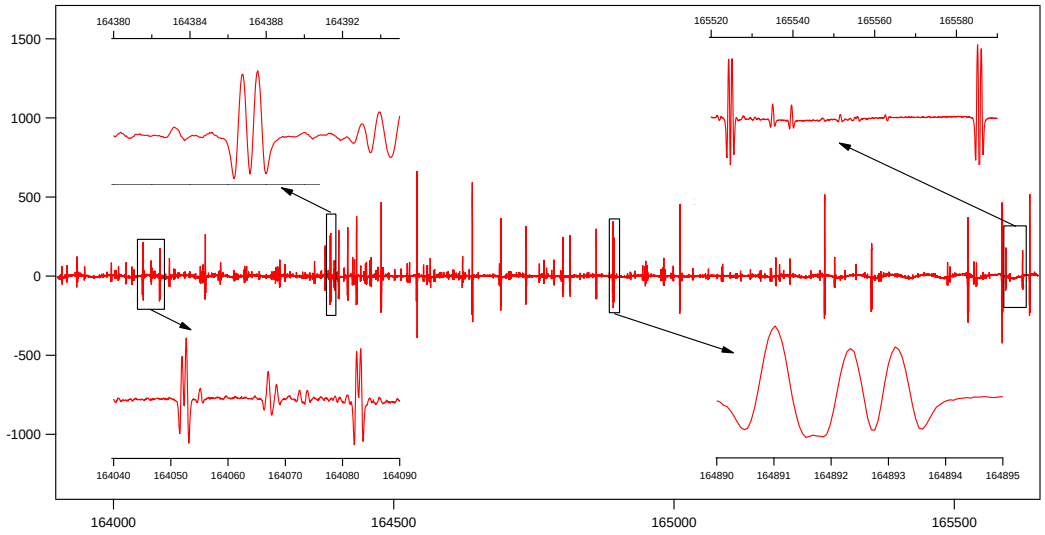

Figure 3.9: A/E Splitting in Band 5. Upper Left: $37_{8,30} \leftarrow 37_{7,31}$, Lower Left 2 sets of A/E Splits: lower frequency: $38_{8,31} \leftarrow 38_{7,32}$ and higher frequency $40_{8,33} \leftarrow 40_{7,34}$, Upper Right 2 sets of A/E splits: lower frequency: $35_{8,28} \leftarrow 35_{7,29}$ and higher frequency: $32_{8,24} \leftarrow 32_{7,25}$, Lower Right: $36_{8,29} \leftarrow 36_{7,30}$.

part of the Hamiltonian is defined as

$$V(\alpha) = F(p_\alpha - \rho P_r)^2 + \frac{1}{2}V_3(1 - \cos 3\alpha) + \frac{1}{2}V_6(1 - \cos 6\alpha) \tag{3.1}$$

where P_r is the angular momentum vector along the ρ axis (defined to be the axis of greatest symmetry for the internal rotor) and F is the rotational constant of the torsional motion. The value of F_o for the final fit was held constant at 157.7631, a reasonable value for a methyl top. Propylene oxide appears to be in the limit where the V_6 term does not contribute significantly to the internal rotation barrier, an assumption which was used in previous studies as well [41]. Analysis including the V_6 term was done, but this did not improve the quality of the fit and was therefore ultimately not included in the final analysis. The final term used in the fit, δ, is the angle between the internal motion axis and the principle axis of the molecule. The fits generated for the A state by SPFIT and the barrier published by Herschbach and Swalen [64] were used as a starting point for this analysis.

The ground torsional state fit, under the $V_6 = 0$ assumption, included 1252 line

Table 3.1: Comparison of key constants from our study and previous work

Parameter	Swalen and Herschbach[64]	This Work	Unit
A	18023.72 (10)	18027.271 (51)	MHz
B	6682.12 (10)	6678.736 (50)	MHz
C	5951.48 (10)	5951.3816 (13)	MHz
D_J	2.97 (50)	14.7073(19)	kHz
D_{JK}	4.2 (2.0)	-31.9081(53)	kHz
D_K	19.50 (50)	19.7306(35)	kHz
d_j	—	5.70622(89)	kHz
d_k	—	-10.3404(18)	kHz
H_J	—	0.0355(16)	Hz
H_{JK}	—	-0.1644(82)	Hz
H_{KJ}	—	0.216(11)	Hz
H_K	—	-0.0851(48)	Hz
h_j	—	0.01672(79)	Hz
h_{jk}	—	-0.0677(34)	Hz
h_k	—	0.0430(25)	Hz
F_o	—	157.7631(00)	GHz
V_T	895(5)	881(5)	cm^{-1}
δ	—	1.076(18)	radians

assignments from 100 GHz to 1 THz and converged with a RMS of 110 kHz. This RMS is a reasonable value, as it is below the spectral resolution, and hence the frequency uncertainty, for the lines measured in the higher frequency bands. All of the lines included in this fit are lines that have not been measured in any previous studies. The A/E splitting included assignments up to $J = 52$ and to a frequency of 300 GHz, after which point separate A and E state assignments became difficult due to broadened lineshapes and line confusion. For the blended transitions at higher frequencies, where the A and E state lines could not be distinguished, the full set of A and E state components for a given set of lines were assigned to the same frequency.

The results of the analysis can be found in Table 3.1. The inclusion of additional centrifugal distortion constants changed the A and B rotational constants from the values reported by Herschbach and Swalen [64]. The quartic centrifugal distortion constants from the current work are 2-3 orders of magnitude higher precision than those previously reported. We are the first to determine the sextic centrifugal distor-

tion constants for this molecule. The barrier to internal rotation was determined to be 881 cm^{-1}, 14 cm^{-1} lower than the original value calculated by Swalen and Herschbach, and within their published uncertainty. Overall, this fit is in good agreement with the results reported by Swalen and Herschbach, and offers an improvement in determination of the centrifugal distortion parameters.

In relation to astronomical observations, a plethora of lines have been detected in this study that can be used as targets for interstellar searches for propylene oxide, specifically searches that target star-forming regions. With the extension of the assignment up to 1 THz we open up a large spectral range that can now be probed with far-infrared telescopes. These powerful observational tools have the potential to give us much insight into the formation of chiral molecules in the interstellar medium.

3.4 Conclusion

We have presented the spectrum of propylene oxide from 70 GHz to 1 THz. The resultant spectral fit defines the ground torsional state of the molecule well, producing accurate line centers up to 1 THz and $J < 70$, and has improved on previous values of molecular constants. With our analysis of the A/E splitting we have calculated that the methyl group experiences a barrier to internal rotation of 881 cm^{-1}. It is our hope that with the spectra presented in this paper astronomical studies can progress in the search for propylene oxide in key regions of the interstellar medium.

Appendix A Ice Experiment

This appendix contains additional information pertaining to the results obtained in the experiments outlined in Chapters 2 and 3.

A.1 Temperature Programmed Desorption of Pure H_2O Ices

The following spectra (Figures A.1–A.7) show the scans taken at each temperature that were used to construct the plot shown in Figure 2.2.

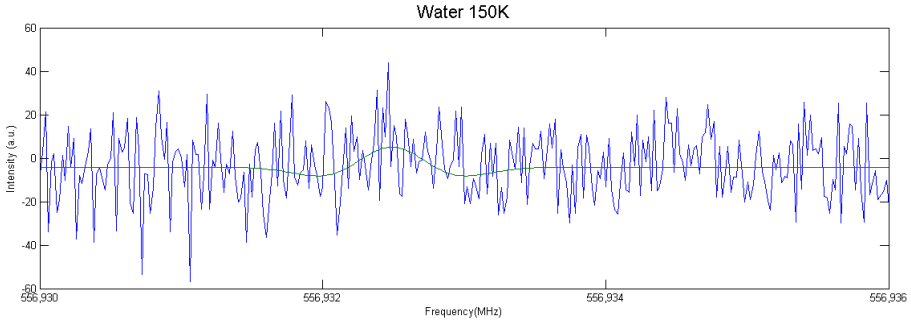

Figure A.1: H_2O TPD 150 K

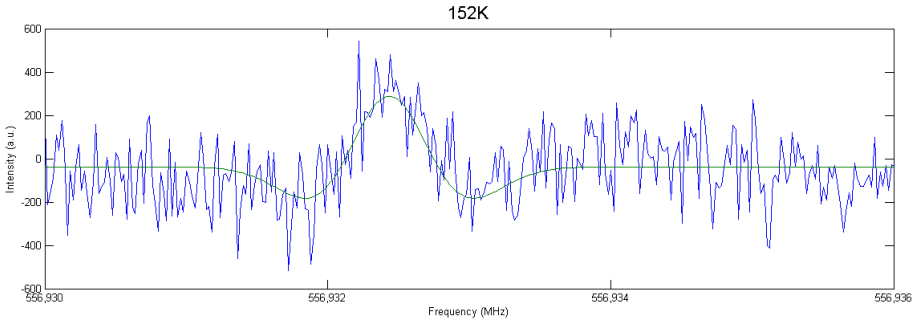

Figure A.2: H_2O TPD 152 K

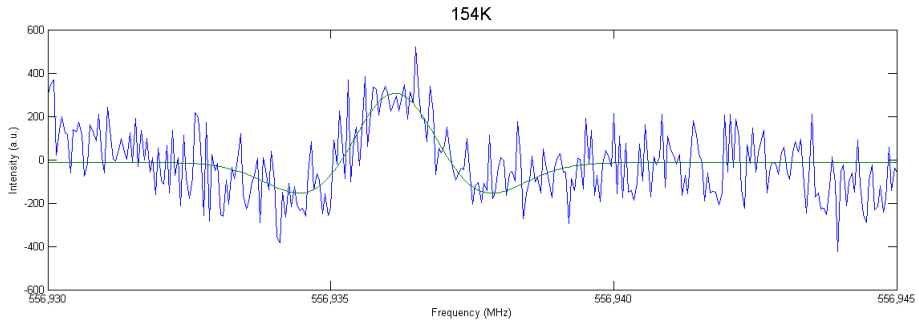

Figure A.3: H_2O TPD 154 K

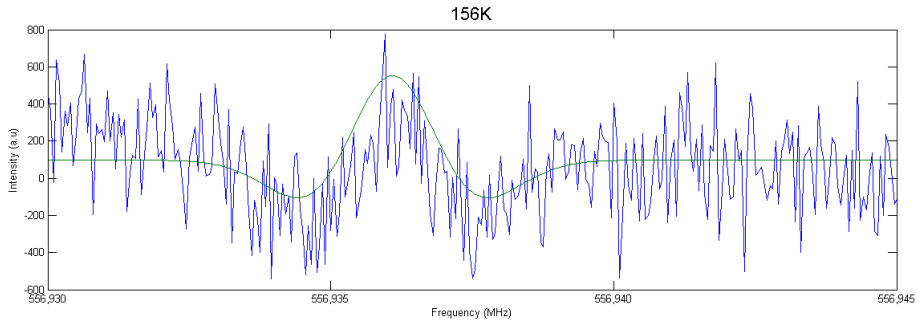

Figure A.4: H_2O TPD 156 K

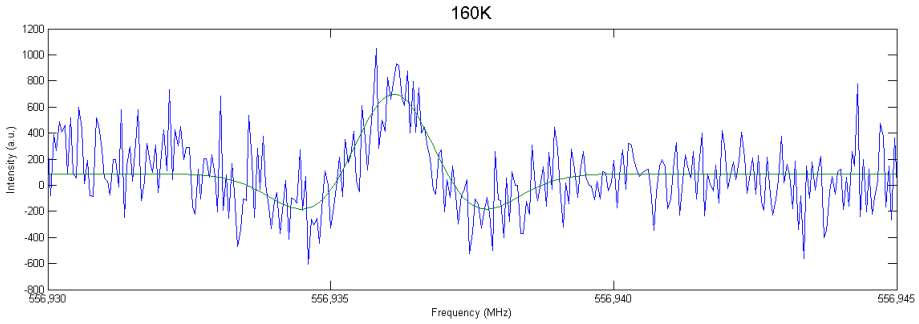

Figure A.5: H_2O TPD 160 K

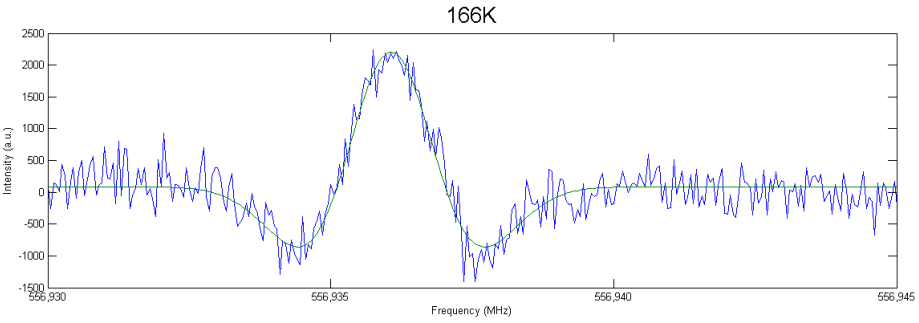

Figure A.6: H_2O TPD 166 K

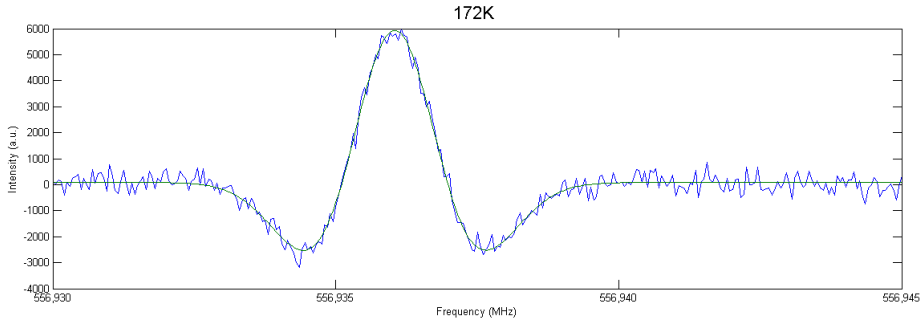

Figure A.7: H_2O TPD 172 K

Fits generated by taking the second derivative of a Gaussian lineshape:

$$f(x) = \frac{ae^{-\frac{(b-x)^2}{2c^2}}(b^2 - 2bx - c^2 + x^2)}{c^4} \tag{A.1}$$

where f(x) models the intensity at a frequency x, a and c are fitting parameters relating to the peak height and width respectively, and b is the parameter for the peak center. The table below provides the fitting parameters for the above data where b = 556936 MHz.

Table A.1: Fit Data for H_2O TPD

Temperature (K)	a (95% Conf. bounds)	c (95% Conf. bounds)
150	-5.27 (-13.36, 2.822)	0.7583 (0.3984, 1.118)
152	-241.6 (-335.4, -147.7)	0.8616 (0.75757, 0.9657)
154	-307.4 (-412.3, -202.5)	0.9815 (0.8766, 1.086)
156	-432.9 (-628.9, -237)	0.9769 (0.8384, 1.115)
160	-541.5 (-710.1, -372.9)	0.9436(0.8517, 1.035)
166	-1929(-2139, -1720)	0.9548(0.9224, 0.9872)
172	-5066(-5281,-4852)	0.9309(0.9186, 0.9432)

The integrated intensity is given by:

$$\int_{-\infty}^{\infty} ae^{-\frac{(x-b)^2}{2c^2}}\,dx = ac\sqrt{2\pi} \tag{A.2}$$

where the parameters a, b, and c are the same parameters used in the fits. The fitting parameters can thereby be directly used to calculate an integrated intensity. The results for this analysis are given in Table A.2.

Table A.2: Integrated Intensities for H_2O TPD

Temperature (K)	Integrated Intensity (95% Conf. Interval)
150	10.019 (16.0995)
152	521.69 (212.22)
154	756.20 (270.42)
156	1060.1 (502.82)
160	1280.8 (417.85)
166	4617.5 (525.38)
172	11823 (524.39)

A.2 Methanol Photolysis

The individual spectra taken for each H_2CO and CH_3OH line is shown in Figures A.8 and A.9.

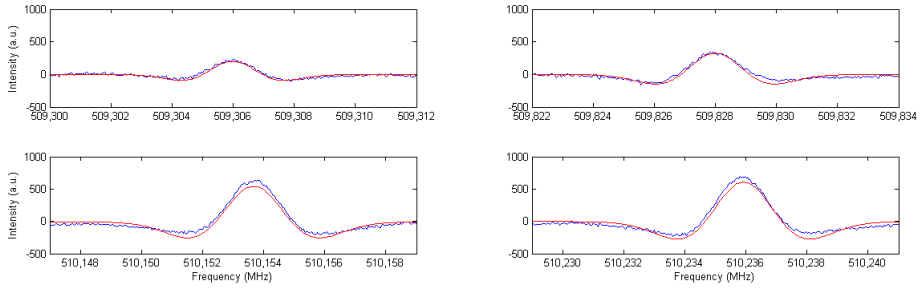

Figure A.8: H_2CO Data With Fits

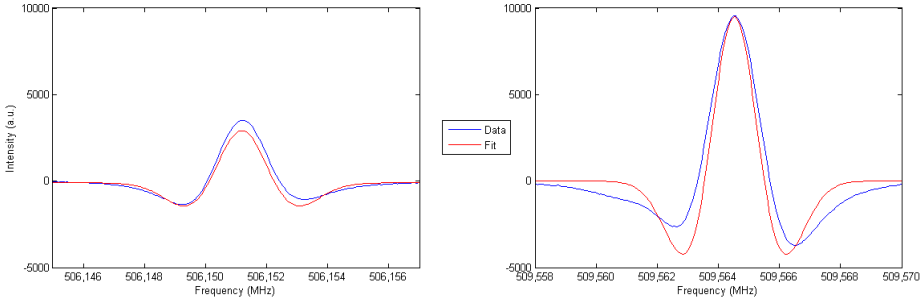

Figure A.9: CH_3OH Data With Fits

As in the previous section the data is fit with the second derivative of a Gaussian lineshape. The fitting parameters are outlined in the tables below where b will be the frequency.

Table A.3: Fit Data for H_2CO produced from CH_3OH photolysis

Frequency (MHz)	a (95% Conf. bounds)	c (95% Conf. bounds)
509306	-188.5 (–206.9,-170.2)	0.9683 (0.9383, 0.9982)
509830	-410.3 (-443.9, -376.7)	1.122 (1.093, 1.152)
510155.7	-860.5 (-930.1, -791)	1.25 (1.217, 1.282)
510237.9	-965.3 (-1041, -889.5))	1.26 (1.228, 1.292)

Table A.4: Fit Data for CH_3OH during CH_3OH photolysis

Frequency (MHz)	a (95% Conf. bounds)	c (95% Conf. bounds)
506153.3	-3590 (-3895, -3285)	1.093 (1.063, 1.122)
509564.6	-9110 (-10020, -8202)	0.9796 (0.9486, 1.011)

Appendix B Propylene Oxide Experiment

B.1 Propylene Oxide Spectral Fitting using only V_3 barrier

This output files from the XIAM fitting program for propylene oxide presents the fitting setting, the fit parameters, the correlation matrix, the cofreedom matix, and the eigenvalue/eigenvector matix.

```
 Rotational, Centrifugal Distortion, Internal Rotation Calculation (V2.5e)
                     Holger Hartwig 08-Nov-96 (hartwig@phc.uni-kiel.de)

 Please cite: H.Hartwig and H.Dreizler, Z.Naturforsch, 51a (1996) 923.

 Calculation date and time:  Type help now for the list of parameters :
-Propylene Oxide: AJ Mesko; Prediction Attempt 1

   nzyk       100   print        4   eval         0   dfreq        0
   orger        0   ints         0   maxm         8   woods       33
   ndata        0   nfold        3   spin         0   ntop         1
   adjf         0   maxvm        0   aprint      75   xprint      20
   ncycl      100   svderr       0   fitscl       0   reduct       0
   rofit    .0000000D+00   eps      .1000000D-11   defer    .1000000D-04
   weigf    .0000000D+00   convg    .9990000D+00   lambda   .1000000D-04
   freq_l   .7000000D+02   freq_h   .3000000D+03   limit    .1000000D+00
   temp     .2980000D+03
 Using Watson A Reduction

 assumed sizeb           1
 \\ set (adj  or 16)
 \\ set (adj  or  8)
 \\ set (adj  or  1)
 \\ adj  1: adjust F according to rho, beta and gamma
 \\ adj  8: adjust rho according to F0 = 1/(2 I_alpha)
 \\ adj 16: adjust beta and gamma  according delta + epsil
 new adj :  25
 BJ           12.353023550
 BK           -6.401626440
 B-            5.670877120
 DJ            2.910760E-6
 DJK           3.469500E-6
 DK           19.874200E-6
 dj            0.191890E-6
 dk            2.585700E-6
 H_J           0.001840E-9
 HJK           0.001000E-9
 HKJ           0.001000E-9
 H_K           0.001000E-9
 h_j           0.001000E-9
 hjk          -0.020550E-9
 h_k           0.001000E-9
 mu_x          0.950000000
 mu_y          1.670000000
 mu_z          0.560000000
\F           166.116064534
 V1n           5000.000000
\rho           0.057722269
\beta          0.930417129
 F0          157.763100000
 delta         0.417130400

 fit  0.1D+00 0.1D+01   BJ          1.00
 fit  0.1D+00 0.1D+01   BK          1.00
 fit  0.1D+00 0.1D+01   B-          1.00
 fit  0.1D+00 0.1D+01   DJ          1.00
 fit  0.1D+00 0.1D+01   DJK         1.00
 fit  0.1D+00 0.1D+01   DK          1.00
 fit  0.1D+00 0.1D+01   dj          1.00
 fit  0.1D+00 0.1D+01   dk          1.00
 fit  0.1D+00 0.1D+01   H_J         1.00
 fit  0.1D+00 0.1D+01   HJK         1.00
 fit  0.1D+00 0.1D+01   HKJ         1.00
```

```
 fit  0.1D+00 0.1D+01   H_K         1.00
 fit  0.1D+00 0.1D+01   h_j         1.00
 fit  0.1D+00 0.1D+01   h_k         1.00
 fit  0.1D+00 0.1D+01   hjk         1.00
 dqx  0.1D+00 0.1D+01   V1n_1       1.00
 dqx  0.1D+00 0.1D+01   delta_1     1.00

   /A     S     0
   /E     S     1

  V  0

   ndata 1252   Data Points1252   Splittings   0
   Effective Data Points  12.5

\\\\\\\\\\\\\\\\\\\\\\\\\\\\\\\\\\\\\\\\\\\\\\\\\\\\\\\\\\\\\\\\\\\\\\\\\\\\\\\\\\\\\\\\\\\\\\\\\\\\\\\\\
\\Lines and Iterations Omitted For Space
\\\\\\\\\\\\\\\\\\\\\\\\\\\\\\\\\\\\\\\\\\\\\\\\\\\\\\\\\\\\\\\\\\\\\\\\\\\\\\\\\\\\\\\\\\\\\\\\\\\\\\\\\

  Lines fitted =         1252
 MICROWAVE RMS =            0.109325 MHz   = [(sum(o-c)^2)/n]^(1/2)
     RMS ERROR =            1.093247       = [(sum((o-c)/err)^2)/n]^(1/2)


 RMS deviations (MHz), B and V sorted
  B  V   n splittings MHz
  B  V   n abs. freq. MHz
  1  11252          0.109325          0.110809

            Parameters  and  Errors
 BJ          12.353003124 { 0.000000738}
 BK          -6.401621508 { 0.000000616}
 B-           5.674267619 { 0.000050411}
 DJ          14.707253E-6 { 0.001891E-6}
 DJK        -31.908106E-6 { 0.005291E-6}
 DK          19.730649E-6 { 0.003535E-6}
 dj           5.706226E-6 { 0.000896E-6}
 dk         -10.340473E-6 { 0.001821E-6}
 Vss          0.000000E-9 {     fixed  }
 Vcc          0.000000E-9 {     fixed  }
 H_J          0.035494E-9 { 0.001594E-9}           35.49351714E-12     1.59379493E-12
 HJK         -0.164406E-9 { 0.008165E-9}         -164.40566514E-12     8.16486773E-12
 HKJ          0.215596E-9 { 0.011329E-9}          215.59601296E-12    11.32947019E-12
 H_K         -0.085150E-9 { 0.004756E-9}          -85.15013785E-12     4.75603116E-12
 h_j          0.016721E-9 { 0.000790E-9}           16.72146576E-12   790.34987433E-15
 hjk         -0.067696E-9 { 0.003404E-9}          -67.69575346E-12     3.40441226E-12
 h_k          0.042987E-9 { 0.002469E-9}           42.98709394E-12     2.46880532E-12
 mu_x         0.950000000 {     fixed  }
 mu_y         1.670000000 {     fixed  }
 mu_z         0.560000000 {     fixed  }
 P_x          0.000000E-9 {     fixed  }
 P_y          0.000000E-9 {     fixed  }
 P_z          0.000000E-9 {     fixed  }
\F          174.700494695 {     derived}
 V1n        26414.559060 {  145.808100}
 V2n          0.000000E-9 {     fixed  }
\rho          0.102103591 {     derived}
\beta         1.394147354 {     derived}
\gamma        0.000000E-9 {     derived}
 F0         157.763100000 {     fixed  }
 epsil        0.000000E-9 {     fixed  }
 delta        1.075104421 { 0.017726682}

 Standard Deviation       0.110119 MHz

------------------------------------- B =  1
 Rotational Constants and Errors (in GHz)
      B_x      18.027270744       0.000050634
      B_y       6.678735505       0.000050197
      B_z       5.951381616       0.000001298
 Ray's kappa   -0.87954
 F0(calc)     157.763100000       0.000000000
 I_alpha        3.203404789       0.000000000
 <(i,x)  <(i,y)  <(i,z)       28.4011       90.0000       61.5989
d<(i,x) d<(i,y) d<(i,z)        1.0157        0.0000        1.0157

 V1n_1     10.540236 kj +/- 0.058182 kj         2.517430 kcal +/- 0.013896 kcal
          881.094726 cm +/-   4.8636 cm    s=  67.199604


 Errors of fitted linear combinations
    0.000000738    0.000000616    0.000050411    0.000000002    0.000000005
    0.000000004    0.000000001    0.000000002    0.000000000    0.000000000
    0.000000000    0.000000000    0.000000000    0.000000000    0.000000000
  145.808100232    0.017726682

 Correlation Matrix of fitted linear combinations
 BJ      1.000
 BK     -0.838  1.000
 B-      0.296 -0.016  1.000
 DJ      0.788 -0.830 -0.231  1.000
 DJK    -0.627  0.757  0.374 -0.962  1.000
```

```
DK      0.545 -0.674 -0.422  0.921 -0.989  1.000
dj      0.738 -0.799 -0.170  0.963 -0.961  0.937  1.000
dk     -0.615  0.716  0.350 -0.949  0.984 -0.973 -0.964  1.000
H_J     0.515 -0.642 -0.523  0.927 -0.969  0.963  0.898 -0.961  1.000
HJK    -0.409  0.565  0.601 -0.873  0.946 -0.955 -0.854  0.938 -0.991  1.000
HKJ     0.348 -0.510 -0.645  0.835 -0.921  0.938  0.815 -0.914  0.978 -0.997  1.000
H_K    -0.295  0.465  0.683 -0.799  0.892 -0.913 -0.776  0.886 -0.962  0.988 -0.997  1.000
h_j     0.489 -0.624 -0.523  0.914 -0.970  0.970  0.907 -0.967  0.996 -0.992  0.981 -0.965  1.000
h_k     0.301 -0.471 -0.679  0.803 -0.894  0.913  0.781 -0.893  0.965 -0.988  0.995 -0.996  0.968  1.000
hjk    -0.397  0.551  0.608 -0.865  0.939 -0.949 -0.849  0.939 -0.989  0.999 -0.996  0.988 -0.991 -0.992  1.000
V1n_1   0.546 -0.331  0.857  0.083  0.046 -0.098  0.165  0.029 -0.246  0.334 -0.391  0.441 -0.240 -0.436  0.345  1.000
delta_  0.337 -0.062  0.997 -0.191  0.334 -0.383 -0.125  0.310 -0.493  0.574 -0.621  0.661 -0.492 -0.657  0.582  0.896  1.000
strongest correlation between 15 and 10 ( 0.9986)

Freedom Cofreedom Matrix of linear comb.
BJ      0.093
BK      0.641  0.109
B-      0.969  0.994  0.001
DJ      0.485  0.649  0.977  0.010
DJK     0.694  0.563  0.963  0.371  0.004
DK      0.735  0.626  0.952  0.459  0.154  0.008
dj      0.802  0.775  0.693  0.505  0.524  0.589  0.015
dk      0.855  0.775  0.943  0.534  0.386  0.440  0.479  0.030
H_J     0.643  0.771  0.916  0.224  0.357  0.386  0.645  0.502  0.004
HJK     0.752  0.708  0.894  0.474  0.235  0.245  0.719  0.538  0.245  0.001
HKJ     0.783  0.741  0.873  0.536  0.312  0.241  0.756  0.585  0.328  0.112  0.001
H_K     0.807  0.769  0.854  0.584  0.381  0.292  0.788  0.628  0.392  0.193  0.083  0.002
h_j     0.910  0.884  0.777  0.617  0.492  0.488  0.362  0.451  0.281  0.347  0.435  0.504  0.006
h_k     0.932  0.880  0.846  0.725  0.598  0.564  0.744  0.456  0.482  0.345  0.272  0.264  0.446  0.014
hjk     0.925  0.862  0.872  0.676  0.538  0.517  0.672  0.312  0.369  0.211  0.273  0.358  0.312  0.190  0.005
V1n_1   0.907  0.966  0.110  0.989  0.999  0.998  0.692  0.974  0.976  0.971  0.959  0.947  0.828  0.936  0.947  0.005
delta_  0.962  0.993  0.018  0.982  0.971  0.961  0.695  0.950  0.925  0.905  0.885  0.866  0.785  0.857  0.882  0.097  0.001
minimum cofreedom between 17 and  3 ( 0.0177)

 Eigenvalues and Eigenvector Matrix of SVD-FIT

0.236343D-06  -0.001 0.002 0.392-0.033 0.087-0.052-0.020 0.012-0.114 0.470-0.577 0.222-0.068-0.033 0.085 0.058 0.449
0.100198D-05  -0.009 0.006-0.494-0.067 0.133-0.071-0.048 0.020-0.118 0.382-0.390 0.123-0.072-0.019 0.067-0.127-0.610
0.776595D-04   0.033-0.037-0.424 0.197-0.386 0.182 0.138-0.044 0.134-0.123-0.242 0.227 0.079-0.026-0.012 0.632 0.159
0.235074D-03  -0.041 0.040-0.252-0.278 0.248 0.006-0.074 0.016-0.360 0.357 0.348-0.359-0.130 0.026 0.063 0.461 0.218
0.945032D-03  -0.074 0.011 0.118-0.345-0.476 0.621 0.030-0.015-0.401 0.045 0.078 0.144-0.073-0.039 0.101-0.182-0.091
0.221019D-02   0.137-0.105 0.055 0.548-0.364 0.054-0.099 0.062 0.138 0.351 0.104-0.391-0.287-0.101 0.329-0.090-0.044
0.508526D-02  -0.051 0.011-0.127-0.139-0.020-0.088-0.697 0.181 0.041-0.339-0.075 0.177-0.473-0.016 0.204 0.003 0.127
0.927874D-02  -0.073-0.259 0.031-0.245-0.482-0.568 0.079-0.120-0.279-0.160-0.234-0.345-0.024 0.032-0.106 0.000-0.024
0.129164D-01   0.071-0.004-0.019 0.164-0.086 0.117-0.262-0.328-0.007 0.179 0.027 0.021-0.234 0.475-0.673-0.051 0.024
0.490536D-01  -0.223 0.279-0.092-0.139-0.014 0.126-0.198-0.528 0.263 0.029-0.140-0.280 0.075-0.555-0.115-0.089 0.091
0.127599D+00   0.657-0.047-0.020 0.206 0.115-0.079-0.070-0.311-0.462-0.152 0.062 0.179 0.006-0.359-0.009-0.021 0.018
0.190914D+00  -0.310 0.427 0.109 0.172 0.021-0.202 0.355-0.351-0.146-0.098 0.105 0.218-0.479 0.088 0.203 0.097-0.111
0.359015D+00   0.331 0.714-0.032-0.007-0.060 0.074 0.024 0.258-0.096-0.168-0.288-0.358 0.063 0.219-0.014-0.041 0.032
0.519877D+00   0.341-0.212 0.280-0.315 0.167 0.207 0.217-0.056 0.315-0.115-0.169-0.195-0.441-0.050-0.050 0.286-0.282
0.165411D+01  -0.288 0.053 0.202 0.274 0.043 0.039-0.034 0.445-0.261-0.062-0.046-0.041-0.123-0.441-0.480 0.200-0.201
0.462189D+01   0.053 0.198 0.418-0.059-0.167-0.151-0.402-0.124 0.059 0.145 0.130 0.122 0.352 0.083 0.127 0.417-0.418
0.944680D+01   0.267 0.245-0.092-0.290-0.300-0.301 0.144 0.235 0.288 0.304 0.303 0.299-0.164-0.250-0.237-0.094 0.092
```

B.2 Propylene Oxide Spectral Assignments

The file below presents the assigned spectral lines used in the above fit. In the layout of the file the first set of quantum numbers correspond the J, K_a, and K_c of the upper state and the second set correspond to the lower state. The values that follow the lower quantum state describe the state of internal motion of the line. S 1 tags the line as an A state and S 2 tags the line as E states. The spectral line center follows that, and the error is last.

```
\\\\\\\\\\\\\\\\\\\\\\\\\\\\\\\\\\\\\\\\\\\\\\\\\\\\\\\\\\\\\\\\\\\\\\\\\\\\\\\\\\\
Propylene Oxide Spectral Line Assignments
\\\\\\\\\\\\\\\\\\\\\\\\\\\\\\\\\\\\\\\\\\\\\\\\\\\\\\\\\\\\\\\\\\\\\\\\\\\\\\\\\\\

(J Ka Kc)u  (J  Ka Kc)l  IntMot      Freq          Unc. MHz
 28  8 20    28  7 21    S 2  =  170333.0835 MHz   Err   .1
 28  8 20    28  7 21    S 1  =  170333.8651 MHz   Err   .1
 29  8 21    29  7 22    S 1  =  169428.4514 MHz   Err   .1
```

```
29  8 21    29  7 22    S 2  =  169427.6210 MHz   Err   .1
30  8 22    30  7 23    S 2  =  168360.2004 MHz   Err   .1
30  8 22    30  7 23    S 1  =  168361.0576 MHz   Err   .1
31  8 23    31  7 24    S 1  =  167095.1823 MHz   Err   .1
31  8 23    31  7 24    S 2  =  167094.3012 MHz   Err   .1
32  8 24    32  7 25    S 1  =  165586.0651 MHz   Err   .1
32  8 24    32  7 25    S 2  =  165585.1756 MHz   Err   .1
33  8 25    33  7 26    S 2  =  163779.4671 MHz   Err   .1
33  8 25    33  7 26    S 1  =  163780.3902 MHz   Err   .1
34  8 26    34  7 27    S 2  =  161617.2736 MHz   Err   .1
34  8 26    34  7 27    S 1  =  161618.2228 MHz   Err   .1
35  8 27    35  7 28    S 1  =  159036.9274 MHz   Err   .1
35  8 27    35  7 28    S 2  =  159035.9338 MHz   Err   .1
38  8 30    38  7 31    S 1  =  148300.3773 MHz   Err   .1
38  8 30    38  7 31    S 2  =  148299.2164 MHz   Err   .1
33  9 24    33  8 25    S 1  =  192226.6861 MHz   Err   .1
33  9 24    33  8 25    S 2  =  192225.9291 MHz   Err   .1
36  9 27    36  8 28    S 1  =  188861.5759 MHz   Err   .1
36  9 27    36  8 28    S 2  =  188860.7380 MHz   Err   .1
37  9 28    37  8 29    S 1  =  187364.2904 MHz   Err   .1
37  9 28    37  8 29    S 2  =  187363.4294 MHz   Err   .1
38  9 29    38  8 30    S 2  =  185609.5824 MHz   Err   .1
38  9 29    38  8 30    S 1  =  185610.4827 MHz   Err   .1
40  9 31    40  8 32    S 2  =  181111.3263 MHz   Err   .1
40  9 31    40  8 32    S 1  =  181112.2536 MHz   Err   .1
41  9 32    41  8 33    S 1  =  178243.7554 MHz   Err   .1
41  9 32    41  8 33    S 2  =  178242.7899 MHz   Err   .1
42  9 33    42  8 34    S 2  =  174880.1716 MHz   Err   .1
42  9 33    42  8 34    S 1  =  174881.1716 MHz   Err   .1
43  9 34    43  8 35    S 1  =  170979.2516 MHz   Err   .1
43  9 34    43  8 35    S 2  =  170978.2066 MHz   Err   .1
44  9 35    44  8 36    S 1  =  166522.0085 MHz   Err   .1
44  9 35    44  8 36    S 2  =  166520.9189 MHz   Err   .1
45  9 36    45  8 37    S 2  =  161537.3606 MHz   Err   .1
45  9 36    45  8 37    S 1  =  161538.5063 MHz   Err   .1
47  9 38    47  8 39    S 2  =  150407.5990 MHz   Err   .1
47  9 38    47  8 39    S 1  =  150408.7282 MHz   Err   .1
50 10 40    50  9 41    S 1  =  184693.0803 MHz   Err   .1
50 10 40    50  9 41    S 2  =  184692.0380 MHz   Err   .1
51 10 41    51  9 42    S 1  =  179362.6734 MHz   Err   .1
51 10 41    51  9 42    S 2  =  179361.6232 MHz   Err   .1
52 10 42    52  9 43    S 2  =  173544.3751 MHz   Err   .1
52 10 42    52  9 43    S 1  =  173545.4806 MHz   Err   .1
49 10 39    49  9 40    S 1  =  189461.2385 MHz   Err   .1
49 10 39    49  9 40    S 2  =  189460.2353 MHz   Err   .1
47 10 37    47  9 38    S 2  =  197277.1871 MHz   Err   .1
47 10 37    47  9 38    S 1  =  197278.1046 MHz   Err   .1
45 10 35    45  9 36    S 1  =  203076.2167 MHz   Err   .1
45 10 35    45  9 36    S 2  =  203075.3504 MHz   Err   .1
44 10 34    44  9 35    S 1  =  205371.7004 MHz   Err   .1
44 10 34    44  9 35    S 2  =  205370.8591 MHz   Err   .1
43 10 33    43  9 34    S 2  =  207346.3044 MHz   Err   .1
43 10 33    43  9 34    S 1  =  207347.1302 MHz   Err   .1
42 10 32    42  9 33    S 2  =  209055.3664 MHz   Err   .1
42 10 32    42  9 33    S 1  =  209056.1710 MHz   Err   .1
40 10 30    40  9 31    S 2  =  211847.7598 MHz   Err   .1
40 10 30    40  9 31    S 1  =  211848.5302 MHz   Err   .1
26  8 19    26  7 20    S 1  =  171917.4912 MHz   Err   .1
26  8 19    26  7 20    S 2  =  171916.2273 MHz   Err   .1
28  8 21    28  7 22    S 1  =  170731.2016 MHz   Err   .1
28  8 21    28  7 22    S 2  =  170730.2279 MHz   Err   .1
29  8 22    29  7 23    S 1  =  170057.8952 MHz   Err   .1
29  8 22    29  7 23    S 2  =  170056.9780 MHz   Err   .1
30  8 23    30  7 24    S 1  =  169337.4658 MHz   Err   .1
30  8 23    30  7 24    S 2  =  169336.5753 MHz   Err   .1
31  8 24    31  7 25    S 2  =  168578.4261 MHz   Err   .1
31  8 24    31  7 25    S 1  =  168579.2948 MHz   Err   .1
32  8 25    32  7 26    S 1  =  167797.1844 MHz   Err   .1
32  8 25    32  7 26    S 2  =  167796.3249 MHz   Err   .1
33  8 26    33  7 27    S 2  =  167009.3436 MHz   Err   .1
33  8 26    33  7 27    S 1  =  167010.1846 MHz   Err   .1
34  8 27    34  7 28    S 1  =  166242.6838 MHz   Err   .1
34  8 27    34  7 28    S 2  =  166241.8521 MHz   Err   .1
35  8 28    35  7 29    S 1  =  165525.0947 MHz   Err   .1
35  8 28    35  7 29    S 2  =  165524.2748 MHz   Err   .1
36  8 29    36  7 30    S 1  =  164893.1373 MHz   Err   .1
36  8 29    36  7 30    S 2  =  164892.3337 MHz   Err   .1
37  8 30    37  7 31    S 2  =  164386.7558 MHz   Err   .1
37  8 30    37  7 31    S 1  =  164387.5502 MHz   Err   .1
38  8 31    38  7 32    S 2  =  164051.9611 MHz   Err   .1
38  8 31    38  7 32    S 1  =  164052.6825 MHz   Err   .1
40  8 33    40  7 34    S 2  =  164082.4752 MHz   Err   .1
40  8 33    40  7 34    S 1  =  164083.1760 MHz   Err   .1
33  9 25    33  8 26    S 1  =  192548.8019 MHz   Err   .1
33  9 25    33  8 26    S 2  =  192547.8766 MHz   Err   .1
34  9 26    34  8 27    S 1  =  191762.6970 MHz   Err   .1
34  9 26    34  8 27    S 2  =  191761.8179 MHz   Err   .1
35  9 27    35  8 28    S 1  =  190920.3607 MHz   Err   .1
35  9 27    35  8 28    S 2  =  190919.5098 MHz   Err   .1
36  9 28    36  8 29    S 1  =  190027.7969 MHz   Err   .1
36  9 28    36  8 29    S 2  =  190026.9490 MHz   Err   .1
37  9 29    37  8 30    S 1  =  189094.4951 MHz   Err   .1
```

```
37  9 29    37  8 30    S 2  =  189093.6650 MHz   Err   .1
38  9 30    38  8 31    S 2  =  188133.6841 MHz   Err   .1
38  9 30    38  8 31    S 1  =  188134.5061 MHz   Err   .1
39  9 31    39  8 32    S 1  =  187166.6083 MHz   Err   .1
39  9 31    39  8 32    S 2  =  187165.7972 MHz   Err   .1
40  9 32    40  8 33    S 1  =  186215.0057 MHz   Err   .1
40  9 32    40  8 33    S 2  =  186214.2038 MHz   Err   .1
41  9 33    41  8 34    S 1  =  185309.7469 MHz   Err   .1
41  9 33    41  8 34    S 2  =  185308.9571 MHz   Err   .1
42  9 34    42  8 35    S 1  =  184485.9481 MHz   Err   .1
42  9 34    42  8 35    S 2  =  184485.1730 MHz   Err   .1
43  9 35    43  8 36    S 2  =  183783.2673 MHz   Err   .1
43  9 35    43  8 36    S 1  =  183784.0222 MHz   Err   .1
44  9 36    44  8 37    S 2  =  183247.3070 MHz   Err   .1
44  9 36    44  8 37    S 1  =  183248.0426 MHz   Err   .1
45  9 37    45  8 38    S 2  =  182924.1470 MHz   Err   .1
45  9 37    45  8 38    S 1  =  182924.8670 MHz   Err   .1
46  9 38    46  8 39    S 1  =  182862.2339 MHz   Err   .1
46  9 38    46  8 39    S 2  =  182861.5610 MHz   Err   .1
47  9 39    47  8 40    S 1  =  183106.9939 MHz   Err   .1
47  9 39    47  8 40    S 2  =  183106.3904 MHz   Err   .1
49 10 40    49  9 41    S 2  =  202893.5742 MHz   Err   .1
49 10 40    49  9 41    S 1  =  202894.2936 MHz   Err   .1
48 10 39    48  9 40    S 1  =  203787.3994 MHz   Err   .1
48 10 39    48  9 40    S 2  =  203786.6581 MHz   Err   .1
47 10 38    47  9 39    S 2  =  204796.3017 MHz   Err   .1
47 10 38    47  9 39    S 1  =  204797.0427 MHz   Err   .1
46 10 37    46  9 38    S 1  =  205883.7525 MHz   Err   .1
46 10 37    46  9 38    S 2  =  205882.9870 MHz   Err   .1
45 10 36    45  9 37    S 2  =  207011.7516 MHz   Err   .1
45 10 36    45  9 37    S 1  =  207012.5149 MHz   Err   .1
44 10 35    44  9 36    S 2  =  208153.4005 MHz   Err   .1
44 10 35    44  9 36    S 1  =  208154.1520 MHz   Err   .1
42 10 33    42  9 34    S 1  =  210385.7003 MHz   Err   .1
42 10 33    42  9 34    S 2  =  210384.9164 MHz   Err   .1
41 10 32    41  9 33    S 1  =  211443.1580 MHz   Err   .1
41 10 32    41  9 33    S 2  =  211442.3689 MHz   Err   .1
40 10 31    40  9 32    S 1  =  212447.5308 MHz   Err   .1
40 10 31    40  9 32    S 2  =  212446.7227 MHz   Err   .1
36 10 27    36  9 28    S 2  =  215848.8275 MHz   Err   .1
36 10 27    36  9 28    S 1  =  215849.8488 MHz   Err   .1
37 10 28    37  9 29    S 2  =  215093.1508 MHz   Err   .1
37 10 28    37  9 29    S 1  =  215094.0786 MHz   Err   .1
38 10 29    38  9 30    S 2  =  214274.3276 MHz   Err   .1
38 10 29    38  9 30    S 1  =  214275.1913 MHz   Err   .1
39 10 30    39  9 31    S 2  =  213391.7742 MHz   Err   .1
40 17 23    39 18 21    S 2  =  98341.5121  MHz   Err   .1
40 17 23    39 18 21    S 1  =  98342.1411  MHz   Err   .1
40 17 24    39 18 21    S 1  =  98342.1411  MHz   Err   .1
40 17 23    39 18 22    S 1  =  98342.1411  MHz   Err   .1
40 17 24    39 18 22    S 1  =  98342.1411  MHz   Err   .1
40 17 24    39 18 22    S 2  =  98342.1411  MHz   Err   .1
29 11 19    28 12 17    S 2  =  99684.7561  MHz   Err   .1
29 11 19    28 12 17    S 1  =  99684.7561  MHz   Err   .1
29 11 19    28 12 16    S 1  =  99684.7561  MHz   Err   .1
29 11 18    28 12 17    S 1  =  99684.7561  MHz   Err   .1
29 11 18    28 12 16    S 1  =  99684.7561  MHz   Err   .1
29 11 18    28 12 16    S 2  =  99685.6718  MHz   Err   .1
31 12 20    30 13 18    S 2  =  101589.3785 MHz   Err   .1
31 12 20    30 13 17    S 1  =  101589.3785 MHz   Err   .1
31 12 19    30 13 18    S 1  =  101589.3785 MHz   Err   .1
31 12 19    30 13 17    S 1  =  101589.3785 MHz   Err   .1
31 12 20    30 13 18    S 1  =  101590.1785 MHz   Err   .1
31 12 19    30 13 17    S 2  =  101590.1785 MHz   Err   .1
31 12 20    30 13 18    S 2  =  101589.3785 MHz   Err   .1
31 12 20    30 13 18    S 1  =  101589.3785 MHz   Err   .1
31 12 20    30 13 17    S 1  =  101589.3785 MHz   Err   .1
31 12 19    30 13 18    S 1  =  101589.3785 MHz   Err   .1
31 12 19    30 13 17    S 1  =  101589.3785 MHz   Err   .1
31 12 19    30 13 17    S 2  =  101590.1785 MHz   Err   .1
39 10 30    39  9 31    S 1  =  213392.6022 MHz   Err   .1
17  4 14    16  5 11    S 1  =  112134.9298 MHz   Err   .1
30 11 20    29 12 18    S 1  =  112612.7394 MHz   Err   .1
30 11 20    29 12 17    S 1  =  112612.7394 MHz   Err   .1
30 11 19    29 12 17    S 1  =  112612.7394 MHz   Err   .1
30 11 19    29 12 18    S 1  =  112612.7394 MHz   Err   .1
21  1 20    21  0 21    S 1  =  113041.8455 MHz   Err   .1
 9  2  8     8  2  7    S 1  =  113085.6391 MHz   Err   .1
24  2 22    24  1 23    S 1  =  113149.2753 MHz   Err   .1
 9  1  9     8  0  8    S 1  =  113153.1065 MHz   Err   .1
 9  7  3     8  7  2    S 1  =  113828.2385 MHz   Err   .1
 9  7  2     8  7  1    S 1  =  113828.2385 MHz   Err   .1
 9  3  7     8  3  6    S 1  =  114055.2814 MHz   Err   .1
 9  3  6     8  3  5    S 1  =  114492.9544 MHz   Err   .1
13 13  1    14 12  2    S 1  =  115339.0176 MHz   Err   .1
13 13  0    14 12  3    S 1  =  115339.0176 MHz   Err   .1
 9  1  8     8  1  7    S 1  =  115763.9025 MHz   Err   .1
19  5 14    18  6 13    S 1  =  115813.4099 MHz   Err   .1
 9  2  7     8  2  6    S 1  =  116227.1329 MHz   Err   .1
17  4 13    16  5 12    S 1  =  116479.1066 MHz   Err   .1
24  3 22    24  2 23    S 1  =  116999.8411 MHz   Err   .1
23  7 16    22  8 15    S 1  =  118402.9042 MHz   Err   .1
```

```
 6  2  4     5  1  5    S 1  =  118659.7268 MHz   Err   .1
22  1 21    22  0 22    S 1  =  119193.4365 MHz   Err   .1
10  0 10     9  1  9    S 1  =  119747.6982 MHz   Err   .1
 5  3  3     4  2  2    S 1  =  121412.4889 MHz   Err   .1
10  1 10     9  1  9    S 1  =  121648.6850 MHz   Err   .1
10  1 10     9  0  9    S 1  =  124268.8223 MHz   Err   .1
18  4 15    17  5 12    S 1  =  124834.8227 MHz   Err   .1
23  1 22    23  0 23    S 1  =  125297.3759 MHz   Err   .1
10  4  7     9  4  6    S 1  =  126742.6109 MHz   Err   .1
10  3  8     9  3  7    S 1  =  126746.8818 MHz   Err   .1
17  6 11    17  5 12    S 1  =  126748.3543 MHz   Err   .1
17  6 12    17  5 13    S 1  =  127054.8020 MHz   Err   .1
16  6 10    16  5 11    S 1  =  127206.7876 MHz   Err   .1
16  6 11    16  5 12    S 1  =  127377.5839 MHz   Err   .1
10  3  7     9  3  6    S 1  =  127474.2997 MHz   Err   .1
17  3 15    16  4 12    S 1  =  127518.7136 MHz   Err   .1
30  6 25    30  5 26    S 1  =  127567.0080 MHz   Err   .1
15  6  9    15  5 10    S 1  =  127567.9332 MHz   Err   .1
15  6 10    15  5 11    S 1  =  127659.0079 MHz   Err   .1
14  6  8    14  5  9    S 1  =  127852.2198 MHz   Err   .1
14  6  9    14  5 10    S 1  =  127898.4565 MHz   Err   .1
13  6  7    13  5  8    S 1  =  128075.4552 MHz   Err   .1
13  6  8    13  5  9    S 1  =  128097.5476 MHz   Err   .1
20  5 16    19  6 14    S 1  =  128098.8015 MHz   Err   .1
10  1  9     9  1  8    S 1  =  128226.0831 MHz   Err   .1
22  6 16    21  7 15    S 1  =  130218.6194 MHz   Err   .1
30  3 27    30  2 28    S 1  =  130807.1226 MHz   Err   .1
24  1 23    24  0 24    S 1  =  131365.0983 MHz   Err   .1
18  4 14    17  5 13    S 1  =  131394.6420 MHz   Err   .1
24  7 18    23  8 15    S 1  =  131549.9263 MHz   Err   .1
24  7 17    23  8 16    S 1  =  131603.6343 MHz   Err   .1
11  0 11    10  1 10    S 1  =  132290.8582 MHz   Err   .1
26  8 18    25  9 17    S 1  =  133233.1833 MHz   Err   .1
11  1 11    10  1 10    S 1  =  133643.2673 MHz   Err   .1
 6  3  3     5  2  3    S 1  =  133703.3084 MHz   Err   .1
11  0 11    10  0 10    S 1  =  134191.8538 MHz   Err   .1
 6  3  3     5  2  4    S 1  =  134872.9785 MHz   Err   .1
11  1 11    10  0 10    S 1  =  135544.2610 MHz   Err   .1
 9  2  8     8  1  7    S 1  =  135998.1461 MHz   Err   .1
30 10 21    29 11 18    S 1  =  136741.0223 MHz   Err   .1
30 10 21    29 11 19    S 1  =  136741.0223 MHz   Err   .1
30  7 23    30  6 24    S 1  =  136896.8128 MHz   Err   .1
18  3 16    17  4 13    S 1  =  137044.0029 MHz   Err   .1
16  3 13    15  4 12    S 1  =  137207.8101 MHz   Err   .1
19  4 16    18  5 13    S 1  =  137310.3548 MHz   Err   .1
11  2 10    10  2  9    S 1  =  137816.5282 MHz   Err   .1
11 10  1    10 10  0    S 1  =  139084.9429 MHz   Err   .1
11 10  2    10 10  1    S 1  =  139084.9429 MHz   Err   .1
11  9  2    10  9  1    S 1  =  139104.6855 MHz   Err   .1
11  9  3    10  9  2    S 1  =  139104.6855 MHz   Err   .1
11  8  4    10  8  3    S 1  =  139131.6930 MHz   Err   .1
11  8  3    10  8  2    S 1  =  139131.6930 MHz   Err   .1
11  7  5    10  7  4    S 1  =  139170.5748 MHz   Err   .1
11  7  4    10  7  3    S 1  =  139170.5748 MHz   Err   .1
11  6  6    10  6  5    S 1  =  139230.5427 MHz   Err   .1
11  6  5    10  6  4    S 1  =  139230.5427 MHz   Err   .1
11  5  7    10  5  6    S 1  =  139330.3520 MHz   Err   .1
11  5  6    10  5  5    S 1  =  139332.8988 MHz   Err   .1
11  3  9    10  3  8    S 1  =  139422.2974 MHz   Err   .1
11  4  8    10  4  7    S 1  =  139487.0307 MHz   Err   .1
11  4  7    10  4  6    S 1  =  139567.3981 MHz   Err   .1
29  7 22    29  6 23    S 1  =  139608.0845 MHz   Err   .1
12  0 12    11  1 11    S 1  =  144667.5809 MHz   Err   .1
30  7 24    30  6 25    S 1  =  144944.5860 MHz   Err   .1
26  7 19    26  6 20    S 1  =  145237.3600 MHz   Err   .1
12  1 12    11  1 11    S 1  =  145614.3148 MHz   Err   .1
28  7 22    28  6 23    S 1  =  145902.5849 MHz   Err   .1
12  0 12    11  0 11    S 1  =  146020.0009 MHz   Err   .1
25  7 18    25  6 19    S 1  =  146476.6767 MHz   Err   .1
27  7 21    27  6 22    S 1  =  146479.3401 MHz   Err   .1
12  1 12    11  0 11    S 1  =  146966.6898 MHz   Err   .1
26  7 20    26  6 21    S 1  =  147078.7593 MHz   Err   .1
24  7 17    24  6 18    S 1  =  147490.3495 MHz   Err   .1
25  7 19    25  6 20    S 1  =  147675.9714 MHz   Err   .1
23  7 16    23  6 17    S 1  =  148322.4464 MHz   Err   .1
23  7 17    23  6 18    S 1  =  148794.2267 MHz   Err   .1
22  7 15    22  6 16    S 1  =  149008.8444 MHz   Err   .1
21  7 15    21  6 16    S 1  =  149743.8688 MHz   Err   .1
20  7 13    20  6 14    S 1  =  150050.5582 MHz   Err   .1
12  2 11    11  2 10    S 1  =  150104.9552 MHz   Err   .1
12 11  1    11 11  0    S 1  =  151722.4722 MHz   Err   .1
12 11  2    11 11  1    S 1  =  151722.4722 MHz   Err   .1
12 10  3    11 10  2    S 1  =  151741.7004 MHz   Err   .1
12 10  2    11 10  1    S 1  =  151741.7004 MHz   Err   .1
12  9  3    11  9  2    S 1  =  151767.1382 MHz   Err   .1
12  9  4    11  9  3    S 1  =  151767.1382 MHz   Err   .1
12  8  5    11  8  4    S 1  =  151801.7762 MHz   Err   .1
12  8  4    11  8  3    S 1  =  151801.7762 MHz   Err   .1
12  7  6    12  6  7    S 1  =  151838.8155 MHz   Err   .1
12  7  5    12  6  7    S 1  =  151838.8155 MHz   Err   .1
12  7  6    11  7  5    S 1  =  151852.1178 MHz   Err   .1
12  7  5    11  7  4    S 1  =  151852.1178 MHz   Err   .1
```

```
11  7  5    11  6  5    S 1  =  151916.5227 MHz   Err   .1
12  3  9    11  3  8    S 1  =  153735.5840 MHz   Err   .1
17  3 14    16  4 13    S 1  =  154156.0586 MHz   Err   .1
11  2 10    10  1  9    S 1  =  155300.7409 MHz   Err   .1
28  1 27    28  0 28    S 1  =  155424.2333 MHz   Err   .1
28  2 27    28  1 28    S 1  =  155479.3406 MHz   Err   .1
12  2 10    11  2  9    S 1  =  155518.8411 MHz   Err   .1
13  0 13    12  1 12    S 1  =  156912.0285 MHz   Err   .1
13  1 13    12  1 12    S 1  =  157565.9280 MHz   Err   .1
 6  4  3     5  3  2    S 1  =  157740.6141 MHz   Err   .1
13  0 13    12  0 12    S 1  =  157858.6941 MHz   Err   .1
15  2 13    14  3 12    S 1  =  158964.7754 MHz   Err   .1
21  3 19    20  4 16    S 1  =  159043.0963 MHz   Err   .1
10  2  8     9  1  8    S 1  =  159156.2748 MHz   Err   .1
28  8 20    27  9 19    S 1  =  159641.4311 MHz   Err   .1
13  4  9    13  1 12    S 1  =  161023.0722 MHz   Err   .1
14  4 10    14  1 13    S 1  =  162593.2086 MHz   Err   .1
20  4 16    19  5 15    S 1  =  163018.5246 MHz   Err   .1
16  3 14    16  0 16    S 1  =  163280.5078 MHz   Err   .1
13 12  2    12 12  1    S 1  =  164358.7221 MHz   Err   .1
13 12  1    12 12  0    S 1  =  164358.7221 MHz   Err   .1
13 11  3    12 11  2    S 1  =  164377.7145 MHz   Err   .1
13 11  2    12 11  1    S 1  =  164377.7145 MHz   Err   .1
13 10  4    12 10  3    S 1  =  164401.8635 MHz   Err   .1
13 10  3    12 10  2    S 1  =  164401.8635 MHz   Err   .1
13  9  5    12  9  4    S 1  =  164433.7431 MHz   Err   .1
13  9  4    12  9  3    S 1  =  164433.7431 MHz   Err   .1
13  8  6    12  8  5    S 1  =  164477.6843 MHz   Err   .1
13  8  5    12  8  4    S 1  =  164477.6843 MHz   Err   .1
13  7  7    12  7  6    S 1  =  164541.4570 MHz   Err   .1
13  7  6    12  7  5    S 1  =  164541.4570 MHz   Err   .1
13  3 11    12  3 10    S 1  =  164691.3143 MHz   Err   .1
13  1 12    12  1 11    S 1  =  164736.1891 MHz   Err   .1
13  5  8    12  5  7    S 1  =  164814.5006 MHz   Err   .1
13  4 10    12  4  9    S 1  =  165010.6621 MHz   Err   .1
13  4  9    12  4  8    S 1  =  165268.8942 MHz   Err   .1
13  3 10    12  3  9    S 1  =  167004.7462 MHz   Err   .1
23  5 19    22  6 16    S 1  =  167432.0936 MHz   Err   .1
27  3 25    26  4 22    S 1  =  168249.6639 MHz   Err   .1
13  2 11    12  2 10    S 1  =  168434.3057 MHz   Err   .1
 5  5  1     4  4  0    S 1  =  168527.1013 MHz   Err   .1
 5  5  0     4  4  0    S 1  =  168527.1013 MHz   Err   .1
 5  5  1     4  4  1    S 1  =  168527.1013 MHz   Err   .1
 5  5  0     4  4  1    S 1  =  168527.1013 MHz   Err   .1
14  0 14    13  1 13    S 1  =  169055.4148 MHz   Err   .1
25  3 23    24  4 20    S 1  =  170025.4558 MHz   Err   .1
14  1 14    13  0 13    S 1  =  170155.9214 MHz   Err   .1
 7  4  4     6  3  3    S 1  =  170324.8149 MHz   Err   .1
 7  4  4     6  3  4    S 1  =  170408.1536 MHz   Err   .1
28  8 20    28  7 22    S 1  =  170758.4826 MHz   Err   .1
24  8 16    24  7 17    S 1  =  172833.6085 MHz   Err   .1
29  8 21    28  9 20    S 1  =  172947.3907 MHz   Err   .1
23  8 15    23  7 16    S 1  =  173260.1217 MHz   Err   .1
23  8 15    23  7 17    S 1  =  173289.2880 MHz   Err   .1
21  8 13    21  7 14    S 1  =  173947.3846 MHz   Err   .1
19  8 12    19  7 12    S 1  =  174456.5098 MHz   Err   .1
19  8 11    19  7 12    S 1  =  174456.5098 MHz   Err   .1
14  2 13    13  2 12    S 1  =  174526.2348 MHz   Err   .1
26  1 26    25  2 24    S 1  =  174680.8670 MHz   Err   .1
26  0 26    25  1 24    S 1  =  174862.8832 MHz   Err   .1
16  8  9    16  7  9    S 1  =  174969.0038 MHz   Err   .1
16  8  8    16  7  9    S 1  =  174969.0038 MHz   Err   .1
16  2 14    15  3 13    S 1  =  175542.2310 MHz   Err   .1
14  1 13    13  1 12    S 1  =  176638.7716 MHz   Err   .1
14 13  2    13 13  1    S 1  =  176993.5903 MHz   Err   .1
14 13  1    13 13  0    S 1  =  176993.5903 MHz   Err   .1
14 12  2    13 12  1    S 1  =  177012.3997 MHz   Err   .1
14 12  3    13 12  2    S 1  =  177012.3997 MHz   Err   .1
14 11  3    13 11  2    S 1  =  177035.7285 MHz   Err   .1
14 11  4    13 11  3    S 1  =  177035.7285 MHz   Err   .1
21  4 17    20  5 16    S 1  =  179800.3076 MHz   Err   .1
10  3  7     9  2  7    S 1  =  180143.4790 MHz   Err   .1
14  3 11    13  3 10    S 1  =  180333.7283 MHz   Err   .1
15  1 14    14  2 13    S 1  =  180811.7724 MHz   Err   .1
22  3 20    21  4 18    S 1  =  180907.4228 MHz   Err   .1
11  1 10    10  0 10    S 1  =  181013.8887 MHz   Err   .1
 6  5  2     5  4  2    S 1  =  181168.5598 MHz   Err   .1
 6  5  1     5  4  2    S 1  =  181168.5598 MHz   Err   .1
14  2 12    13  2 11    S 1  =  181226.5762 MHz   Err   .1
15  1 15    14  1 14    S 1  =  181426.1087 MHz   Err   .1
15  0 15    14  0 14    S 1  =  181570.5032 MHz   Err   .1
16  3 13    16  0 16    S 1  =  181677.0295 MHz   Err   .1
15  1 15    14  0 14    S 1  =  181872.7687 MHz   Err   .1
18  4 14    18  1 17    S 1  =  182202.0156 MHz   Err   .1
23  4 20    22  5 17    S 1  =  182751.1485 MHz   Err   .1
 8  4  5     7  3  4    S 1  =  182844.4427 MHz   Err   .1
 8  4  4     7  3  4    S 1  =  182856.2571 MHz   Err   .1
 8  4  5     7  3  5    S 1  =  183051.5465 MHz   Err   .1
 8  4  4     7  3  5    S 1  =  183063.3767 MHz   Err   .1
24  2 23    23  3 21    S 1  =  183077.6377 MHz   Err   .1
18  2 16    17  3 14    S 1  =  184190.2113 MHz   Err   .1
15  2 14    14  2 13    S 1  =  186662.7173 MHz   Err   .1
```

```
12  2 10    11  1 10    S 1  =  188402.4113 MHz   Err   .1
15  1 14    14  1 13    S 1  =  188453.4089 MHz   Err   .1
19  3 16    18  4 15    S 1  =  189181.1119 MHz   Err   .1
15 13  3    14 13  2    S 1  =  189645.6934 MHz   Err   .1
15 13  2    14 13  1    S 1  =  189645.6934 MHz   Err   .1
15 12  3    14 12  2    S 1  =  189668.4929 MHz   Err   .1
15 12  4    14 12  3    S 1  =  189668.4929 MHz   Err   .1
10  3  7     9  2  8    S 1  =  189674.0656 MHz   Err   .1
15 11  5    14 11  4    S 1  =  189696.7656 MHz   Err   .1
15 11  4    14 11  3    S 1  =  189696.7656 MHz   Err   .1
23  3 21    22  4 19    S 1  =  189699.2224 MHz   Err   .1
15 10  6    14 10  5    S 1  =  189733.1700 MHz   Err   .1
15 10  5    14 10  4    S 1  =  189733.1700 MHz   Err   .1
15  9  6    14  9  5    S 1  =  189781.4556 MHz   Err   .1
15  9  7    14  9  6    S 1  =  189781.4556 MHz   Err   .1
15  3 13    14  3 12    S 1  =  189800.3197 MHz   Err   .1
15  8  8    14  8  7    S 1  =  189848.4469 MHz   Err   .1
15  8  7    14  8  6    S 1  =  189848.4469 MHz   Err   .1
15  7  9    14  7  8    S 1  =  189946.1243 MHz   Err   .1
15  7  8    14  7  7    S 1  =  189946.1243 MHz   Err   .1
15  5 11    14  5 10    S 1  =  190337.1312 MHz   Err   .1
15  5 10    14  5  9    S 1  =  190383.6940 MHz   Err   .1
15  4 12    14  4 11    S 1  =  190551.4533 MHz   Err   .1
10  2  8     9  1  9    S 1  =  191147.4421 MHz   Err   .1
20  2 18    20  1 20    S 1  =  191147.4421 MHz   Err   .1
15  4 11    14  4 10    S 1  =  191226.3889 MHz   Err   .1
11  3  8    10  2  8    S 1  =  191306.7378 MHz   Err   .1
24  4 21    23  5 18    S 1  =  192287.0461 MHz   Err   .1
16  0 16    15  1 15    S 1  =  193137.9086 MHz   Err   .1
16  1 16    15  1 15    S 1  =  193340.8818 MHz   Err   .1
16  0 16    15  0 15    S 1  =  193440.1477 MHz   Err   .1
16  1 16    15  0 15    S 1  =  193643.1569 MHz   Err   .1
19  2 17    18  3 15    S 1  =  193650.7047 MHz   Err   .1
15  3 12    14  3 11    S 1  =  193682.1582 MHz   Err   .1
11  2 10    10  1 10    S 1  =  193869.1820 MHz   Err   .1
15  2 13    14  2 12    S 1  =  193879.3206 MHz   Err   .1
16  1 15    15  2 14    S 1  =  194366.0446 MHz   Err   .1
29  9 20    29  8 22    S 1  =  195103.3770 MHz   Err   .1
28  9 19    28  8 20    S 1  =  195571.3817 MHz   Err   .1
26  9 17    26  8 18    S 1  =  196432.2417 MHz   Err   .1
25  9 16    25  8 17    S 1  =  196789.7513 MHz   Err   .1
21  9 13    21  8 13    S 1  =  197836.6454 MHz   Err   .1
21  9 12    21  8 13    S 1  =  197836.6454 MHz   Err   .1
20  9 12    20  8 12    S 1  =  198020.1809 MHz   Err   .1
20  3 17    19  4 15    S 1  =  198020.1809 MHz   Err   .1
20  9 11    20  8 12    S 1  =  198020.1809 MHz   Err   .1
24  3 22    23  4 20    S 1  =  198055.5409 MHz   Err   .1
12  3 10    11  2  9    S 1  =  198133.8562 MHz   Err   .1
19  9 11    19  8 11    S 1  =  198178.4980 MHz   Err   .1
19  9 10    19  8 11    S 1  =  198178.4980 MHz   Err   .1
19  9 11    19  8 12    S 1  =  198178.4980 MHz   Err   .1
19  9 10    19  8 12    S 1  =  198178.4980 MHz   Err   .1
18  9 10    18  8 10    S 1  =  198314.0917 MHz   Err   .1
18  9  9    18  8 10    S 1  =  198314.0917 MHz   Err   .1
18  9 10    18  8 11    S 1  =  198314.0917 MHz   Err   .1
18  9  9    18  8 11    S 1  =  198314.0917 MHz   Err   .1
17  9  9    17  8  9    S 1  =  198429.3628 MHz   Err   .1
17  9  8    17  8  9    S 1  =  198429.3628 MHz   Err   .1
17  9  9    17  8 10    S 1  =  198429.3628 MHz   Err   .1
17  9  8    17  8 10    S 1  =  198429.3628 MHz   Err   .1
16  9  7    16  8  8    S 1  =  198526.4744 MHz   Err   .1
16  9  8    16  8  8    S 1  =  198526.4744 MHz   Err   .1
16  9  8    16  8  9    S 1  =  198526.4744 MHz   Err   .1
16  9  7    16  8  9    S 1  =  198526.4744 MHz   Err   .1
15  9  6    15  8  7    S 1  =  198607.6187 MHz   Err   .1
15  9  7    15  8  7    S 1  =  198607.6187 MHz   Err   .1
15  9  7    15  8  8    S 1  =  198607.6187 MHz   Err   .1
15  9  6    15  8  8    S 1  =  198607.6187 MHz   Err   .1
14  9  6    14  8  6    S 1  =  198674.6069 MHz   Err   .1
14  9  5    14  8  6    S 1  =  198674.6069 MHz   Err   .1
14  9  5    14  8  7    S 1  =  198674.6069 MHz   Err   .1
14  9  6    14  8  7    S 1  =  198674.6069 MHz   Err   .1
13  9  5    13  8  5    S 1  =  198729.2285 MHz   Err   .1
13  9  4    13  8  5    S 1  =  198729.2285 MHz   Err   .1
13  9  4    13  8  6    S 1  =  198729.2285 MHz   Err   .1
13  9  5    13  8  6    S 1  =  198729.2285 MHz   Err   .1
16  2 15    15  2 14    S 1  =  198754.2079 MHz   Err   .1
12  9  4    12  8  4    S 1  =  198773.1379 MHz   Err   .1
12  9  4    12  8  5    S 1  =  198773.1379 MHz   Err   .1
12  9  3    12  8  4    S 1  =  198773.1379 MHz   Err   .1
12  9  3    12  8  5    S 1  =  198773.1379 MHz   Err   .1
11  9  2    11  8  3    S 1  =  198807.9585 MHz   Err   .1
11  9  3    11  8  4    S 1  =  198807.9585 MHz   Err   .1
11  9  3    11  8  3    S 1  =  198807.9585 MHz   Err   .1
11  9  2    11  8  4    S 1  =  198807.9585 MHz   Err   .1
10  9  2    10  8  2    S 1  =  198834.8931 MHz   Err   .1
10  9  1    10  8  2    S 1  =  198834.8931 MHz   Err   .1
10  9  2    10  8  3    S 1  =  198834.8931 MHz   Err   .1
10  9  1    10  8  3    S 1  =  198834.8931 MHz   Err   .1
 9  9  0     9  8  1    S 1  =  198855.3934 MHz   Err   .1
 9  9  1     9  8  2    S 1  =  198855.3934 MHz   Err   .1
 9  9  1     9  8  1    S 1  =  198855.3934 MHz   Err   .1
```

```
 9  9  0     9  8  2    S 1  =  198855.3934 MHz   Err   .1
16  1 15    15  1 14    S 1  =  200217.0147 MHz   Err   .1
25  4 22    24  5 19    S 1  =  200770.1269 MHz   Err   .1
16  3 14    15  3 13    S 1  =  202279.2182 MHz   Err   .1
16 13  3    15 13  2    S 1  =  202299.8334 MHz   Err   .1
16 13  4    15 13  3    S 1  =  202299.8334 MHz   Err   .1
16 12  4    15 12  3    S 1  =  202327.0639 MHz   Err   .1
16 12  5    15 12  4    S 1  =  202327.0639 MHz   Err   .1
16 11  6    15 11  5    S 1  =  202361.0840 MHz   Err   .1
16 11  5    15 11  4    S 1  =  202361.0840 MHz   Err   .1
16 10  6    15 10  5    S 1  =  202404.8686 MHz   Err   .1
16 10  7    15 10  6    S 1  =  202404.8686 MHz   Err   .1
16  9  8    15  9  7    S 1  =  202463.2493 MHz   Err   .1
16  9  7    15  9  6    S 1  =  202463.2493 MHz   Err   .1
16  8  9    15  8  8    S 1  =  202544.3681 MHz   Err   .1
16  8  8    15  8  7    S 1  =  202544.3681 MHz   Err   .1
16  7 10    15  7  9    S 1  =  202662.9710 MHz   Err   .1
16  7  9    15  7  8    S 1  =  202662.9710 MHz   Err   .1
16  5 12    15  5 11    S 1  =  203128.0693 MHz   Err   .1
16  5 11    15  5 10    S 1  =  203211.5082 MHz   Err   .1
16  4 13    15  4 12    S 1  =  203312.5338 MHz   Err   .1
13  2 11    12  1 11    S 1  =  204124.6536 MHz   Err   .1
16  4 12    15  4 11    S 1  =  204334.1127 MHz   Err   .1
17  1 17    16  1 16    S 1  =  205248.4651 MHz   Err   .1
17  0 17    16  0 16    S 1  =  205316.0996 MHz   Err   .1
17  1 17    16  0 16    S 1  =  205451.4375 MHz   Err   .1
16  2 14    15  2 13    S 1  =  206377.7575 MHz   Err   .1
16  3 13    15  3 12    S 1  =  207005.1271 MHz   Err   .1
20  3 17    19  4 16    S 1  =  207042.6380 MHz   Err   .1
13  3 11    12  2 10    S 1  =  207306.2935 MHz   Err   .1
17  1 16    16  2 15    S 1  =  207573.3449 MHz   Err   .1
10  4  6     9  3  7    S 1  =  208467.5846 MHz   Err   .1
17  2 16    16  2 15    S 1  =  210805.2261 MHz   Err   .1
17  1 16    16  1 15    S 1  =  211961.4680 MHz   Err   .1
11  2  9    10  1 10    S 1  =  211996.4609 MHz   Err   .1
17  3 15    16  3 14    S 1  =  214702.0331 MHz   Err   .1
16  5 12    16  2 14    S 1  =  214982.2550 MHz   Err   .1
17 12  6    16 12  5    S 1  =  214988.3874 MHz   Err   .1
17 12  5    16 12  4    S 1  =  214988.3874 MHz   Err   .1
17 11  7    16 11  6    S 1  =  215028.8406 MHz   Err   .1
17 11  6    16 11  5    S 1  =  215028.8406 MHz   Err   .1
17 10  8    16 10  7    S 1  =  215081.0436 MHz   Err   .1
17 10  7    16 10  6    S 1  =  215081.0436 MHz   Err   .1
17  9  9    16  9  8    S 1  =  215150.8312 MHz   Err   .1
17  9  8    16  9  7    S 1  =  215150.8312 MHz   Err   .1
17  8 10    16  8  9    S 1  =  215247.9760 MHz   Err   .1
17  8  9    16  8  8    S 1  =  215247.9760 MHz   Err   .1
17  6 12    16  6 11    S 1  =  215610.4803 MHz   Err   .1
17  5 13    16  5 12    S 1  =  215933.1463 MHz   Err   .1
17  4 14    16  4 13    S 1  =  216056.8910 MHz   Err   .1
17  5 12    16  5 11    S 1  =  216076.2294 MHz   Err   .1
14  3 12    13  2 11    S 1  =  216141.1894 MHz   Err   .1
18  0 18    17  1 17    S 1  =  217061.0152 MHz   Err   .1
18  1 18    17  1 17    S 1  =  217150.6996 MHz   Err   .1
18  0 18    17  0 17    S 1  =  217196.3241 MHz   Err   .1
 7  6  2     6  5  1    S 1  =  217208.4089 MHz   Err   .1
 7  6  1     6  5  1    S 1  =  217208.4089 MHz   Err   .1
 7  6  2     6  5  2    S 1  =  217208.4089 MHz   Err   .1
 7  6  1     6  5  2    S 1  =  217208.4089 MHz   Err   .1
18  1 18    17  0 17    S 1  =  217286.0270 MHz   Err   .1
17  4 13    16  4 12    S 1  =  217541.2428 MHz   Err   .1
17  2 15    16  2 14    S 1  =  218710.4647 MHz   Err   .1
 9  5  5     8  4  4    S 1  =  219040.8557 MHz   Err   .1
30 10 21    30  9 21    S 1  =  219193.5053 MHz   Err   .1
17  3 14    16  3 13    S 1  =  220260.8035 MHz   Err   .1
18  1 17    17  2 16    S 1  =  220477.6184 MHz   Err   .1
26 10 17    26  9 17    S 1  =  220532.0641 MHz   Err   .1
26 10 16    26  9 17    S 1  =  220532.0641 MHz   Err   .1
14  2 12    13  1 12    S 1  =  220615.1229 MHz   Err   .1
12  3  9    11  2 10    S 1  =  220671.5927 MHz   Err   .1
16 10  6    16  9  7    S 1  =  222014.2552 MHz   Err   .1
16 10  7    16  9  7    S 1  =  222014.2552 MHz   Err   .1
16 10  6    16  9  8    S 1  =  222014.2552 MHz   Err   .1
16 10  7    16  9  8    S 1  =  222014.2552 MHz   Err   .1
15 10  6    15  9  7    S 1  =  222072.6382 MHz   Err   .1
15 10  6    15  9  6    S 1  =  222072.6382 MHz   Err   .1
15 10  5    15  9  7    S 1  =  222072.6382 MHz   Err   .1
15 10  5    15  9  6    S 1  =  222072.6382 MHz   Err   .1
14 10  5    14  9  6    S 1  =  222120.9407 MHz   Err   .1
14 10  5    14  9  5    S 1  =  222120.9407 MHz   Err   .1
14 10  4    14  9  5    S 1  =  222120.9407 MHz   Err   .1
14 10  4    14  9  6    S 1  =  222120.9407 MHz   Err   .1
13 10  4    13  9  5    S 1  =  222160.4828 MHz   Err   .1
13 10  4    13  9  4    S 1  =  222160.4828 MHz   Err   .1
13 10  3    13  9  5    S 1  =  222160.4828 MHz   Err   .1
13 10  3    13  9  4    S 1  =  222160.4828 MHz   Err   .1
18  2 17    17  2 16    S 1  =  222820.9582 MHz   Err   .1
18  1 17    17  1 16    S 1  =  223709.4942 MHz   Err   .1
21  3 18    20  4 17    S 1  =  224977.5102 MHz   Err   .1
40  0 40    39  1 39    S 1  =  478430.6857 MHz   Err   .1
40  1 40    39  1 39    S 1  =  478430.6857 MHz   Err   .1
40  0 40    39  0 39    S 1  =  478430.6857 MHz   Err   .1
```

```
40  1 40    39  0 39    S 1  =  478430.6857 MHz   Err   .1
41  0 41    40  1 40    S 1  =  490283.3688 MHz   Err   .1
41  1 41    40  1 40    S 1  =  490283.3688 MHz   Err   .1
41  0 41    40  0 40    S 1  =  490283.3688 MHz   Err   .1
41  1 41    40  0 40    S 1  =  490283.3688 MHz   Err   .1
41  1 40    40  2 39    S 1  =  496226.0912 MHz   Err   .1
41  2 40    40  2 39    S 1  =  496226.0912 MHz   Err   .1
41  1 40    40  1 39    S 1  =  496226.0912 MHz   Err   .1
41  2 40    40  1 39    S 1  =  496226.0912 MHz   Err   .1
42  1 41    41  2 40    S 1  =  508074.5860 MHz   Err   .1
42  2 41    41  2 40    S 1  =  508074.5860 MHz   Err   .1
42  1 41    41  1 40    S 1  =  508074.5860 MHz   Err   .1
42  2 41    41  1 40    S 1  =  508074.5860 MHz   Err   .1
42  1 41    41  2 40    S 1  =  508074.5860 MHz   Err   .1
42  2 41    41  2 40    S 1  =  508074.5860 MHz   Err   .1
42  1 41    41  1 40    S 1  =  508074.5860 MHz   Err   .1
42  2 41    41  1 40    S 1  =  508074.5860 MHz   Err   .1
43  1 42    42  2 41    S 1  =  519920.5746 MHz   Err   .1
43  2 42    42  2 41    S 1  =  519920.5746 MHz   Err   .1
43  1 42    42  1 41    S 1  =  519920.5746 MHz   Err   .1
43  2 42    42  1 41    S 1  =  519920.5746 MHz   Err   .1
44  0 44    43  1 43    S 1  =  525826.2775 MHz   Err   .1
44  1 44    43  1 43    S 1  =  525826.2775 MHz   Err   .1
44  0 44    43  0 43    S 1  =  525826.2775 MHz   Err   .1
44  1 44    43  0 43    S 1  =  525826.2775 MHz   Err   .1
44  0 44    43  1 43    S 1  =  525826.2775 MHz   Err   .1
44  1 44    43  1 43    S 1  =  525826.2775 MHz   Err   .1
44  0 44    43  0 43    S 1  =  525826.2775 MHz   Err   .1
44  1 44    43  0 43    S 1  =  525826.2775 MHz   Err   .1
15 15  0    14 14  0    S 1  =  528689.3975 MHz   Err   .1
15 15  0    14 14  1    S 1  =  528689.3975 MHz   Err   .1
15 15  1    14 14  0    S 1  =  528689.3975 MHz   Err   .1
15 15  1    14 14  1    S 1  =  528689.3975 MHz   Err   .1
44  1 43    43  2 42    S 1  =  531764.0195 MHz   Err   .1
44  2 43    43  2 42    S 1  =  531764.0195 MHz   Err   .1
44  1 43    43  1 42    S 1  =  531764.0195 MHz   Err   .1
44  2 43    43  1 42    S 1  =  531764.0195 MHz   Err   .1
19 13  7    18 12  7    S 1  =  532487.9085 MHz   Err   .1
19 13  7    18 12  6    S 1  =  532487.9085 MHz   Err   .1
19 13  6    18 12  6    S 1  =  532487.9085 MHz   Err   .1
19 13  6    18 12  7    S 1  =  532487.9085 MHz   Err   .1
23 11 13    22 10 12    S 1  =  536102.5444 MHz   Err   .1
23 11 12    22 10 12    S 1  =  536102.5444 MHz   Err   .1
23 11 13    22 10 13    S 1  =  536102.5444 MHz   Err   .1
23 11 12    22 10 13    S 1  =  536102.5444 MHz   Err   .1
25 10 16    24  9 15    S 1  =  537688.4900 MHz   Err   .1
25 10 15    24  9 15    S 1  =  537688.4900 MHz   Err   .1
25 10 16    24  9 16    S 1  =  537688.4900 MHz   Err   .1
25 10 15    24  9 16    S 1  =  537688.4900 MHz   Err   .1
43  0 43    42  1 42    S 1  =  513981.1910 MHz   Err   .1
43  1 43    42  1 42    S 1  =  513981.1910 MHz   Err   .1
43  0 43    42  0 42    S 1  =  513981.1910 MHz   Err   .1
43  1 43    42  0 42    S 1  =  513981.1910 MHz   Err   .1
45  0 45    44  1 44    S 1  =  537668.7190 MHz   Err   .1
45  1 45    44  1 44    S 1  =  537668.7190 MHz   Err   .1
45  0 45    44  0 44    S 1  =  537668.7190 MHz   Err   .1
45  1 45    44  0 44    S 1  =  537668.7190 MHz   Err   .1
44  2 42    43  3 41    S 1  =  537740.7136 MHz   Err   .1
44  3 42    43  3 41    S 1  =  537744.0218 MHz   Err   .1
44  2 42    43  2 41    S 1  =  537744.0218 MHz   Err   .1
44  3 42    43  2 41    S 1  =  537747.3584 MHz   Err   .1
16 15  1    15 14  1    S 1  =  541321.0475 MHz   Err   .1
16 15  1    15 14  2    S 1  =  541321.0475 MHz   Err   .1
16 15  2    15 14  1    S 1  =  541321.0475 MHz   Err   .1
16 15  2    15 14  2    S 1  =  541321.0475 MHz   Err   .1
45  1 44    44  2 43    S 1  =  543604.8788 MHz   Err   .1
45  2 44    44  2 43    S 1  =  543604.8788 MHz   Err   .1
45  1 44    44  1 43    S 1  =  543604.8788 MHz   Err   .1
45  2 44    44  1 43    S 1  =  543604.8788 MHz   Err   .1
18 14  5    17 13  5    S 1  =  543226.4302 MHz   Err   .1
18 14  5    17 13  4    S 1  =  543226.4302 MHz   Err   .1
18 14  4    17 13  5    S 1  =  543226.4302 MHz   Err   .1
18 14  4    17 13  4    S 1  =  543226.4302 MHz   Err   .1
17 15  2    16 14  3    S 1  =  553951.0856 MHz   Err   .1
17 15  3    16 14  2    S 1  =  553951.0856 MHz   Err   .1
17 15  2    16 14  2    S 1  =  553951.0856 MHz   Err   .1
17 15  3    16 14  3    S 1  =  553951.0856 MHz   Err   .1
46  1 45    45  2 44    S 1  =  555443.0443 MHz   Err   .1
46  2 45    45  2 44    S 1  =  555443.0443 MHz   Err   .1
46  1 45    45  1 44    S 1  =  555443.0443 MHz   Err   .1
46  2 45    45  1 44    S 1  =  555443.0443 MHz   Err   .1
21 13  8    20 12  9    S 1  =  557722.2977 MHz   Err   .1
21 13  8    20 12  8    S 1  =  557722.2977 MHz   Err   .1
21 13  9    20 12  8    S 1  =  557722.2977 MHz   Err   .1
21 13  9    20 12  9    S 1  =  557722.2977 MHz   Err   .1
23 12 11    22 11 11    S 1  =  559535.8348 MHz   Err   .1
23 12 12    22 11 12    S 1  =  559535.8348 MHz   Err   .1
23 12 12    22 11 11    S 1  =  559535.8348 MHz   Err   .1
23 12 11    22 11 12    S 1  =  559535.8348 MHz   Err   .1
47  0 47    46  1 46    S 1  =  561345.2611 MHz   Err   .1
47  1 47    46  1 46    S 1  =  561345.2611 MHz   Err   .1
47  0 47    46  0 46    S 1  =  561345.2611 MHz   Err   .1
```

```
47  1 47    46  0 46    S 1  =  561345.2611 MHz   Err   .1
16 16  0    15 15  0    S 1  =  564665.7111 MHz   Err   .1
16 16  1    15 15  1    S 1  =  564665.7111 MHz   Err   .1
16 16  1    15 15  0    S 1  =  564665.7111 MHz   Err   .1
16 16  0    15 15  1    S 1  =  564665.7111 MHz   Err   .1
18 15  4    17 14  3    S 1  =  566579.3045 MHz   Err   .1
18 15  3    17 14  4    S 1  =  566579.3045 MHz   Err   .1
18 15  3    17 14  3    S 1  =  566579.3045 MHz   Err   .1
18 15  4    17 14  4    S 1  =  566579.3045 MHz   Err   .1
47  1 46    46  2 45    S 1  =  567278.4590 MHz   Err   .1
47  2 46    46  2 45    S 1  =  567278.4590 MHz   Err   .1
47  1 46    46  1 45    S 1  =  567278.4590 MHz   Err   .1
47  2 46    46  1 45    S 1  =  567278.4590 MHz   Err   .1
20 14  6    19 13  7    S 1  =  568473.4048 MHz   Err   .1
20 14  6    19 13  6    S 1  =  568473.4048 MHz   Err   .1
20 14  7    19 13  6    S 1  =  568473.4048 MHz   Err   .1
20 14  7    19 13  7    S 1  =  568473.4048 MHz   Err   .1
40  0 40    39  1 39    S 1  =  478430.6857 MHz   Err   .1
40  1 40    39  1 39    S 1  =  478430.6857 MHz   Err   .1
40  0 40    39  0 39    S 1  =  478430.6857 MHz   Err   .1
40  1 40    39  0 39    S 1  =  478430.6857 MHz   Err   .1
41  0 41    40  1 40    S 1  =  490283.3688 MHz   Err   .1
41  1 41    40  1 40    S 1  =  490283.3688 MHz   Err   .1
41  0 41    40  0 40    S 1  =  490283.3688 MHz   Err   .1
41  1 41    40  0 40    S 1  =  490283.3688 MHz   Err   .1
41  1 40    40  2 39    S 1  =  496226.0912 MHz   Err   .1
41  2 40    40  2 39    S 1  =  496226.0912 MHz   Err   .1
41  1 40    40  1 39    S 1  =  496226.0912 MHz   Err   .1
41  2 40    40  1 39    S 1  =  496226.0912 MHz   Err   .1
42  1 41    41  2 40    S 1  =  508074.5860 MHz   Err   .1
42  2 41    41  2 40    S 1  =  508074.5860 MHz   Err   .1
42  1 41    41  1 40    S 1  =  508074.5860 MHz   Err   .1
42  2 41    41  1 40    S 1  =  508074.5860 MHz   Err   .1
42  1 41    41  2 40    S 1  =  508074.5860 MHz   Err   .1
42  2 41    41  2 40    S 1  =  508074.5860 MHz   Err   .1
42  1 41    41  1 40    S 1  =  508074.5860 MHz   Err   .1
42  2 41    41  1 40    S 1  =  508074.5860 MHz   Err   .1
43  1 42    42  2 41    S 1  =  519920.5746 MHz   Err   .1
43  2 42    42  2 41    S 1  =  519920.5746 MHz   Err   .1
43  1 42    42  1 41    S 1  =  519920.5746 MHz   Err   .1
43  2 42    42  1 41    S 1  =  519920.5746 MHz   Err   .1
44  0 44    43  1 43    S 1  =  525826.2775 MHz   Err   .1
44  1 44    43  1 43    S 1  =  525826.2775 MHz   Err   .1
44  0 44    43  0 43    S 1  =  525826.2775 MHz   Err   .1
44  1 44    43  0 43    S 1  =  525826.2775 MHz   Err   .1
44  0 44    43  1 43    S 1  =  525826.2775 MHz   Err   .1
44  1 44    43  1 43    S 1  =  525826.2775 MHz   Err   .1
44  0 44    43  0 43    S 1  =  525826.2775 MHz   Err   .1
44  1 44    43  0 43    S 1  =  525826.2775 MHz   Err   .1
15 15  0    14 14  0    S 1  =  528689.3975 MHz   Err   .1
15 15  0    14 14  1    S 1  =  528689.3975 MHz   Err   .1
15 15  1    14 14  0    S 1  =  528689.3975 MHz   Err   .1
15 15  1    14 14  1    S 1  =  528689.3975 MHz   Err   .1
44  1 43    43  2 42    S 1  =  531764.0195 MHz   Err   .1
44  2 43    43  2 42    S 1  =  531764.0195 MHz   Err   .1
44  1 43    43  1 42    S 1  =  531764.0195 MHz   Err   .1
44  2 43    43  1 42    S 1  =  531764.0195 MHz   Err   .1
19 13  7    18 12  7    S 1  =  532487.9085 MHz   Err   .1
19 13  7    18 12  6    S 1  =  532487.9085 MHz   Err   .1
19 13  6    18 12  6    S 1  =  532487.9085 MHz   Err   .1
19 13  6    18 12  7    S 1  =  532487.9085 MHz   Err   .1
23 11 13    22 10 12    S 1  =  536102.5444 MHz   Err   .1
23 11 12    22 10 12    S 1  =  536102.5444 MHz   Err   .1
23 11 13    22 10 13    S 1  =  536102.5444 MHz   Err   .1
23 11 12    22 10 13    S 1  =  536102.5444 MHz   Err   .1
25 10 16    24  9 15    S 1  =  537688.4900 MHz   Err   .1
25 10 15    24  9 15    S 1  =  537688.4900 MHz   Err   .1
25 10 16    24  9 16    S 1  =  537688.4900 MHz   Err   .1
25 10 15    24  9 16    S 1  =  537688.4900 MHz   Err   .1
43  0 43    42  1 42    S 1  =  513981.1910 MHz   Err   .1
43  1 43    42  1 42    S 1  =  513981.1910 MHz   Err   .1
43  0 43    42  0 42    S 1  =  513981.1910 MHz   Err   .1
43  1 43    42  0 42    S 1  =  513981.1910 MHz   Err   .1
45  0 45    44  1 44    S 1  =  537668.7190 MHz   Err   .1
45  1 45    44  1 44    S 1  =  537668.7190 MHz   Err   .1
45  0 45    44  0 44    S 1  =  537668.7190 MHz   Err   .1
45  1 45    44  0 44    S 1  =  537668.7190 MHz   Err   .1
16 15  1    15 14  1    S 1  =  541321.0475 MHz   Err   .1
16 15  1    15 14  2    S 1  =  541321.0475 MHz   Err   .1
16 15  2    15 14  1    S 1  =  541321.0475 MHz   Err   .1
16 15  2    15 14  2    S 1  =  541321.0475 MHz   Err   .1
45  1 44    44  2 43    S 1  =  543604.8788 MHz   Err   .1
45  2 44    44  2 43    S 1  =  543604.8788 MHz   Err   .1
45  1 44    44  1 43    S 1  =  543604.8788 MHz   Err   .1
45  2 44    44  1 43    S 1  =  543604.8788 MHz   Err   .1
18 14  5    17 13  5    S 1  =  543226.4302 MHz   Err   .1
18 14  5    17 13  4    S 1  =  543226.4302 MHz   Err   .1
18 14  4    17 13  5    S 1  =  543226.4302 MHz   Err   .1
18 14  4    17 13  4    S 1  =  543226.4302 MHz   Err   .1
17 15  2    16 14  3    S 1  =  553951.0856 MHz   Err   .1
17 15  3    16 14  2    S 1  =  553951.0856 MHz   Err   .1
17 15  2    16 14  2    S 1  =  553951.0856 MHz   Err   .1
```

```
17 15  3    16 14  3    S 1  =  553951.0856 MHz   Err   .1
46  1 45    45  2 44    S 1  =  555443.0443 MHz   Err   .1
46  2 45    45  2 44    S 1  =  555443.0443 MHz   Err   .1
46  1 45    45  1 44    S 1  =  555443.0443 MHz   Err   .1
46  2 45    45  1 44    S 1  =  555443.0443 MHz   Err   .1
21 13  8    20 12  9    S 1  =  557722.2977 MHz   Err   .1
21 13  8    20 12  8    S 1  =  557722.2977 MHz   Err   .1
21 13  9    20 12  8    S 1  =  557722.2977 MHz   Err   .1
21 13  9    20 12  9    S 1  =  557722.2977 MHz   Err   .1
23 12 11    22 11 11    S 1  =  559535.8348 MHz   Err   .1
23 12 12    22 11 12    S 1  =  559535.8348 MHz   Err   .1
23 12 12    22 11 11    S 1  =  559535.8348 MHz   Err   .1
23 12 11    22 11 12    S 1  =  559535.8348 MHz   Err   .1
47  0 47    46  1 46    S 1  =  561345.2611 MHz   Err   .1
47  1 47    46  1 46    S 1  =  561345.2611 MHz   Err   .1
47  0 47    46  0 46    S 1  =  561345.2611 MHz   Err   .1
47  1 47    46  0 46    S 1  =  561345.2611 MHz   Err   .1
16 16  0    15 15  0    S 1  =  564665.7111 MHz   Err   .1
16 16  1    15 15  1    S 1  =  564665.7111 MHz   Err   .1
16 16  1    15 15  0    S 1  =  564665.7111 MHz   Err   .1
16 16  0    15 15  1    S 1  =  564665.7111 MHz   Err   .1
18 15  4    17 14  3    S 1  =  566579.3045 MHz   Err   .1
18 15  3    17 14  4    S 1  =  566579.3045 MHz   Err   .1
18 15  3    17 14  3    S 1  =  566579.3045 MHz   Err   .1
18 15  4    17 14  4    S 1  =  566579.3045 MHz   Err   .1
47  1 46    46  2 45    S 1  =  567278.4590 MHz   Err   .1
47  2 46    46  2 45    S 1  =  567278.4590 MHz   Err   .1
47  1 46    46  1 45    S 1  =  567278.4590 MHz   Err   .1
47  2 46    46  1 45    S 1  =  567278.4590 MHz   Err   .1
20 14  6    19 13  7    S 1  =  568473.4048 MHz   Err   .1
20 14  6    19 13  6    S 1  =  568473.4048 MHz   Err   .1
20 14  7    19 13  6    S 1  =  568473.4048 MHz   Err   .1
20 14  7    19 13  7    S 1  =  568473.4048 MHz   Err   .1
22 13  9    21 12  9    S 1  =  570332.4776 MHz   Err   .1
22 13  9    21 12 10    S 1  =  570332.4776 MHz   Err   .1
22 13 10    21 12  9    S 1  =  570332.4776 MHz   Err   .1
22 13 10    21 12 10    S 1  =  570332.4776 MHz   Err   .1
37 25 12    37 24 13    S 1  =  571653.0264 MHz   Err   .1
37 25 12    37 24 14    S 1  =  571653.0264 MHz   Err   .1
37 25 13    37 24 13    S 1  =  571653.0264 MHz   Err   .1
37 25 13    37 24 14    S 1  =  571653.0264 MHz   Err   .1
38 25 14    38 24 14    S 1  =  571596.8148 MHz   Err   .1
38 25 13    38 24 15    S 1  =  571596.8148 MHz   Err   .1
38 25 13    38 24 14    S 1  =  571596.8148 MHz   Err   .1
38 25 14    38 24 15    S 1  =  571596.8148 MHz   Err   .1
39 25 14    39 24 15    S 1  =  571536.7694 MHz   Err   .1
39 25 15    39 24 16    S 1  =  571536.7694 MHz   Err   .1
39 25 15    39 24 15    S 1  =  571536.7694 MHz   Err   .1
39 25 14    39 24 16    S 1  =  571536.7694 MHz   Err   .1
24 12 12    23 11 12    S 1  =  572123.8580 MHz   Err   .1
24 12 12    23 11 13    S 1  =  572123.8580 MHz   Err   .1
24 12 13    23 11 12    S 1  =  572123.8580 MHz   Err   .1
24 12 13    23 11 13    S 1  =  572123.8580 MHz   Err   .1
38 25 14    38 24 14    S 1  =  571596.8148 MHz   Err   .1
38 25 13    38 24 15    S 1  =  571596.8148 MHz   Err   .1
38 25 13    38 24 14    S 1  =  571596.8148 MHz   Err   .1
38 25 14    38 24 15    S 1  =  571596.8148 MHz   Err   .1
37 25 12    37 24 13    S 1  =  571653.0264 MHz   Err   .1
37 25 12    37 24 14    S 1  =  571653.0264 MHz   Err   .1
37 25 13    37 24 13    S 1  =  571653.0264 MHz   Err   .1
37 25 13    37 24 14    S 1  =  571653.0264 MHz   Err   .1
36 25 11    36 24 12    S 1  =  571705.5522 MHz   Err   .1
36 25 11    36 24 13    S 1  =  571705.5522 MHz   Err   .1
36 25 12    36 24 12    S 1  =  571705.5522 MHz   Err   .1
36 25 12    36 24 13    S 1  =  571705.5522 MHz   Err   .1
35 25 10    35 24 11    S 1  =  571754.8085 MHz   Err   .1
35 25 10    35 24 12    S 1  =  571754.8085 MHz   Err   .1
35 25 11    35 24 11    S 1  =  571754.8085 MHz   Err   .1
35 25 11    35 24 12    S 1  =  571754.8085 MHz   Err   .1
34 25 10    34 24 10    S 1  =  571800.5669 MHz   Err   .1
34 25  9    34 24 11    S 1  =  571800.5669 MHz   Err   .1
34 25  9    34 24 10    S 1  =  571800.5669 MHz   Err   .1
34 25 10    34 24 11    S 1  =  571800.5669 MHz   Err   .1
33 25  8    33 24  9    S 1  =  571843.2434 MHz   Err   .1
33 25  9    33 24 10    S 1  =  571843.2434 MHz   Err   .1
33 25  9    33 24  9    S 1  =  571843.2434 MHz   Err   .1
33 25  8    33 24 10    S 1  =  571843.2434 MHz   Err   .1
32 25  7    32 24  8    S 1  =  571882.9952 MHz   Err   .1
32 25  8    32 24  8    S 1  =  571882.9952 MHz   Err   .1
32 25  8    32 24  9    S 1  =  571882.9952 MHz   Err   .1
32 25  7    32 24  9    S 1  =  571882.9952 MHz   Err   .1
31 25  6    31 24  7    S 1  =  571919.7075 MHz   Err   .1
31 25  6    31 24  8    S 1  =  571919.7075 MHz   Err   .1
31 25  7    31 24  7    S 1  =  571919.7075 MHz   Err   .1
31 25  7    31 24  8    S 1  =  571919.7075 MHz   Err   .1
30 25  6    30 24  6    S 1  =  571953.9904 MHz   Err   .1
30 25  5    30 24  7    S 1  =  571953.9904 MHz   Err   .1
30 25  5    30 24  6    S 1  =  571953.9904 MHz   Err   .1
30 25  6    30 24  7    S 1  =  571953.9904 MHz   Err   .1
39 25 14    39 24 15    S 1  =  571536.7694 MHz   Err   .1
39 25 15    39 24 16    S 1  =  571536.7694 MHz   Err   .1
39 25 15    39 24 15    S 1  =  571536.7694 MHz   Err   .1
```

```
39 25 14    39 24 16    S 1  =  571536.7694 MHz   Err   .1
40 25 15    40 24 16    S 1  =  571472.7162 MHz   Err   .1
40 25 15    40 24 17    S 1  =  571472.7162 MHz   Err   .1
40 25 16    40 24 16    S 1  =  571472.7162 MHz   Err   .1
40 25 16    40 24 17    S 1  =  571472.7162 MHz   Err   .1
41 25 16    41 24 17    S 1  =  571404.4845 MHz   Err   .1
41 25 16    41 24 18    S 1  =  571404.4845 MHz   Err   .1
41 25 17    41 24 17    S 1  =  571404.4845 MHz   Err   .1
41 25 17    41 24 18    S 1  =  571404.4845 MHz   Err   .1
42 25 17    42 24 18    S 1  =  571331.7836 MHz   Err   .1
42 25 17    42 24 19    S 1  =  571331.7836 MHz   Err   .1
42 25 18    42 24 18    S 1  =  571331.7836 MHz   Err   .1
42 25 18    42 24 19    S 1  =  571331.7836 MHz   Err   .1
43 25 18    43 24 19    S 1  =  571254.7061 MHz   Err   .1
43 25 18    43 24 20    S 1  =  571254.7061 MHz   Err   .1
43 25 19    43 24 19    S 1  =  571254.7061 MHz   Err   .1
43 25 19    43 24 20    S 1  =  571254.7061 MHz   Err   .1
44 25 19    44 24 20    S 1  =  571172.6217 MHz   Err   .1
44 25 20    44 24 21    S 1  =  571172.6217 MHz   Err   .1
44 25 20    44 24 20    S 1  =  571172.6217 MHz   Err   .1
44 25 19    44 24 21    S 1  =  571172.6217 MHz   Err   .1
45 25 20    45 24 21    S 1  =  571085.6158 MHz   Err   .1
45 25 20    45 24 22    S 1  =  571085.6158 MHz   Err   .1
45 25 21    45 24 21    S 1  =  571085.6158 MHz   Err   .1
45 25 21    45 24 22    S 1  =  571085.6158 MHz   Err   .1
46 25 21    46 24 22    S 1  =  570993.4292 MHz   Err   .1
46 25 21    46 24 23    S 1  =  570993.4292 MHz   Err   .1
46 25 22    46 24 22    S 1  =  570993.4292 MHz   Err   .1
46 25 22    46 24 23    S 1  =  570993.4292 MHz   Err   .1
47 25 23    47 24 23    S 1  =  570895.7880 MHz   Err   .1
47 25 22    47 24 24    S 1  =  570895.7880 MHz   Err   .1
47 25 22    47 24 23    S 1  =  570895.7880 MHz   Err   .1
47 25 23    47 24 24    S 1  =  570895.7880 MHz   Err   .1
48 25 24    48 24 24    S 1  =  570792.4941 MHz   Err   .1
48 25 23    48 24 25    S 1  =  570792.4941 MHz   Err   .1
48 25 23    48 24 24    S 1  =  570792.4941 MHz   Err   .1
48 25 24    48 24 25    S 1  =  570792.4941 MHz   Err   .1
49 25 24    49 24 25    S 1  =  570683.3177 MHz   Err   .1
49 25 25    49 24 26    S 1  =  570683.3177 MHz   Err   .1
49 25 25    49 24 25    S 1  =  570683.3177 MHz   Err   .1
49 25 24    49 24 26    S 1  =  570683.3177 MHz   Err   .1
50 25 25    50 24 26    S 1  =  570568.0376 MHz   Err   .1
50 25 25    50 24 27    S 1  =  570568.0376 MHz   Err   .1
50 25 26    50 24 26    S 1  =  570568.0376 MHz   Err   .1
50 25 26    50 24 27    S 1  =  570568.0376 MHz   Err   .1
51 25 26    51 24 28    S 1  =  570446.3786 MHz   Err   .1
51 25 26    51 24 27    S 1  =  570446.3786 MHz   Err   .1
51 25 27    51 24 27    S 1  =  570446.3786 MHz   Err   .1
51 25 27    51 24 28    S 1  =  570446.3786 MHz   Err   .1
52 25 28    52 24 29    S 1  =  570318.1215 MHz   Err   .1
52 25 28    52 24 28    S 1  =  570318.1215 MHz   Err   .1
52 25 27    52 24 28    S 1  =  570318.1215 MHz   Err   .1
52 25 27    52 24 29    S 1  =  570318.1215 MHz   Err   .1
53 25 29    53 24 29    S 1  =  570183.0195 MHz   Err   .1
53 25 28    53 24 30    S 1  =  570183.0195 MHz   Err   .1
53 25 28    53 24 29    S 1  =  570183.0195 MHz   Err   .1
53 25 29    53 24 30    S 1  =  570183.0195 MHz   Err   .1
54 25 29    54 24 30    S 1  =  570040.8041 MHz   Err   .1
54 25 29    54 24 31    S 1  =  570040.8041 MHz   Err   .1
54 25 30    54 24 30    S 1  =  570040.8041 MHz   Err   .1
54 25 30    54 24 31    S 1  =  570040.8041 MHz   Err   .1
55 25 30    55 24 31    S 1  =  569891.1556 MHz   Err   .1
55 25 30    55 24 32    S 1  =  569891.1556 MHz   Err   .1
55 25 31    55 24 31    S 1  =  569891.1556 MHz   Err   .1
55 25 31    55 24 32    S 1  =  569891.1556 MHz   Err   .1
56 25 32    56 24 32    S 1  =  569733.9663 MHz   Err   .1
56 25 31    56 24 33    S 1  =  569733.9663 MHz   Err   .1
56 25 31    56 24 32    S 1  =  569733.9663 MHz   Err   .1
56 25 32    56 24 33    S 1  =  569733.9663 MHz   Err   .1
57 25 33    57 24 33    S 1  =  569568.7264 MHz   Err   .1
57 25 32    57 24 34    S 1  =  569568.7264 MHz   Err   .1
57 25 32    57 24 33    S 1  =  569568.7264 MHz   Err   .1
57 25 33    57 24 34    S 1  =  569568.7264 MHz   Err   .1
58 25 33    58 24 34    S 1  =  569395.3808 MHz   Err   .1
58 25 33    58 24 35    S 1  =  569395.3808 MHz   Err   .1
58 25 34    58 24 34    S 1  =  569395.3808 MHz   Err   .1
58 25 34    58 24 35    S 1  =  569395.3808 MHz   Err   .1
59 25 34    59 24 36    S 1  =  569213.2202 MHz   Err   .1
59 25 34    59 24 35    S 1  =  569213.2202 MHz   Err   .1
59 25 35    59 24 35    S 1  =  569213.2202 MHz   Err   .1
59 25 35    59 24 36    S 1  =  569213.2202 MHz   Err   .1
60 25 35    60 24 36    S 1  =  569022.9605 MHz   Err   .1
60 25 36    60 24 37    S 1  =  569022.9605 MHz   Err   .1
60 25 36    60 24 36    S 1  =  569022.9605 MHz   Err   .1
60 25 35    60 24 37    S 1  =  569022.9605 MHz   Err   .1
61 25 36    61 24 38    S 1  =  568823.0660 MHz   Err   .1
61 25 36    61 24 37    S 1  =  568823.0660 MHz   Err   .1
61 25 37    61 24 37    S 1  =  568823.0660 MHz   Err   .1
61 25 37    61 24 38    S 1  =  568823.0660 MHz   Err   .1
62 25 37    62 24 38    S 1  =  568613.9349 MHz   Err   .1
62 25 37    62 24 39    S 1  =  568613.9349 MHz   Err   .1
62 25 38    62 24 38    S 1  =  568613.9349 MHz   Err   .1
```

```
62 25 38    62 24 39    S 1  =  568613.9349 MHz   Err   .1
63 25 38    63 24 40    S 1  =  568395.0372 MHz   Err   .1
63 25 38    63 24 39    S 1  =  568395.0372 MHz   Err   .1
63 25 39    63 24 39    S 1  =  568395.0372 MHz   Err   .1
63 25 39    63 24 40    S 1  =  568395.0372 MHz   Err   .1
64 25 39    64 24 40    S 1  =  568166.1922 MHz   Err   .1
64 25 39    64 24 41    S 1  =  568166.1922 MHz   Err   .1
64 25 40    64 24 40    S 1  =  568166.1922 MHz   Err   .1
64 25 40    64 24 41    S 1  =  568166.1922 MHz   Err   .1
38 25 14    38 24 14    S 1  =  571596.8148 MHz   Err   .1
38 25 13    38 24 15    S 1  =  571596.8148 MHz   Err   .1
38 25 13    38 24 14    S 1  =  571596.8148 MHz   Err   .1
38 25 14    38 24 15    S 1  =  571596.8148 MHz   Err   .1
37 25 12    37 24 13    S 1  =  571653.0264 MHz   Err   .1
37 25 12    37 24 14    S 1  =  571653.0264 MHz   Err   .1
37 25 13    37 24 13    S 1  =  571653.0264 MHz   Err   .1
37 25 13    37 24 14    S 1  =  571653.0264 MHz   Err   .1
36 25 11    36 24 12    S 1  =  571705.5522 MHz   Err   .1
36 25 11    36 24 13    S 1  =  571705.5522 MHz   Err   .1
36 25 12    36 24 12    S 1  =  571705.5522 MHz   Err   .1
36 25 12    36 24 13    S 1  =  571705.5522 MHz   Err   .1
35 25 10    35 24 11    S 1  =  571754.8085 MHz   Err   .1
35 25 10    35 24 12    S 1  =  571754.8085 MHz   Err   .1
35 25 11    35 24 11    S 1  =  571754.8085 MHz   Err   .1
35 25 11    35 24 12    S 1  =  571754.8085 MHz   Err   .1
34 25 10    34 24 10    S 1  =  571800.5669 MHz   Err   .1
34 25  9    34 24 11    S 1  =  571800.5669 MHz   Err   .1
34 25  9    34 24 10    S 1  =  571800.5669 MHz   Err   .1
34 25 10    34 24 11    S 1  =  571800.5669 MHz   Err   .1
33 25  8    33 24  9    S 1  =  571843.2434 MHz   Err   .1
33 25  9    33 24 10    S 1  =  571843.2434 MHz   Err   .1
33 25  9    33 24  9    S 1  =  571843.2434 MHz   Err   .1
33 25  8    33 24 10    S 1  =  571843.2434 MHz   Err   .1
32 25  7    32 24  8    S 1  =  571882.9952 MHz   Err   .1
32 25  8    32 24  8    S 1  =  571882.9952 MHz   Err   .1
32 25  8    32 24  9    S 1  =  571882.9952 MHz   Err   .1
32 25  7    32 24  9    S 1  =  571882.9952 MHz   Err   .1
31 25  6    31 24  7    S 1  =  571919.7075 MHz   Err   .1
31 25  7    31 24  8    S 1  =  571919.7075 MHz   Err   .1
31 25  7    31 24  7    S 1  =  571919.7075 MHz   Err   .1
31 25  6    31 24  8    S 1  =  571919.7075 MHz   Err   .1
30 25  6    30 24  7    S 1  =  571953.9904 MHz   Err   .1
30 25  6    30 24  6    S 1  =  571953.9904 MHz   Err   .1
30 25  5    30 24  6    S 1  =  571953.9904 MHz   Err   .1
30 25  5    30 24  7    S 1  =  571953.9904 MHz   Err   .1
29 25  4    29 24  5    S 1  =  571985.7391 MHz   Err   .1
29 25  4    29 24  6    S 1  =  571985.7391 MHz   Err   .1
29 25  5    29 24  5    S 1  =  571985.7391 MHz   Err   .1
29 25  5    29 24  6    S 1  =  571985.7391 MHz   Err   .1
28 25  4    28 24  4    S 1  =  572014.9992 MHz   Err   .1
28 25  3    28 24  5    S 1  =  572014.9992 MHz   Err   .1
28 25  3    28 24  4    S 1  =  572014.9992 MHz   Err   .1
28 25  4    28 24  5    S 1  =  572014.9992 MHz   Err   .1
27 25  2    27 24  3    S 1  =  572042.0342 MHz   Err   .1
27 25  3    27 24  4    S 1  =  572042.0342 MHz   Err   .1
27 25  3    27 24  3    S 1  =  572042.0342 MHz   Err   .1
27 25  2    27 24  4    S 1  =  572042.0342 MHz   Err   .1
26 25  2    26 24  2    S 1  =  572066.9476 MHz   Err   .1
26 25  1    26 24  3    S 1  =  572066.9476 MHz   Err   .1
26 25  1    26 24  2    S 1  =  572066.9476 MHz   Err   .1
26 25  2    26 24  3    S 1  =  572066.9476 MHz   Err   .1
25 25  0    25 24  1    S 1  =  572089.8344 MHz   Err   .1
25 25  0    25 24  2    S 1  =  572089.8344 MHz   Err   .1
25 25  1    25 24  1    S 1  =  572089.8344 MHz   Err   .1
25 25  1    25 24  2    S 1  =  572089.8344 MHz   Err   .1
48  0 48    47  1 47    S 1  =  573179.3192 MHz   Err   .1
48  1 48    47  1 47    S 1  =  573179.3192 MHz   Err   .1
48  0 48    47  0 47    S 1  =  573179.3192 MHz   Err   .1
48  1 48    47  0 47    S 1  =  573179.3192 MHz   Err   .1
47  2 45    46  3 44    S 1  =  573246.8041 MHz   Err   .1
47  3 45    46  3 44    S 1  =  573246.8041 MHz   Err   .1
47  2 45    46  2 44    S 1  =  573246.8041 MHz   Err   .1
47  3 45    46  2 44    S 1  =  573246.8041 MHz   Err   .1
46  4 42    45  5 41    S 1  =  573279.4045 MHz   Err   .1
45 10 35    44 10 34    S 1  =  573372.9191 MHz   Err   .1
46  5 42    45  5 41    S 1  =  573647.8909 MHz   Err   .1
46  4 42    45  4 41    S 1  =  573800.6337 MHz   Err   .1
26 11 16    25 10 15    S 1  =  573778.7320 MHz   Err   .1
26 11 15    25 10 15    S 1  =  573778.7320 MHz   Err   .1
26 11 16    25 10 16    S 1  =  573778.7320 MHz   Err   .1
26 11 15    25 10 16    S 1  =  573778.7320 MHz   Err   .1
46  5 42    45  4 41    S 1  =  574169.0924 MHz   Err   .1
45  9 37    44  9 36    S 1  =  574343.6258 MHz   Err   .1
28 10 19    27  9 18    S 1  =  575148.3093 MHz   Err   .1
28 10 18    27  9 18    S 1  =  575148.3093 MHz   Err   .1
28 10 19    27  9 19    S 1  =  575148.3093 MHz   Err   .1
28 10 18    27  9 19    S 1  =  575148.3093 MHz   Err   .1
45  9 36    44  9 35    S 1  =  575668.3867 MHz   Err   .1
46  5 41    45  6 40    S 1  =  575974.7124 MHz   Err   .1
17 16  1    16 15  1    S 1  =  577295.6119 MHz   Err   .1
17 16  1    16 15  2    S 1  =  577295.6119 MHz   Err   .1
17 16  2    16 15  1    S 1  =  577295.6119 MHz   Err   .1
```

```
17 16  2    16 15  2    S 1  =  577295.6119 MHz   Err   .1
48  1 47    47  2 46    S 1  =  579111.1458 MHz   Err   .1
48  2 47    47  2 46    S 1  =  579111.1458 MHz   Err   .1
48  1 47    47  1 46    S 1  =  579111.1458 MHz   Err   .1
48  2 47    47  1 46    S 1  =  579111.1458 MHz   Err   .1
19 15  4    18 14  4    S 1  =  579205.2243 MHz   Err   .1
19 15  4    18 14  5    S 1  =  579205.2243 MHz   Err   .1
19 15  5    18 14  4    S 1  =  579205.2243 MHz   Err   .1
19 15  5    18 14  5    S 1  =  579205.2243 MHz   Err   .1
47  3 44    46  4 43    S 1  =  579276.4248 MHz   Err   .1
47  4 44    46  3 43    S 1  =  579316.8224 MHz   Err   .1
47  4 44    46  4 43    S 1  =  579292.8476 MHz   Err   .1
47  3 44    46  3 43    S 1  =  579300.3477 MHz   Err   .1
46  6 41    45  6 40    S 1  =  579768.6708 MHz   Err   .1
45  8 37    44  8 36    S 1  =  580651.9203 MHz   Err   .1
21 14  7    20 13  7    S 1  =  581091.9277 MHz   Err   .1
21 14  7    20 13  8    S 1  =  581091.9277 MHz   Err   .1
21 14  8    20 13  7    S 1  =  581091.9277 MHz   Err   .1
21 14  8    20 13  8    S 1  =  581091.9277 MHz   Err   .1
46  5 41    45  5 40    S 1  =  581077.3087 MHz   Err   .1
46 22 24    45 22 23    S 1  =  581264.2168 MHz   Err   .1
46 22 25    45 22 24    S 1  =  581264.2168 MHz   Err   .1
46 21 25    45 21 24    S 1  =  581391.2717 MHz   Err   .1
46 21 26    45 21 25    S 1  =  581391.2717 MHz   Err   .1
46 20 26    45 20 25    S 1  =  581535.2652 MHz   Err   .1
46 20 27    45 20 26    S 1  =  581535.2652 MHz   Err   .1
46 19 27    45 19 26    S 1  =  581700.1170 MHz   Err   .1
46 19 28    45 19 27    S 1  =  581700.1170 MHz   Err   .1
46 18 28    45 18 27    S 1  =  581890.9217 MHz   Err   .1
46 18 29    45 18 28    S 1  =  581890.9217 MHz   Err   .1
46 17 29    45 17 28    S 1  =  582114.4895 MHz   Err   .1
46 17 30    45 17 29    S 1  =  582114.4895 MHz   Err   .1
46 16 30    45 16 29    S 1  =  582379.9677 MHz   Err   .1
46 16 31    45 16 30    S 1  =  582379.9677 MHz   Err   .1
46 15 32    45 15 31    S 1  =  582700.0991 MHz   Err   .1
46 15 31    45 15 30    S 1  =  582700.0991 MHz   Err   .1
23 13 10    22 12 10    S 1  =  582937.1677 MHz   Err   .1
23 13 10    22 12 11    S 1  =  582937.1677 MHz   Err   .1
23 13 11    22 12 10    S 1  =  582937.1677 MHz   Err   .1
23 13 11    22 12 11    S 1  =  582937.1677 MHz   Err   .1
46 14 33    45 14 32    S 1  =  583093.1237 MHz   Err   .1
46 14 32    45 14 31    S 1  =  583093.1237 MHz   Err   .1
46 13 34    45 13 33    S 1  =  583586.1558 MHz   Err   .1
46 13 33    45 13 32    S 1  =  583586.1558 MHz   Err   .1
45  7 38    44  7 37    S 1  =  584257.0560 MHz   Err   .1
25 12 13    24 11 13    S 1  =  584702.8542 MHz   Err   .1
25 12 13    24 11 14    S 1  =  584702.8542 MHz   Err   .1
25 12 14    24 11 13    S 1  =  584702.8542 MHz   Err   .1
25 12 14    24 11 14    S 1  =  584702.8542 MHz   Err   .1
46  7 40    45  7 39    S 1  =  584832.3471 MHz   Err   .1
46  6 41    45  5 40    S 1  =  584871.2287 MHz   Err   .1
49  0 49    48  1 48    S 1  =  585010.4820 MHz   Err   .1
49  1 49    48  1 48    S 1  =  585010.4820 MHz   Err   .1
49  0 49    48  0 48    S 1  =  585010.4820 MHz   Err   .1
49  1 49    48  0 48    S 1  =  585010.4820 MHz   Err   .1
46 11 36    45 11 35    S 1  =  585061.1649 MHz   Err   .1
48  2 46    47  3 45    S 1  =  585075.9864 MHz   Err   .1
48  3 46    47  3 45    S 1  =  585075.9864 MHz   Err   .1
48  2 46    47  2 45    S 1  =  585075.9864 MHz   Err   .1
48  3 46    47  2 45    S 1  =  585075.9864 MHz   Err   .1
46 11 35    45 11 34    S 1  =  585085.8467 MHz   Err   .1
47  4 43    46  5 42    S 1  =  585206.8930 MHz   Err   .1
33  8 26    32  7 25    S 1  =  585379.3013 MHz   Err   .1
47  5 43    46  5 42    S 1  =  585466.2010 MHz   Err   .1
47  4 43    46  4 42    S 1  =  585575.3675 MHz   Err   .1
47  5 43    46  4 42    S 1  =  585834.6648 MHz   Err   .1
46 10 37    45 10 36    S 1  =  586158.3065 MHz   Err   .1
27 11 17    26 10 16    S 1  =  586309.9545 MHz   Err   .1
27 11 16    26 10 16    S 1  =  586309.9545 MHz   Err   .1
27 11 17    26 10 17    S 1  =  586309.9545 MHz   Err   .1
27 11 16    26 10 17    S 1  =  586309.9545 MHz   Err   .1
46 10 36    45 10 35    S 1  =  586408.8765 MHz   Err   .1
46  9 38    45  9 37    S 1  =  587287.0899 MHz   Err   .1
46  8 39    45  8 38    S 1  =  587349.6957 MHz   Err   .1
29 10 20    28  9 19    S 1  =  587587.2785 MHz   Err   .1
29 10 19    28  9 19    S 1  =  587587.2785 MHz   Err   .1
29 10 20    28  9 20    S 1  =  587587.2785 MHz   Err   .1
29 10 19    28  9 20    S 1  =  587587.2785 MHz   Err   .1
31  9 23    30  8 22    S 1  =  588086.1368 MHz   Err   .1
33  8 25    32  7 26    S 1  =  588152.5324 MHz   Err   .1
47  5 42    46  6 41    S 1  =  588850.3493 MHz   Err   .1
46  9 37    45  9 36    S 1  =  589085.1945 MHz   Err   .1
18 16  2    17 15  2    S 1  =  589923.8492 MHz   Err   .1
18 16  2    17 15  3    S 1  =  589923.8492 MHz   Err   .1
18 16  3    17 15  2    S 1  =  589923.8492 MHz   Err   .1
18 16  3    17 15  3    S 1  =  589923.8492 MHz   Err   .1
46  6 40    45  6 39    S 1  =  590556.1970 MHz   Err   .1
48  3 45    47  4 44    S 1  =  591103.3034 MHz   Err   .1
48  4 45    47  4 44    S 1  =  591114.5432 MHz   Err   .1
48  3 45    47  3 44    S 1  =  591119.6051 MHz   Err   .1
48  4 45    47  3 44    S 1  =  591130.8615 MHz   Err   .1
35  7 29    34  6 29    S 1  =  591530.9229 MHz   Err   .1
```

```
47  6 42    46  6 41    S 1  =  591648.6937 MHz   Err   .1
20 15  5    19 14  5    S 1  =  591828.6805 MHz   Err   .1
20 15  5    19 14  6    S 1  =  591828.6805 MHz   Err   .1
20 15  6    19 14  5    S 1  =  591828.6805 MHz   Err   .1
20 15  6    19 14  6    S 1  =  591828.6805 MHz   Err   .1
47  5 42    46  5 41    S 1  =  592644.3385 MHz   Err   .1
28  5 24    27  2 25    S 1  =  592781.5901 MHz   Err   .1
22 14  8    21 13  8    S 1  =  593706.5752 MHz   Err   .1
22 14  9    21 13  9    S 1  =  593706.5752 MHz   Err   .1
22 14  9    21 13  8    S 1  =  593706.5752 MHz   Err   .1
22 14  8    21 13  9    S 1  =  593706.5752 MHz   Err   .1
47 33 14    46 33 13    S 1  =  593013.3884 MHz   Err   .1
47 33 15    46 33 14    S 1  =  593013.3884 MHz   Err   .1
47 32 15    46 32 14    S 1  =  593070.2712 MHz   Err   .1
47 32 16    46 32 15    S 1  =  593070.2712 MHz   Err   .1
47 31 16    46 31 15    S 1  =  593129.5116 MHz   Err   .1
47 31 17    46 31 16    S 1  =  593129.5116 MHz   Err   .1
47 30 17    46 30 16    S 1  =  593192.0123 MHz   Err   .1
47 30 18    46 30 17    S 1  =  593192.0123 MHz   Err   .1
47 29 18    46 29 17    S 1  =  593258.3020 MHz   Err   .1
47 29 19    46 29 18    S 1  =  593258.3020 MHz   Err   .1
47 27 20    46 27 19    S 1  =  593404.7766 MHz   Err   .1
47 27 21    46 27 20    S 1  =  593404.7766 MHz   Err   .1
47 26 21    46 26 20    S 1  =  593486.7200 MHz   Err   .1
47 26 22    46 26 21    S 1  =  593486.7200 MHz   Err   .1
47 25 22    46 25 21    S 1  =  593575.8183 MHz   Err   .1
47 25 23    46 25 22    S 1  =  593575.8183 MHz   Err   .1
22 14  8    21 13  8    S 1  =  593706.5752 MHz   Err   .1
22 14  9    21 13  9    S 1  =  593706.5752 MHz   Err   .1
22 14  9    21 13  8    S 1  =  593706.5752 MHz   Err   .1
22 14  8    21 13  9    S 1  =  593706.5752 MHz   Err   .1
47 23 24    46 23 23    S 1  =  593781.3567 MHz   Err   .1
47 23 25    46 23 24    S 1  =  593781.3567 MHz   Err   .1
47 22 25    46 22 24    S 1  =  593901.3780 MHz   Err   .1
47 22 26    46 22 25    S 1  =  593901.3780 MHz   Err   .1
47 21 26    46 21 25    S 1  =  594036.3585 MHz   Err   .1
47 21 27    46 21 26    S 1  =  594036.3585 MHz   Err   .1
47 20 27    46 20 26    S 1  =  594189.2639 MHz   Err   .1
47 20 28    46 20 27    S 1  =  594189.2639 MHz   Err   .1
47 19 28    46 19 27    S 1  =  594364.8081 MHz   Err   .1
47 19 29    46 19 28    S 1  =  594364.8081 MHz   Err   .1
47 26 21    47 25 22    S 1  =  594251.5414 MHz   Err   .1
47 26 21    47 25 23    S 1  =  594251.5414 MHz   Err   .1
47 26 22    47 25 22    S 1  =  594251.5414 MHz   Err   .1
47 26 22    47 25 23    S 1  =  594251.5414 MHz   Err   .1
46 26 20    46 25 21    S 1  =  594340.6424 MHz   Err   .1
46 26 20    46 25 22    S 1  =  594340.6424 MHz   Err   .1
46 26 21    46 25 21    S 1  =  594340.6424 MHz   Err   .1
46 26 21    46 25 22    S 1  =  594340.6424 MHz   Err   .1
45 26 19    45 25 20    S 1  =  594424.9324 MHz   Err   .1
45 26 19    45 25 21    S 1  =  594424.9324 MHz   Err   .1
45 26 20    45 25 20    S 1  =  594424.9324 MHz   Err   .1
45 26 20    45 25 21    S 1  =  594424.9324 MHz   Err   .1
32  5 27    31  4 28    S 1  =  594417.2251 MHz   Err   .1
44 26 18    44 25 19    S 1  =  594504.3486 MHz   Err   .1
44 26 19    44 25 20    S 1  =  594504.3486 MHz   Err   .1
44 26 19    44 25 19    S 1  =  594504.3486 MHz   Err   .1
44 26 18    44 25 20    S 1  =  594504.3486 MHz   Err   .1
46  8 38    45  8 37    S 1  =  594507.3654 MHz   Err   .1
47 18 29    46 18 28    S 1  =  594567.9841 MHz   Err   .1
47 18 30    46 18 29    S 1  =  594567.9841 MHz   Err   .1
43 26 17    43 25 19    S 1  =  594579.5282 MHz   Err   .1
43 26 17    43 25 18    S 1  =  594579.5282 MHz   Err   .1
43 26 18    43 25 18    S 1  =  594579.5282 MHz   Err   .1
43 26 18    43 25 19    S 1  =  594579.5282 MHz   Err   .1
42 26 16    42 25 18    S 1  =  594650.3502 MHz   Err   .1
42 26 16    42 25 17    S 1  =  594650.3502 MHz   Err   .1
42 26 17    42 25 17    S 1  =  594650.3502 MHz   Err   .1
42 26 17    42 25 18    S 1  =  594650.3502 MHz   Err   .1
41 26 15    41 25 16    S 1  =  594717.0316 MHz   Err   .1
41 26 15    41 25 17    S 1  =  594717.0316 MHz   Err   .1
41 26 16    41 25 16    S 1  =  594717.0316 MHz   Err   .1
41 26 16    41 25 17    S 1  =  594717.0316 MHz   Err   .1
40 26 14    40 25 15    S 1  =  594779.7456 MHz   Err   .1
40 26 14    40 25 16    S 1  =  594779.7456 MHz   Err   .1
40 26 15    40 25 15    S 1  =  594779.7456 MHz   Err   .1
40 26 15    40 25 16    S 1  =  594779.7456 MHz   Err   .1
47 17 30    46 17 29    S 1  =  594806.3001 MHz   Err   .1
47 17 31    46 17 30    S 1  =  594806.3001 MHz   Err   .1
39 26 13    39 25 14    S 1  =  594838.7279 MHz   Err   .1
39 26 13    39 25 15    S 1  =  594838.7279 MHz   Err   .1
39 26 14    39 25 14    S 1  =  594838.7279 MHz   Err   .1
39 26 14    39 25 15    S 1  =  594838.7279 MHz   Err   .1
38 26 12    38 25 13    S 1  =  594894.0777 MHz   Err   .1
38 26 12    38 25 14    S 1  =  594894.0777 MHz   Err   .1
38 26 13    38 25 13    S 1  =  594894.0777 MHz   Err   .1
38 26 13    38 25 14    S 1  =  594894.0777 MHz   Err   .1
37 26 11    37 25 12    S 1  =  594945.9687 MHz   Err   .1
37 26 11    37 25 13    S 1  =  594945.9687 MHz   Err   .1
37 26 12    37 25 12    S 1  =  594945.9687 MHz   Err   .1
37 26 12    37 25 13    S 1  =  594945.9687 MHz   Err   .1
36 26 10    36 25 11    S 1  =  594994.5930 MHz   Err   .1
```

```
 36 26 10    36 25 12    S 1  =  594994.5930 MHz   Err   .1
 36 26 11    36 25 11    S 1  =  594994.5930 MHz   Err   .1
 36 26 11    36 25 12    S 1  =  594994.5930 MHz   Err   .1
 35 26  9    35 25 10    S 1  =  595040.1258 MHz   Err   .1
 35 26  9    35 25 11    S 1  =  595040.1258 MHz   Err   .1
 35 26 10    35 25 10    S 1  =  595040.1258 MHz   Err   .1
 35 26 10    35 25 11    S 1  =  595040.1258 MHz   Err   .1
 34 26  8    34 25  9    S 1  =  595082.6593 MHz   Err   .1
 34 26  9    34 25  9    S 1  =  595082.6593 MHz   Err   .1
 34 26  9    34 25 10    S 1  =  595082.6593 MHz   Err   .1
 34 26  8    34 25 10    S 1  =  595082.6593 MHz   Err   .1
 33 26  7    33 25  8    S 1  =  595122.3316 MHz   Err   .1
 33 26  7    33 25  9    S 1  =  595122.3316 MHz   Err   .1
 33 26  8    33 25  8    S 1  =  595122.3316 MHz   Err   .1
 33 26  8    33 25  9    S 1  =  595122.3316 MHz   Err   .1
 32 26  6    32 25  7    S 1  =  595159.3574 MHz   Err   .1
 32 26  6    32 25  8    S 1  =  595159.3574 MHz   Err   .1
 32 26  7    32 25  7    S 1  =  595159.3574 MHz   Err   .1
 32 26  7    32 25  8    S 1  =  595159.3574 MHz   Err   .1
 31 26  5    31 25  6    S 1  =  595193.7827 MHz   Err   .1
 31 26  6    31 25  6    S 1  =  595193.7827 MHz   Err   .1
 31 26  6    31 25  7    S 1  =  595193.7827 MHz   Err   .1
 31 26  5    31 25  7    S 1  =  595193.7827 MHz   Err   .1
 30 26  4    30 25  5    S 1  =  595225.7688 MHz   Err   .1
 30 26  4    30 25  6    S 1  =  595225.7688 MHz   Err   .1
 30 26  5    30 25  5    S 1  =  595225.7688 MHz   Err   .1
 30 26  5    30 25  6    S 1  =  595225.7688 MHz   Err   .1
 29 26  3    29 25  4    S 1  =  595255.4667 MHz   Err   .1
 29 26  4    29 25  4    S 1  =  595255.4667 MHz   Err   .1
 29 26  4    29 25  5    S 1  =  595255.4667 MHz   Err   .1
 29 26  3    29 25  5    S 1  =  595255.4667 MHz   Err   .1
 28 26  2    28 25  3    S 1  =  595283.0304 MHz   Err   .1
 28 26  2    28 25  4    S 1  =  595283.0304 MHz   Err   .1
 28 26  3    28 25  3    S 1  =  595283.0304 MHz   Err   .1
 28 26  3    28 25  4    S 1  =  595283.0304 MHz   Err   .1
 27 26  1    27 25  2    S 1  =  595308.4253 MHz   Err   .1
 27 26  1    27 25  3    S 1  =  595308.4253 MHz   Err   .1
 27 26  2    27 25  2    S 1  =  595308.4253 MHz   Err   .1
 27 26  2    27 25  3    S 1  =  595308.4253 MHz   Err   .1
 26 26  1    26 25  1    S 1  =  595332.0664 MHz   Err   .1
 26 26  0    26 25  2    S 1  =  595332.0664 MHz   Err   .1
 26 26  0    26 25  1    S 1  =  595332.0664 MHz   Err   .1
 26 26  1    26 25  2    S 1  =  595332.0664 MHz   Err   .1
 47 15 33    46 15 32    S 1  =  595431.6057 MHz   Err   .1
 47 15 32    46 15 31    S 1  =  595431.6057 MHz   Err   .1
 47  6 42    46  5 41    S 1  =  595442.6586 MHz   Err   .1
 24 13 11    23 12 11    S 1  =  595535.7149 MHz   Err   .1
 24 13 11    23 12 12    S 1  =  595535.7149 MHz   Err   .1
 24 13 12    23 12 11    S 1  =  595535.7149 MHz   Err   .1
 24 13 12    23 12 12    S 1  =  595535.7149 MHz   Err   .1
 34  6 28    33  5 29    S 1  =  595822.5341 MHz   Err   .1
 47 14 34    46 14 33    S 1  =  595852.0836 MHz   Err   .1
 47 14 33    46 14 32    S 1  =  595852.0836 MHz   Err   .1
\-------------------------------------------------------------------------------
\------------------end of data--------------------------------------------------
```

Bibliography

1. H. S. P. Müller, D. A. Thorwirth, Roth, G. Winnewisser, *J. Mol. Struct.* 215–227 (2005).
2. E. Herbst, E. F. van Dishoeck, *Annual Review of Astronomy and Astrophysics* **47**, 427–480 (2009).
3. A. Horn *et al.*, *The Astrophysical Journal* **611**, 605–614 (2004).
4. K. I. Öberg, S. Bottinelli, J. K. Jørgensen, E. F. van Dishoeck, *The Astrophysical Journal* **716**, 825–834 (06/2010).
5. K. I. Öberg, E. F. van Dishoeck, H. Linnartz, presented at the Organic Matter in Space, vol. 4, pp. 449–450, DOI: 10.1017/S1743921308022151.
6. J. . M. Hollis, F. J. Lovas, P. R. Jewell, *Journal* (2000).
7. A. C. Cheung, D. M. Rank, C. H. Townes, D. D. Thornton, W. J. Welch, *Phys. Rev. Lett.* **21**, 1701–1705 (25 12/1968).
8. L. E. Snyder, D. Buhl, *ApJ* **163**, L47 (01/1971).
9. M. B. Bell *et al.*, *The Astrophysical Journal Letters* **483**, L61 (1997).
10. J. Cami, J. Bernard-Salas, E. Peeters, S. E. Malek, *Science* **329**, 1180–1182, ISSN: 0036-8075 (2010).
11. K. Sellgren, K. I. Uchida, M. W. Werner, *The Astrophysical Journal* **659**, 1338 (2007).
12. W. W. Duley, A. Hu, *The Astrophysical Journal Letters* **745**, L11 (2012).
13. K. Sellgren *et al.*, *The Astrophysical Journal Letters* **722**, L54 (2010).
14. Y. Zhang, S. Kwok, *The Astrophysical Journal* **730**, 126 (2011).
15. B. A. McGuire *et al.*, *Science*, ISSN: 0036-8075, DOI: 10.1126/science.aae0328 (2016).
16. E. Herbst, *Phys. Chem. Chem. Phys.* **16**, 3344–3359 (8 2014).
17. J. Hagege, P. C. Roberge, C. Vermeil, *Trans. Faraday Soc.* **64**, 3288–3299 (1968).
18. A. Chang, S. Lin, *Chemical Physics Letters* **384**, 229–235, ISSN: 0009-2614 (2004).
19. W. S. Xia, R. S. Zhu, M. C. Lin, A. M. Mebel, *Faraday Discuss.* **119**, 191–205 (2002).
20. M. Bertin *et al.*, *The Astrophysical Journal Letters* **817**, L12 (2016).
21. J. R. Cronin, C. B. Moore, *Science* **172**, 1327–1329 (1971).
22. J. L. Bada, *Astrobiology* **1**, 259–269 (07/2004).

23. S. Pizzarello, X. Feng, S. Epstein, J. Cronin, *Geochimica et Cosmochimica Acta* **58**, 5579–5587, ISSN: 0016-7037 (1994).
24. A. S. Burton *et al.*, *Meteoritics & Planetary Science* **49**, 2074–2086, ISSN: 1945-5100 (2014).
25. A. S. Burton *et al.*, *Meteoritics & Planetary Science* **50**, 470–482, ISSN: 1945-5100 (2015).
26. J. E. Elsila, D. P. Glavin, J. P. Dworkin, *Meteoritics & Planetary Science* **44**, 1323–1330 (2009).
27. A. Singh, A. Misra, P. Tandon, *Research in Astronomy and Astrophysics* **13**, 912 (2013).
28. G. W. Fuchs *et al.*, *Faraday Discuss.* **133**, 331–345 (2006).
29. K. I. Öberg, R. T. Garrod, E. F. van Dishoeck, H. Linnartz, *A&A* **504**, 891–913, ISSN: 1432-0746 (09/2009).
30. P. Carroll, B. J. Drouin, S. L. Widicus Weaver, *The Astroph* **723**, 845 (2010).
31. N. F. W. Ligterink *et al.*, *Astronomy and Astrophysics* **584**, A56 (12/2015).
32. H. J. Fraser, M. P. Collings, M. R. S. McCoustra, D. A. Williams, *Monthly Notices of the Royal Astronomical Society* **327**, 1165–1172 (2001).
33. Öberg, K. I., Fayolle, E. C., Cuppen, H. M., van Dishoeck, E. F., Linnartz, H., *A&A* **505**, 183–194 (2009).
34. M. Klussmann, D. G. Blackmond, in *Chemical Evolution II: From the Origins of Life to Modern Society*, chap. 8, pp. 133–145, DOI: 10.1021/bk-2009-1025.ch007.
35. Y. Saito, H. Hyuga, *Rev. Mod. Phys.* **85**, 603–621 (2 04/2013).
36. F. Frank, *Biochimica et Biophysica Acta* **11**, 459–463, ISSN: 0006-3002 (1953).
37. K. Soai, T. Shibata, H. Morioka, K. Choji, *Nature* **378**, 767–768 (12/1995).
38. M. Engel, S. Macko, *Nature* **389**, 265–268 (07/1997).
39. K. Soai, T. Kawasaki, A. Matsumoto, *Accounts of Chemical Research* **47**, PMID: 25511374, 3643–3654 (2014).
40. J. J. Flores, W. A. Bonner, G. A. Massey, *J Am Chem Soc* **99**, 3622–5 (05/1997).
41. J. D. Swalen, D. R. Herschbach, *The Journal of Chemical Physics* **27**, 100–108 (1957).
42. C. C. Lin, J. D. Swalen, *Rev. Mod. Phys.* **31**, 841–892 (4 10/1959).
43. R. A. Creswell, R. Schwendeman, *Journal of Molecular Spectroscopy* **64**, 295–301, ISSN: 0022-2852 (1977).
44. M. Imachi, R. Kuczkowski, *Journal of Molecular Structure* **96**, 55–60, ISSN: 0022-2860 (1983).
45. M. Tobin, *Spectrochimica Acta* **16**, 1108–1110, ISSN: 0371-1951 (1960).

46. W. Fateley, F. A. Miller, *Spectrochimica Acta* **19**, 611–628, ISSN: 0371-1951 (1963).

47. F. Winther, D. Hummel, *Spectrochimica Acta Part A: Molecular Spectroscopy* **25**, 417–423, ISSN: 0584-8539 (1969).

48. V. Barone, M. Biczysko, J. Bloino, C. Puzzarini, *The Journal of Chemical Physics* **141**, DOI: http://dx.doi.org/10.1063/1.4887357 (2014).

49. J. R. Villarreal, J. Laane, *The Journal of Chemical Physics* **62**, 303–304 (1975).

50. S. Turchini *et al.*, *Phys. Rev. A* **70**, 014502 (1 07/2004).

51. S. Stranges *et al.*, *The Journal of Chemical Physics* **122**, DOI: http://dx.doi.org/10.1063/1.1940632 (2005).

52. G. A. Garcia, H. Dossmann, L. Nahon, S. Daly, I. Powis, *Phys. Chem. Chem. Phys.* **16**, 16214–16224 (30 2014).

53. G. Contini *et al.*, *The Journal of Chemical Physics* **127**, DOI: http://dx.doi.org/10.1063/1.2779324 (2007).

54. A. Rizzo, O. Vahtras, *The Journal of Chemical Physics* **134**, DOI: http://dx.doi.org/10.1063/1.3602219 (2011).

55. P. L. Polavarapu, B. A. Hess, L. J. Schaad, *The Journal of Chemical Physics* **82**, 1705–1710 (1985).

56. P. Polavarapu, D. Michalska, *Molecular Physics* **52**, 1225–1235 (1984).

57. R. Kawiecki, F. Devlin, P. Stephens, R. Amos, N. Handy, *Chemical Physics Letters* **145**, 411–417, ISSN: 0009-2614 (1988).

58. J. Bloino, V. Barone, *The Journal of Chemical Physics* **136**, DOI: http://dx.doi.org/10.1063/1.3695210 (2012).

59. Y. Enye, PhD thesis, National University of Singapore, 2006.

60. H. M. Pickett, *Journal of Molecular Spectroscopy* **148**, 371–377, ISSN: 0022-2852 (1991).

61. H. Hartwig, H. Dreizler, *Z. Naturforsch* **51a**, 923–32 (1996).

62. J. A. Kroll, S. T. Shipman, S. L. W. Weaver, *Journal of Molecular Spectroscopy* **295**, 52–57, ISSN: 0022-2852 (2014).

63. H. Pickett *et al.*, *J. Quant. Spectrosc. Radiat. Transfer* **60**, 883–90 (1998).

64. D. R. Herschbach, J. D. Swalen, *The Journal of Chemical Physics* **29**, 761–776 (1958).

65. J. Vacherand, B. V. Eijck, J. Burie, J. Demaison, *Journal of Molecular Spectroscopy* **118**, 355–362, ISSN: 0022-2852 (1986).